Universidade Federal de Santa Catarina
Centro de Ciências da Saúde
Programa de Pós-Graduação em Nanotecnologia Farmacêutica

DESENVOLVIMENTO DE SISTEMAS DE LIBERAÇÃO NANO- E/OU MICROESTRUTURADOS CONTENDO SINVASTATINA PARA LIBERAÇÃO COLÔNICA VISANDO O TRATAMENTO DO CÂNCER COLORRETAL

Mariana Dalagnol

Florianópolis
2016

Mariana Dalagnol

DESENVOLVIMENTO DE SISTEMAS DE LIBERAÇÃO NANO- E/OU MICROESTRUTURADOS CONTENDO SINVASTATINA PARA LIBERAÇÃO COLÔNICA VISANDO O TRATAMENTO DO CÂNCER COLORRETAL

Tese apresentada ao Programa de Pós-Graduação em Nanotecnologia Farmacêutica da Universidade Federal de Santa Catarina como requisito parcial à obtenção do grau de Doutor em Nanotecnologia Farmacêutica.

Orientadora: Profª. Drª. Elenara Lemos Senna

Florianópolis
2016

Ficha de identificação da obra elaborada pelo autor,
através do Programa de Geração Automática da Biblioteca Universitária da UFSC.

Dalagnol, Mariana
Desenvolvimento de sistemas de liberação nano- e/ou microestruturados contendo sinvastatina para a liberação colônica visando o tratamento do câncer colorretal / Mariana Dalagnol ; orientadora, Elenara Lemos Senna - Florianópolis, SC, 2016.
191 p.

Tese (doutorado) - Universidade Federal de Santa Catarina, Centro de Ciências da Saúde. Programa de Pós Graduação em Nanotecnologia Farmacêutica.

Inclui referências

1. Nanotecnologia Farmacêutica. 2. Nanotecnologia. 3. Sistemas de liberação de fármacos. 4. Liberação colônica. 5. Câncer. I. Lemos Senna, Elenara . II. Universidade Federal de Santa Catarina. Programa de Pós-Graduação em Nanotecnologia Farmacêutica. III. Título.

Dedico esta conquista àqueles que dão sentido à minha vida: meu pai Sérgio, minha mãe Miriam e minha irmã Raquel.

AGRADECIMENTOS

Aos meus pais Sérgio e Miriam que me ensinaram a correr atrás dos meus sonhos e não desistir nas lutas da vida. Esta conquista só foi possível pois tive vocês ao meu lado. Obrigada pelo orgulho que é ter nascido de vocês!

À minha irmã Raquel por me dar todos os dias o exemplo de profissional que eu quero ser. Obrigada por ser quem você é e por caminharmos juntas nesta vida.

Aos meus dindos Sérgio e Stela por todo carinho e amor que sempre tiveram por mim e por me darem a oportunidade de ser mais que uma afilhada, ser uma filha.

À minha orientadora Profª Drª Elenara Lemos Senna pelos conhecimentos a mim transmitidos, pela confiança, apoio, paciência e dedicação. Obrigada!

À Profª Drª Helena Maria Cabral Marques por ter me recebido na Faculdade de Farmácia da Universidade de Lisboa no meu doutorado sanduiche.

À Profª Drª Maria Cláudia Santos Silva e à Lorena pela colaboração nos experimentos *in vitro*.

Aos meus colegas da farmacotécnica Luís, Talitha, Jana, Marta, Larissa, Mariana, Geci, Priscila, Carine, Aline e Thaisa por todos os momentos compartilhados no lab. Vocês fizeram parte de um momento único na minha vida e serão sempre lembrados com muito carinho.

À Cassi, a amiga que a pós-graduação me deu. Obrigada por transformar todos os momentos que passamos juntas em momentos especiais. Sou grata a Deus por ter colocado no meu caminho uma pessoa como você.

Aos meus amigos de Portugal Diana, André, Carina, Ana Raquel, Melissa, Ana Matos, Eva, Maria Paisana, Joana Marto, Nélio, Mariya Brachkova, Joana Pinto, Vanessa, João, Ana Ester e Joana Silva. Obrigada por terem tornado meu ano em Lisboa inesquecível. Não há distância que seja capaz de diminuir o carinho que sinto por cada um. Vocês são muito especiais!

Às minhas amigas do coração Taty, Déia, Thatha e Lúcia. “Amizade verdadeira não é ser inseparável, é estar separado e nada mudar”. Sou feliz por ter vocês!

À Leka, a irmã que a vida me deu a chance de escolher. Obrigada por ser meu porto seguro. Sou abençoada por ter você na minha vida.

Muito obrigada!

“É que tem mais chão nos meus olhos do que cansaço nas minhas pernas, mais esperança nos meus passos do que tristeza nos meus ombros, mais estrada no meu coração do que medo na minha cabeça.”

Cora Coralina

RESUMO

A liberação colônica de fármacos a partir de nano- e micropartículas por via oral é uma estratégia promissora para o tratamento local de diversas doenças que afetam o cólon, como o câncer colorretal. A sinvastatina é um fármaco inibidor competitivo efetivo da 3-hidroxi-3-metil-glutaril coenzima A redutase e atua diretamente na inibição da via da biossíntese do colesterol. Além do seu efeito redutor dos níveis de colesterol, evidências sugerem que a sinvastatina possui efeitos terapêuticos contra o câncer devido à sua interação com uma série de funções celulares essenciais. Desta maneira, objetivo deste trabalho foi desenvolver carreadores microestruturados gastroresistentes encapsulando nanopartículas de quitosana (CSNP) para a liberação colônica da sinvastatina. As nanopartículas de quitosana (CS) e tripolifosfato (TPP) foram preparadas por meio da técnica de interação iônica. Para aumentar a associação da sinvastatina nas nanopartículas foram adicionadas diferentes concentrações de taurocolato de sódio (STC) ou sulfobutiléter-β-ciclodextrina (SBE-β-CD) nas formulações. Para a quantificação da sinvastatina, uma metodologia de espectroscopia de absorção do ultravioleta foi desenvolvida e validada. As CSNP contendo STC apresentaram teores de sinvastatina entre 66,91 e 225,14 µg/mL e diâmetros variando entre 317,2 e 443,7 nm. Para as CSNP contendo SBE-β-CD os teores variaram de 121,4 a 634,62 µg/mL e os diâmetros de 321,07 a 549,53 nm. A eficiência de encapsulação da sinvastatina foi superior a 91 % e o potencial zeta foi positivo para todas as amostras. Estudos *in vitro* demonstraram que tanto a sinvastatina livre quanto encapsulada ($CSNP_{70}$) exibiram efeitos citotóxicos, além de induzir a morte celular por apoptose, inibir a migração celular e reduzir a capacidade das células HT-29 de formar colônias. As micropartículas encapsulando as CSNP foram obtidas mediante adição das suspensões de nanopartículas em soluções aquosas de Eudragit® S100 pH 7,2 e estes sistemas foram submetidos à

secagem utilizando a técnica de spray-drying. Para avaliar o efeito da concentração de Eudragit® S100 adicionada no controle da liberação do fármaco, diferentes proporções de nanopartículas/Eudragit® S100 (1:4, 1:6 e 1:8) foram testadas. As micropartículas contendo $CSNP_{70}$ apresentaram teores de sinvastatina entre 0,88 e 1,05 % e diâmetros de cerca 3 µm. As micropartículas encapsulando $CSNP_{CD65}$ e $CSNP_{TPP/CD45}$ apresentaram teores de sinvastatina de 0,97 a 1,51 % e diâmetros de cerca de 5 µm. As interações entre os componentes das formulações e as propriedades do estado sólido das partículas foram avaliadas por calorimetria exploratória diferencial, espectroscopia de absorção no infravermelho com transformada de Fourier e difração de raio X. Os ensaios de liberação *in vitro* confirmaram a obtenção de micropartículas gastroresistentes visto que apenas uma pequena fração de sinvastatina foi liberada em meio ácido. Entretanto, as micropartículas promoveram uma liberação sustentada do fármaco em meio tampão fosfato pH 7,2 ao longo de 8 horas, sendo esta liberação afetada pela proporção nanopartículas/Eudragit® S100 utilizada. Estes resultados indicam que estes sistemas de liberação inovadores podem ser promissores para a liberação colônica da sinvastatina visando o tratamento do câncer colorretal.

Palavras-chave: sinvastatina; nanopartículas; interação iônica; quitosana; taurocolato de sódio; sulfobutiléter-β-ciclodextrina; Eudragit® S100; spray-drying; liberação colônica; câncer colorretal.

ABSTRACT

The colonic delivery of drugs from nano- and microparticles after oral administration is a promising strategy for the local treatment of colonic diseases, such as colorectal cancer. Simvastatin (SIM) is a hydroxy-3-methylglutaryl coenzyme A inhibitor that acts directly in the suppression of the cholesterol biosynthesis by the inhibition of the mevalonate pathway. Besides the lip-lowering effect, increasing evidences suggest that simvastatin has therapeutic effects against cancer due to its interaction with essential cellular functions. Therefore, the aim of this study was to develop nano- and/or microparticles containing simvastatin for colonic delivery aiming the treatment of colorectal cancer. The chitosan nanoparticles were prepared using a modified ionic interaction technique by adding sodium taurocholate (STC) and/or sulfobutylether-β-cyclodextrin (SBE-β-CD). To determine the SIM loading in the nano- and/or microparticles an ultraviolet spectroscopy method was developed and validated. The nanoparticles containing STC presented SIM loading ranging between 66.91 and 225.14 μg/mL and mean diameters varying from 317.2 to 443.7 nm. The nanoparticles containing SBE-β-CD exhibited SIM loading between 121.41 and 634.62 μg/mL and mean diameters ranging from 321.07 to 549.53 nm. The encapsulation efficiency of SIM was above 91 % and the zeta potential was positive for all the samples. *In vitro* studies demonstrated that both free and encapsulated SIM exhibited cytotoxic effect, induced apoptosis, inhibited cell migration, and reduced the ability of HT-29 cells to form colonies. The microparticles entrapping chitosan nanoparticles (SDP) were obtained by adding the nanoparticles suspensions in a Eudragit® S100 aqueous solution pH 7.2 and dried using the spray-dryer technique. In order to evaluate the effect of the Eudragit® S100 concentration on SIM release, different nanoparticles/Eudragit® S100 ratios (1:4, 1:6, and 1:8) were tested. The microparticles containing STC showed SIM

loading between 0.88 and 1.05 % with mean diameters around 3 µm. The microparticles containing SBE-β-CD presented SIM loading varying from 0.97 to 1.51 % with mean diameters around 5 µm. The interactions between the components of the formulations and crystallinity properties of the nano- and/or microparticles were assessed by differential scanning calorimetry, Fourier-transformed infrared spectroscopy, and X-ray diffraction techniques. The *in vitro* release studies confirmed the enteric characteristic of all microparticles since a small fraction of SIM was released in the acidic medium. However, the microparticles revealed a sustained drug release in phosphate buffer solution pH 7.2 over 8 hours, that was affected by the nanoparticles/Eudragit® S100 ratios tested. These results indicated that these innovative drug delivery systems could be promising to deliver SIM in the colon for the treatment of colorectal cancer.

Key-words: simvastatin; nanoparticles; ionic interaction; chitosan; sodium taurocholate; sulfobutylether-β-cyclodextrin; Eudragit® S100; spray-drying; colonic delivery; colorectal cancer.

LISTA DE FIGURAS

REVISÃO DA LITERATURA

CAPÍTULO 1

CAPÍTULO 2

LISTA DE TABELAS

CAPÍTULO 1

CAPÍTULO 2

LISTA DE EQUAÇÕES

CAPÍTULO 2

Publicação 1. Spray-Dried Enteric Microparticles Entrapping Sulfobutylether-β-Cyclodextrin/Chitosan Nanoparticles as a New Approach to Deliver Simvastatin in the Colon Aiming the Treatment of the Colorectal Cancer

LISTA DE ABREVIATURAS E SIGLAS

ANOVA – Análise da Variância
AO – acridine orange
CD – cyclodextrin
cmc – critical micellar concentration
CS – chitosan
CSNP – chitosan nanoparticles
DE – dissolution efficiency
DMSO – dimethyl sulfoxide
DNA – ácido desoxirribonucleico
DSC – differential scanning calorimetry
GIT – grastrointestinal tract
EB – ethidium bromide
EE – encapsulation efficiency
FBS – fetal bovin serum
FITC – isotiocianato de fluoresceína
HEPES – 4-(2-hydroxyethyl)-1-piperazineethanesulfonic acid
HMG-CoA – hidroximetilglutaril coenzima A
IC_{50} – 50% inhibitory concentration
ICH – International Conference of Harmonization
INCA – Instituto Nacional do Câncer
MTT – 3-(4,5-dimethyl-2-thiazolyl)-2,5-diphenyl-2H-tetrazolium bromide
NF-κB – fator nuclear kappa B
NP – nanoparticles
PBS – phosphate buffer saline
PDI – polydispersity index
OMS – Organização Mundial da Saúde
RSD – relative standard deviation
SBE-β-CD – sulfobutilether-β-cyclodextrin
SD – standard deviation
SDP – spray-dried powders
SEM – scanning electron microscopy
SIM – simvastatin
SIM-NP – simvastatin nanoparticles

STC – sodium taurocholate
TEM – transmission electronic microscopy
TGI – trato gastrointestinal
TPP – tripolyphosphate
UV – ultraviolet
USP – United States Pharmacopoeia
VEGF – fator de crescimento vascular endotelial
XRD – X-ray diffraction
5-FU – 5-fluoruracil

SUMÁRIO

INTRODUÇÃO

O termo câncer é atribuído a um conjunto de mais de 100 doenças que têm em comum o crescimento desordenado de células que invadem os tecidos e órgãos, podendo espalhar-se para outras regiões do corpo, formando as metástases (INCA, 2016). O câncer é uma das principais causas de morte no mundo de acordo com a mais recente estimativa realizada em 2012 pela Organização Mundial da Saúde. As estatísticas apontaram 14,1 milhões de novos casos de câncer com um total de 8,2 milhões de óbitos em todo o mundo. Esta incidência deve seguir aumentando, atingindo cerca de 21,4 milhões de novos casos com 13,2 milhões de óbitos no ano de 2030. No Brasil, as estimativas para 2016/2017 apontam a ocorrência de aproximadamente 596.070 novos casos de câncer, sendo aproximadamente 34 mil novos casos de câncer colorretal (INCA, 2016).

O câncer colorretal abrange os tumores que acometem um segmento do intestino grosso (cólon) e o reto. O histórico familiar de câncer colorretal e a predisposição genética ao desenvolvimento de doenças inflamatórias do intestino são considerados os fatores de risco mais importantes para o desenvolvimento deste tipo de neoplasia. Além disso, uma dieta baseada em gorduras animais, baixa ingestão de frutas, vegetais e cereais, consumo excessivo de álcool, tabagismo e o aumento da idade também são considerados fatores de risco. Entretanto, cerca de 75% dos cânceres colorretal se dá de forma esporádica, surgindo de mutações somáticas e evolução do clone celular tumoral (KASPER et al., 2006; INCA, 2016).

O tratamento do câncer envolve uma série de intervenções, incluindo suporte psicológico, cirurgia, radioterapia e quimioterapia que objetiva a cura da doença ou o prolongamento do tempo de vida juntamente com uma melhora na qualidade de vida do paciente. A quimioterapia tem como objetivo primário a destruição das células tumorais, preservando as normais. Porém, os agentes citotóxicos tradicionais atuam de maneira não específica, comprometendo tanto as células saudáveis como as células

tumorais, o que explica a ocorrência de efeitos colaterais tóxicos. Sendo assim, o estímulo para a morte celular necessita ser radicalmente modificado para alcançar as células tumorais de maneira mais específica e menos tóxica (KAUFMANN & EARNSHAW, 2000).

A liberação colônica de fármacos após a administração oral é promissora para o tratamento local de diversas doenças que afetam o cólon, como o câncer colorretal (SINGH, 2007). No tratamento destas patologias, altas concentrações do fármaco no local de ação podem ser alcançadas, com a minimização dos efeitos adversos que ocorrem quando o fármaco é liberado no trato gastrointestinal superior ou absorvido sistemicamente (CHOURASIA & JAIN, 2003; BYAT et al., 2008). De acordo com algumas propriedades fisiológicas do trato gastrointestinal, estes sistemas podem ser classificados em sistemas tempo-dependentes, pH-dependentes, microflora-dependentes e pressão luminal-dependentes (FRIEND, 2005; FERRARI et al., 2013). Os sistemas pH-dependentes são os mais comumente empregados no delineamento de formas farmacêuticas de liberação colônica. Estes sistemas levam em consideração o aumento gradativo do pH ao longo do trato gastrointestinal (CHOURASIA & JAIN, 2003; FREIRE et al., 2006; SINGH, 2007). Um sistema de liberação colônico ideal deve prevenir a liberação do fármaco durante a passagem pelo estômago e intestino delgado, e consequentemente ser capaz de liberar o fármaco no cólon (ASGHAR & CHANDRAN, 2006). Para isso, é necessário que a forma farmacêutica seja revestida com um polímero pH-sensível. Estes polímeros devem ser capazes de resistir aos baixos valores de pH do estômago e da porção proximal do intestino delgado e ao mesmo tempo serem capazes de se desintegrar em pH neutro a ligeiramente alcalino do íleo terminal e preferencialmente na junção íleo-cecal. (CHOURASIA & JAIN, 2003). Os polímeros pH-sensíveis mais comumente utilizados são os derivados do ácido acrílico, mais conhecidos como Eudragit®. Mais especificamente o Eudragit® S100, um copolímero do

ácido metacrílico e metil metacrilato, que possui um pH de dissolução acima de 7,0 (PARK et al., 2010).

As nanopartículas são definidas como dispersões particuladas ou partículas sólidas com tamanhos entre 10 – 1000 nm capazes de dissolver, encapsular ou adsorver fármacos na sua matriz (MOHANRAJ & CHEN, 2006). No que diz respeito ao câncer, a administração de nanopartículas tem demonstrado um potencial terapêutico significante, pois aumentam a seletividade do fármaco em relação às células tumorais, reduzindo assim a toxicidade nos tecidos sadios (BRIGGER, DUBERNET, COUVREUR, 2002). Espera-se um acúmulo das nanopartículas nos tecidos tumorais através do efeito de permeação e retenção aumentadas (efeito EPR). Devido à rápida angiogênse, para a obtenção de suprimento adequado de nutrientes e oxigênio, os vasos sanguíneos dos tumores possuem uma arquitetura defeituosa com grandes fendas nas junções entre as células epiteliais, o que leva a um aumento na permeabilidade. Além disso, os tumores são caracterizados por possuir uma drenagem linfática disfuncional, o que auxilia na retenção das nanopartículas nos tumores. Desta maneira, as nanopartículas são capazes de extravasar dos vasos sanguíneos e acumulam-se nos tecidos tumorais, permanecendo retidas por tempo suficiente para sua desintegração e liberação do fármaco nas adjacências das células tumorais (BRANNON-PEPPAS & BLANCHETTE, 2004; WANG & THANAU, 2010; FANG, NAKAMURA, MAEDA, 2011).

Uma vasta gama de materiais tem sido empregada como carreadores de fármacos e dentre eles, os polissacarídeos têm recebido uma maior atenção devido a suas excelentes propriedades físico-químicas e biológicas (LIU et al., 2008). A quitosana é um heteropolímero constituído de unidades de N-acetil-2-amino-2-deoxi-D-glucopiranose e 2-amino-2-deoxi-D-glucopiranose unidas por ligações glicosídicas β-(1→4) e é obtida pela deacetilação termoquímica da quitina, um polímero natural encontrado no exoesqueleto de crustáceos como camarões, lagostas e

caranguejos, insetos e alguns fungos (DASH et al., 2011). A solubilização da quitosana ocorre em soluções de ácidos diluídos (pH < 6,0) devido a quartenização dos grupamentos amino, tornando-se um polímero catiônico (HEZAJI & AMIJI, 2003; RINAUDO, 2006). A quitosana é utilizada para aplicações farmacêuticas e biomédicas, pois possui uma abundante disponibilidade, mucoadesividade única, propriedades farmacológicas inerentes e outras propriedades biológicas benéficas como biocompatibilidade, biodegradabilidade, baixa toxicidade e imunogenicidade (AGRAWAL, STRIJKERS, NICOLAY, 2010; PARK et al., 2010; BALAN & VERESTIUC, 2014).

As estatinas são inibidores competitivos efetivos da 3-hidroxi-3-metil-glutaril coenzima A redutase (HMG-CoA redutase). A inibição da HMG-CoA redutase promove a redução da síntese de colesterol através da prevenção da conversão da 3-hidroxi-3-metil-glutaril coenzima A em mevalonato, um intermediário limitante na via da biossíntese de colesterol no corpo humano (WONG et al., 2002). Além do seu efeito redutor dos níveis de colesterol, evidências sugerem que as estatinas possuem efeitos terapêuticos contra o câncer devido à sua interação com uma série de funções celulares essenciais (HINDLER et al., 2006). A inibição da via do mevalonato inibe a síntese de moléculas importantes como os isoprenóides farnesil pirofosfato e geranil pirofosfato, as quais são responsáveis pela isoprenilação de várias proteínas celulares sinalizadoras. Estas proteínas possuem funções fisiológicas potencialmente envolvidas na carcinogênese, pois estão ligadas aos processos de crescimento, proliferação celular, migração celular e estresse oxidativo. Desta maneira, as propriedades pró-apoptóticas e de inibição do crescimento celular produzidas pelas estatinas parecem ter implicações clínicas no tratamento de diversos tumores (BARDOU, BARKUN, MARTEL, 2010 PISANTI et al., 2014). Por exemplo, estudos *in vitro* e *in vivo* mostraram que as estatinas inibem o crescimento e induzem a apoptose

em linhagens celulares de melanoma, glioma, neuroblastoma e leucemia (HINDLER et al., 2006).

Os potenciais efeitos benéficos das estatinas no câncer colorretal também têm sido extensivamente revisados. Em particular, estudos *in vitro* e *in vivo* realizados por Cho e colaboradores (2008) mostraram que a sinvastatina inibe o desenvolvimento do câncer de cólon pela indução da apoptose, bem como pela supressão da angiogênese. A participação do estresse oxidativo na morte celular por apoptose induzida pela sinvastatina foi descrita por Qi e colaboradores (2010). Neste estudo foi mostrado que a sinvastatina interrompe o sistema de defesa antioxidante, aumentado a produção de espécies oxidativas de oxigênio intracelular em linhagem celular CT26 de carcinoma de cólon murino, promovendo a apoptose. Finalmente, um estudo recente mostrou que o uso de estatinas reduziu a mortalidade de pacientes diagnosticados com câncer colorretal (CARDWELL et al, 2014).

Assim, baseado nos dados da literatura e considerando as potenciais aplicações dos sistemas de liberação cólon-específicos, este trabalho tem como objetivo desenvolver micropartículas gastroresistentes encapsulando nanopartículas de quitosana para a liberação colônica da sinvastatina.

Objetivos

Objetivo Geral

Desenvolver carreadores microestruturados entéricos encapsulando nanocarreadores de quitosana para a liberação colônica da sinvastatina.

Objetivos Específicos

- Preparar carreadores nanoestruturados constituídos de quitosana contendo sinvastatina pela técnica de interação iônica;
- Preparar carreadores microestruturados entéricos encapsulando os carreadores nanoestruturados de quitosana;
- Caracterizar os carreadores nano- e/ou microestruturados quanto ao tamanho, potencial zeta, morfologia, eficiência de encapsulação e teor de sinvastatina;
- Avaliar o efeito da adição de taurocolato de sódio e de sulfobutiléter-β-ciclodextrina no teor e eficiência de encapsulação da sinvastatina nas nanopartículas;
- Avaliar as interações entre os componentes das formulações por calorimetria exploratória diferencial e espectroscopia de infravermelho e avaliar as propriedades do estado sólido das partículas por difração de raio X;
- Avaliar os perfis de liberação da sinvastatina *in vitro* a partir dos carreadores microestruturados entéricos em pH 1,2; 4,5 e 7,2;
- Avaliar a atividade citotóxica e características morfológicas de morte celular *in vitro* da sinvastatina livre e encapsulada sobre a linhagem celular HT-29 (células de adenocarcinoma de cólon humano).

O trabalho mostra-se dividido em revisão da literatura, capítulo 1 correspondente ao desenvolvimento e caracterização de micropartículas entéricas encapsulando nanopartículas de quitosana/tripolifosfato/taurocolato de sódio e a avaliação da atividade antitumoral das nanopartículas e o capítulo 2 que corresponde ao desenvolvimento e caracterização caracterização de micropartículas entéricas encapsulando nanopartículas de quitosana/sulfobituléter-β-ciclodetrina e quitosana/tripolifosfato/sulfobutiléter-β-ciclodextrina.

REVISÃO DA LITERATURA

1. CÂNCER

O câncer é uma das doenças que mais causam temor na sociedade por ter se tornado um estigma de mortalidade e dor. De acordo com o Instituto Nacional do Câncer (INCA), o termo câncer é o nome dado a um conjunto de mais de 100 doenças que têm em comum o crescimento desordenado de células que invadem os tecidos e órgãos, podendo espalhar-se para outras regiões do corpo (INCA, 2016).

Os genes envolvidos nas alterações que levam ao desenvolvimento do câncer podem ser classificados em três tipos: oncogenes, genes supressores de tumor e genes de reparo do DNA. Em condições normais os oncogenes estimulam o crescimento celular apropriado, porém a mutação ou superexpressão dos oncogenes resulta em um "ganho de função", causando um crescimento celular contínuo e descontrolado. Os genes supressores de tumor normalmente inibem o progresso do ciclo celular ou promovem a morte celular programada. Quando a expressão destes genes está ausente, devido a uma mutação ou perda de alelos, ocorre uma perda do controle inibitório normal. Finalmente, os genes de reparo de DNA estão envolvidos no controle da taxa de mutação de outros genes. Quando mutados, os genes de reparo são incapazes de reparar erros e, desta maneira, as mutações nos oncogenes e nos genes supressores de tumor acumulam-se de maneira acelerada (LESLIE et al., 2002). Todas estas alterações genéticas são responsáveis pela malignização (transformação) das células normais, tornando-as cancerosas. A manutenção e o acúmulo dessas células formam os tumores malignos e elas podem adquirir a capacidade de se desprenderem do tumor e migrarem, invadindo inicialmente os tecidos vizinhos, podendo chegar ao interior de um vaso sanguíneo ou linfático e, através destes, disseminarem-se, chegando a órgãos distantes do local onde o tumor se iniciou, formando as metástases (ALMEIDA et al., 2005).

O processo de formação do câncer, ou carcinogênese, em geral se dá lentamente, podendo levar vários anos para que

uma célula tumoral prolifere e dê origem a um tumor visível. A carginogênese possui vários estágios antes de chegar ao tumor propriamente dito. Os estágios da carcinogênese são classificados em:

- *Estágio de iniciação:* neste primeiro estágio as células sofrem o efeito dos agentes carcinogênicos (agentes oncoiniciadores) que provocam modificações em alguns de seus genes. As células se encontram geneticamente alteradas, porém o tumor ainda não é capaz de ser detectado clinicamente. Elas encontram-se "iniciadas" para a ação de um segundo grupo de agentes que atuará no próximo estágio.

-*Estágio de promoção:* neste estágio, as células geneticamente alteradas ("iniciadas"), sofrem ação dos agentes cancerígenos classificados como oncopromotores. A célula iniciada é transformada em célula maligna de maneira lenta e gradual. Para que ocorra essa transformação é necessário um longo e continuado contato com o agente cancerígeno promotor. A suspensão do contato com agentes promotores muitas vezes interrompe o processo nesse estágio.

- *Estágio de progressão:* é o último estágio da carcinogênese e se caracteriza pela multiplicação descontrolada e irreversível das células alteradas. O câncer já está instalado e evolui até o surgimento das primeiras manifestações clínicas da doença (INCA, 2016).

Os fatores de risco para o desenvolvimento do câncer podem ser tanto hereditários quanto relacionados ao meio ambiente, sendo este último responsável por cerca de 80% dos casos. Os fatores ambientais englobam o ambiente geral (água, terra e ar), ambiente ocupacional (quando insalubre), ambiente social e cultural (estilo e hábitos de vida) e o ambiente de consumo (alimentos e medicamentos) (ALMEIDA et al., 2005).

Estatisticamente, o câncer é uma das principais causas de morte no mundo de acordo com estimativas mundiais do projeto Globocan 2012, da Agência Internacional para Pesquisa em Câncer (Iarc, do inglês *International Agency for Research on Cancer*), da Organização Mundial da Saúde

(OMS). As estatísticas apontaram 14,1 milhões de novos casos de câncer com um total de 8,2 milhões de óbitos em todo o mundo. Esta incidência deve seguir aumentando, atingindo cerca de 21,4 milhões de novos casos com 13,2 milhões de óbitos no ano de 2030. No Brasil, as estimativas para 2016, válidas também para o ano de 2017, apontam a ocorrência de aproximadamente 596.070 novos casos de câncer, incluindo os casos de câncer de pele não melanoma, reforçando a magnitude do problema do câncer no país. Entre os homens, são esperados 295.200 novos casos, e entre as mulheres, 300.800. Exceto os cânceres de pele não melanoma, os tipos mais incidentes para o sexo masculino serão o câncer próstata, traquéia, brônquio e pulmão, colorretal e estômago; e para o sexo feminino serão o câncer de mama, colorretal, colo do útero e de traquéia, brônquio e pulmão (INCA, 2016).

O tratamento convencional do câncer envolve uma série de intervenções, incluindo suporte psicológico, cirurgia, radioterapia e quimioterapia que objetiva a cura da doença ou o prolongamento do tempo de vida juntamente com uma melhora na qualidade de vida do paciente.

A técnica cirúrgica pode levar à remoção de tumores de maneira eficaz, caso não haja metástase. A radioterapia (raios gama, radioisótopos como cobalto-60, raios-X e prótons e mésons pi negativos) é geralmente combinada com a técnica cirúrgica para incrementar a eficiência do tratamento. A radioterapia pode também ser utilizada isoladamente para diminuir tumores grandes e diminuir a chance de metástases, porém o tratamento com radiação possui limitações devido aos severos efeitos colaterais. Cerca de um terço dos pacientes alcançam a cura com a utilização desses dois métodos de tratamento locais, que são eficazes quando o tumor não sofreu metástase. Porém, nos cerca de 60 a 70% demais casos a abordagem sistêmica, através da quimioterapia, se faz necessária devido à ocorrência de metástases (ALMEIDA et al., 2005).

A quimioterapia tem como objetivo primário a destruição das células tumorais, preservando as normais.

Porém, os agentes citotóxicos tradicionais atuam de maneira não específica, lesando tanto as células saudáveis como as células tumorais, particularmente as células de rápido crescimento, como as gastrointestinais e as do sistema imunológico. Isto explica a ocorrência de efeitos colaterais tóxicos como náuseas, perda de cabelo e maior susceptibilidade às infecções, acarretando um impacto significante na qualidade de vida do paciente. A erradicação das células tumorais através da quimioterapia é alcançada pelo mecanismo de apoptose (morte celular programada); entretanto, o estímulo para que este processo ocorra necessita ser radicalmente modificado para alcançar as células tumorais de maneira mais específica e menos tóxica (KAUFMANN & EARNSHAW, 2000).

1.1 Câncer colorretal

O câncer colorretal abrange os tumores que acometem um segmento do intestino grosso (cólon) e o reto. De acordo com a última estimativa mundial, este tipo de câncer é o terceiro tipo mais comum entre os homens, com 746 mil novos casos, e o segundo câncer mais incidente nas mulheres, com 614 mil novos casos. Para o Brasil em 2016/2017, as estimativas apontam para aproximadamente 34 mil novos casos de câncer colorretal, sendo 16.660 novos casos em homens e 17.620 novos casos em mulheres. Sem considerar os tumores de pele não melanoma, o câncer colorretal em homens é o segundo mais frequente na Região Sudeste e terceiro nas Regiões Sul e Centro-oeste. Nas Regiões Nordeste e Norte ocupa a quarta posição. Para as mulheres é o segundo mais frequente nas Regiões Sudeste e Sul. Nas Regiões Centro-Oeste, Nordeste e na Região Norte é o terceiro mais frequente (INCA, 2016).

Os fatores de risco mais importantes para o desenvolvimento do câncer colorretal são as doenças inflamatórias do intestino (colite ulcerativa e doença de Crohn), as doenças hereditárias (polipose adenomatosa

familiar e câncer colorretal hereditário sem polipose) e a idade, uma vez que tanto a incidência quanto a mortalidade aumentam com a idade. Além disso, hábitos alimentares baseados em carne vermelha e carnes processadas (mortadelas, presuntos, salsichas, linguiças), consumo de álcool, tabagismo e o excesso de gordura corporal e abdominal também são fatores de risco para o surgimento da doença. Desta maneira, os fatores protetores mais importantes são a atividade física e o consumo de alimentos contendo fibras, ou seja, aqueles de origem vegetal, tais como frutas, hortaliças (legumes e verduras) e cereais integrais. Apesar disso, a maioria dos cânceres colorretais (cerca de 75%) se dá de forma esporádica, surgindo de mutações somáticas e evolução do clone celular tumoral (KASPER et al., 2006; INCA, 2014).

O câncer colorretal é classificado em cinco estágios distintos:

- *Estágio 0*: é o estágio mais inicial do câncer onde os pólipos são formados na mucosa colônica. Durante o exame de colonoscopia, os pólipos são erradicados completamente através da polipectomia, o que previne a evolução para os estágios mais avançados da doença;

- *Estágio I*: neste estágio o pólipo se desenvolve em um tumor e invade a camada mais interna da mucosa colônica. A intervenção cirúrgica é a opção principal de tratamento, onde a porção de tecido canceroso é separada da porção não-cancerosa. A taxa de sobrevivência neste estágio é de aproximadamente 95%;

- *Estágio II*: é caracterizado pela propagação do câncer além do cólon, porém não para os linfonodos, através da metástase. Este estágio é subcaracterizado em estágio IIA, IIB e IIC dependendo da difusão do câncer na camada muscular, na camada externa do cólon ou além do cólon. A cirurgia de ressecção é a única opção de tratamento neste estágio e a taxa de sobrevivência é de 85%;

- *Estágio III*: neste estágio o câncer já se propagou em toda a parede do cólon e também nos linfonodos

adjacentes e a taxa de sobrevivência é cerca de 30 a 60%. Este estágio do câncer é subcategorizado em estágio IIIA, IIIB e IIIC dependendo da difusão do câncer na camada interna, média ou externa do cólon e nos linfonodos adjacentes. Juntamente com a cirurgia, a quimioterapia e outras terapias médicas são requeridas para o tratamento;

- *Estágio IV*: neste estágio o câncer se disseminou rapidamente para outros órgãos do corpo como fígado, ovários, testículos e outros segmentos do intestino, e a taxa de sobrevivência é de apenas 3%. O tratamento inclui ressecção cirúrgica, quimioterapia, radioterapia e remoção cirúrgica das porções cancerosas nos outros órgãos do corpo acometidos pela doença (MISHRA et al., 2013).

A quimioterapia é um dos principais métodos utilizados no tratamento do câncer colorretal e inclui a administração de agentes alquilantes, antimetabólitos, alcaloides, antibióticos antitumorais, enzimas, hormônios e modificadores da resposta biológica que destroem as células malignas, suprimem o crescimento do tumor ou sua divisão celular (MISHRA et al., 2013). O quimioterápico mais comumente aplicado no tratamento do câncer colorretal é o 5-fluorouracila administrado por via intravenosa. Este fármaco é um análogo da pirimidina e age na fase S do crescimento celular, levando a apoptose das células tumorais (BI et al., 2014). Entretanto, possui curta meia-vida plasmática (10 – 25 minutos) e, quando utilizado isoladamente apresenta uma atividade considerada modesta, com taxas de resposta em torno de 10 a 15%. Outros fármacos utilizados no tratamento incluem o raltitrexato, irinotecano e oxaliplatina, os quais também apresentam baixa eficácia quando administrados tanto isoladamente quanto em associação com o 5-fluorouracila (GILL, THOMAS, GOLDBERG, 2003). Além do curto tempo de meia vida plasmática, outro fator agravante para baixa eficácia das quimioterapias tradicionais no tratamento do câncer colorretal é a impossibilidade do fármaco em alcançar o sítio de ação em concentrações adequadas. Desta maneira, um tratamento efetivo demanda

um aumento da dose, o que leva a efeitos indesejados, principalmente devido à toxicidade dos agentes quimioterápicos aos tecidos sadios. Para melhorar esta situação, estratégias têm sido desenvolvidas para promover a liberação de fármacos de maneira mais eficiente no cólon (JAIN et al., 2010; KRISHNAIAH & KHAN, 2002).

2. LIBERAÇÃO COLÔNICA

A liberação colônica de fármacos após a administração oral é promissora para o tratamento local de diversas doenças, principalmente as doenças inflamatórias, a síndrome do intestino irritável e o câncer colorretal (SINGH, 2007). No tratamento destas patologias, altas concentrações do fármaco no local de ação devem ser alcançadas, com a minimização dos efeitos adversos que ocorrem quando o fármaco é liberado no trato gastrointestinal superior e absorvido sistemicamente. Além disso, o cólon é reconhecido por ser um ambiente menos hostil e com menor atividade enzimática do que o estômago e o intestino delgado, e por esta razão espera-se que os fármacos liberados diretamente neste sítio tenham uma maior eficiência de absorção (CHOURASIA & JAIN, 2003; BAYAT et al., 2008).

As formulações colônicas são formas farmacêuticas de liberação retardada, as quais podem ser delineadas de modo a fornecer a completa liberação do fármaco ou permitir o prolongamento da liberação após o seu alcance no cólon (SINGH, 2007). Um sistema de liberação colônico ideal deve prevenir a liberação do fármaco durante a passagem da forma farmacêutica pelo estômago e intestino delgado, e consequentemente ser capaz de liberar o fármaco no cólon (ASGHAR & CHANDRAN, 2006). As estratégias para o desenvolvimento de formas farmacêuticas de liberação colônica baseiam-se em algumas propriedades do trato gastrointestinal e podem ser classificados em: (1) sistemas tempo-dependentes; (2) sistemas pH-dependentes (ou de liberação retardada); (3) sistemas microflora-dependentes e

(4) sistemas pressão luminal-dependentes (FRIEND, 2005; FERRARI et al., 2013).

2.1 Sistemas tempo-dependentes

Os sistemas tempo-dependentes utilizam o tempo compreendido entre a administração da forma farmacêutica por via oral e sua chegada à região colônica. Estes sistemas são úteis para a liberação de fármacos tanto em um tempo pré-determinado, de maneira que o paciente receba o fármaco quando se faz necessário, quanto em um sítio pré-selecionado do trato gastrointestinal. Por estas razões, estes sistemas são úteis no tratamento de patologias às quais dependem do ritmo circadiano (PRASANTH, JAYAPRAKASH, MATHEW, 2012). Nestes sistemas, o sítio de liberação do fármaco é determinado pelo tempo de trânsito da forma farmacêutica ao longo do trato gastrointestinal, o que torna o desenvolvimento um desafio para a obtenção de uma liberação precisa no cólon. De maneira geral, estes sistemas são desenvolvidos de forma que o sítio de liberação não seja afetado pelas diferenças individuais no tempo de esvaziamento gástrico, pH do estômago e intestino delgado ou a presença de bactérias anaeróbicas no cólon. Em média, uma forma farmacêutica administrada por via oral leva cerca de 3 horas para percorrer toda a extensão do intestino delgado até o início do cólon. Em comparação com o tempo de esvaziamento gástrico, o tempo de trânsito no intestino delgado é relativamente constante, sendo assim, os sistemas de liberação de fármacos tempo-dependentes são desenvolvidos baseando-se nesta característica (SINGH, 2007).

2.2 Sistemas pH-dependentes

Os sistemas pH-dependentes são os mais comumente empregados no delineamento de formas farmacêuticas de liberação colônica. Estes sistemas levam em consideração o aumento gradativo do pH a partir do estômago (pH 1 – 2,

podendo alcançar pH 4 durante o período de digestão) para o duodeno (pH 6,6 ± 0,5). No ceco ocorre um decréscimo (pH 6,4 ± 0,4) e então um pequeno aumento do cólon direito para o esquerdo com um valor final de pH de 7,0 ± 0,7 (FREIRE et al., 2006; SINGH, 2007). Para que liberação colônica ocorra de maneira efetiva é necessário que a forma farmacêutica seja revestida com um polímero pH-sensível. Os polímeros utilizados para esta finalidade devem ser capazes de resistir aos baixos valores de pH do estômago e da porção proximal do intestino delgado e ao mesmo tempo serem capazes de se desintegrar em pH neutro a ligeiramente alcalino do íleo terminal e preferencialmente na junção íleo-cecal. Estes processos distribuem o fármaco ao longo do intestino grosso e aumentam o potencial para uma liberação colônica efetiva (CHOURASIA & JAIN, 2003).

Os polímeros pH-sensíveis mais comumente utilizados são os derivados do ácido acrílico, comercialmente conhecidos como Eudragits®. Mais especificamente o Eudragit® S100 (Figura 1), um copolímero do ácido metacrílico e metil metacrilato com razão entre grupamentos carboxílicos e grupamentos éster de aproximadamente 1:2, tem sido amplamente utilizado para liberação colônica. Além deste polímero se dissolver em pH acima de 7,0, ele é solúvel em água, evitando assim o uso de solventes orgânicos durante o processo de revestimento (PARK et al., 2010).

Figura 1. Estrutura química da unidade monomérica do Eudragit® S100.

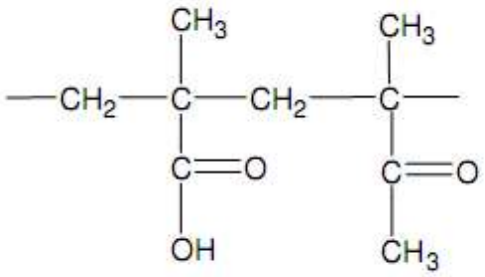

Fonte: www.evonik.com.br

2.3 Sistemas microflora-dependentes

Os sistemas microflora-dependentes exploram a atividade enzimática específica da microflora presente no cólon. As bactérias colônicas são predominantemente de natureza anaeróbica e secretam enzimas que são capazes de metabolizar substratos como carboidratos e proteínas que escapam da digestão pelo trato gastrointestinal superior (SINHA et al., 2004). O cólon possui uma alta contagem bacteriana de cerca de 10^{11} – 10^{12} UFC/mL de conteúdo intestinal, sendo composta por 400 espécies diferentes como *Bacteroides*, *Bifidobacterium*, *Eubacterium, Clostridia, Enterococci, Enterobacteria* etc. Esta vasta microflora obtém energia através da degradação de vários substratos que não são capazes de serem digeridos pelo intestino delgado, como os polissacarídeos. Para que o processo de degradação ocorra, a microflora colônica produz um vasto número de enzimas como a L-arabinofuranosidase, α-D-fucosidase, β-D-galactosidase, β-D-glucosidase e β-D-xilosidase, sendo as três últimas mais ativas no processo de degradação de polissacarídeos (YANG, CHU, FIX, 2002).

Devido ao fato destas enzimas estarem presentes somente no cólon, o uso de polissacarídeos no

desenvolvimento de sistemas de liberação colônica de fármacos é uma estratégia considerada mais específica em comparação com as demais abordagens. Assim que alcançam o cólon, os polissacarídeos podem sofrer endocitose pelos microrganismos, degradação pelas enzimas colônicas ou clivagem da sua estrutura polimérica, levando a uma redução da sua massa molar e consequente perda de força mecânica, tornando-se incapaz de manter a interação com o fármaco (PHILIP & PHILIP, 2010).

2.4 Sistemas pressão luminal-dependentes

Os processos digestivos ao longo do trato gastrointestinal envolvem atividades contráteis do estômago e movimentos peristálticos para a propulsão do conteúdo intestinal. No intestino grosso, o conteúdo é movido de uma porção para a próxima, do cólon ascendente para o transverso, por movimentos peristálticos potentes. Estas fortes ondas peristálticas são de curta duração no cólon, ocorrendo apenas 3 a 4 vezes por dia. Entretanto, estes movimentos aumentam temporariamente a pressão luminal no cólon, formando as bases para o desenvolvimento dos sistemas pressão-luminal dependentes. A pressão luminal resultante do movimento peristáltico é maior no cólon em comparação com a pressão no intestino delgado, a qual é atribuída à diferença de viscosidade do conteúdo luminal. No estômago e intestino delgado os conteúdos são fluidos devido à quantidade abundante de água e sucos digestivos, porém no cólon a viscosidade do conteúdo intestinal é significativamente maior devido à reabsorção de água do lúmen e formação das fezes (PRASANTH, JAYAPRAKASH, MATHEW, 2012).

3. NANOPARTÍCULAS

As nanopartículas são definidas como dispersões particuladas ou partículas sólidas com tamanhos entre 10 – 1000nm as quais são capazes de dissolver, encapsular ou

adsorver fármacos na sua estrutura (MOHANRAJ & CHEN, 2006). Dependendo do método de preparo, composição e organização estrutural, as nanopartículas podem ser classificadas em nanocápsulas e nanoesferas. As nanocápsulas são sistemas vesiculares nos quais o fármaco encontra-se confinado em uma cavidade aquosa ou oleosa, podendo o fármaco estar dissolvido no núcleo ou adsorvido à parede polimérica. As nanoesferas, por sua vez, são sistemas matriciais nos quais o fármaco encontra-se disperso na matriz (SOPPIMATH et al., 2001; SCHAFFAZICK et al., 2003). Nas últimas décadas, o desenvolvimento de nanopartículas tem recebido grande atenção como sistemas de liberação de fármacos devido às suas inúmeras vantagens como: (1) a capacidade de liberar o fármaco diretamente no sítio de ação, aumentando o benefício terapêutico e minimizando os efeitos adversos; (2) o tamanho subcelular destes carreadores de fármaco permite uma maior fagocitose intracelular em comparação a outros sistemas de liberação; (3) a proteção do fármaco frente à degradação em condições fisiológicas e (4) são compatíveis com tecidos e células quando sintetizados a partir de materiais biocompatíveis e biodegradáveis. De acordo com a composição, as nanopartículas podem ser classificadas em lipídicas e poliméricas, sendo estas últimas formadas por polímeros naturais ou sintéticos (MORA-HUERTAS, FESSI, ELAISSARI, 2009).

As nanopartículas poliméricas são amplamente utilizadas para o desenvolvimento de sistemas de liberação de fármacos que possuem problemas de solubilidade, permeabilidade e estabilidade. Uma importante característica das nanopartículas poliméricas reside na sua capacidade de controlar a liberação, sendo de grande interesse para a obtenção de uma liberação sustentada do fármaco incorporado (KUMARI, YADAV, YADAV, 2010; MEI et al., 2013). A escolha do polímero deve preencher alguns requisitos como ser biodegradável ou pelo menos ser totalmente eliminado do organismo em um curto período de tempo, permitindo a administração repetida sem qualquer risco de acúmulo; ser

atóxico e não imunogênico, assim como seus produtos de degradação, e deve ser processado em condições tais que resultem em nanopartículas com características de liberação que atendam os objetivos para os quais foram tencionadas (VAUTHIER & BOUCHEMAL, 2009).

No que diz respeito ao câncer, a administração de nanopartículas tem demonstrado um potencial terapêutico significante, pois aumentam a seletividade do fármaco em relação às células tumorais, reduzindo assim a toxicidade nos tecidos sadios (BRIGGER, DUBERNET, COUVREUR, 2002). De maneira geral, a liberação de fármacos nos tecidos tumorais a partir de nanopartículas pode ser alcançada por vetorização ativa ou passiva. A vetorização passiva faz uso do tamanho inerente das nanopartículas e explora as anormalidades anatômicas e fisiopatológicas da vasculatura dos tumores, como o efeito de permeação e retenção aumentadas (efeito EPR). Esta estratégia é capaz de efetivamente aumentar a biodisponibilidade e eficácia do fármaco administrado. Os tumores sólidos de rápido crescimento sofrem com o inadequado suprimento de nutrientes e oxigênio. Para contornar esta situação uma extensa angiogênese ocorre, resultando em uma alta densidade vascular. Porém, a formação de novos vasos sanguíneos nos tumores ocorre de maneira caótica, gerando uma arquitetura vascular defeituosa com grandes fendas nas junções entre as células epiteliais, o que leva a uma hiperpermeabilidade. As anormalidades dos vasos sanguíneos dos tumores incluem a alta proliferação de células epiteliais, tortuosidade aumentada, deficiência de pericitos (células mesenquimais responsáveis pelo suporte dos vasos sanguíneos pequenos) e formação anômala de membranas (Figura 2). Além disso, a maioria dos tumores sólidos possuem altos níveis de fatores de permeabilidade como a bradicinina, óxido nítrico e peroxinitrito. A produção acentuada destes mediadores de permeabilidade aumenta a permeabilidade dos tecidos tumorais em relação aos tecidos sadios, contribuindo também para o efeito EPR (DANHIER,

FERON, PREÁT, 2010; ACHARYA & SAHOO, 2011). Esta natureza única dos vasos sanguíneos dos tumores facilita a vetorização passiva de macromoléculas ou nanopartículas. Ainda, os tumores são caracterizados por possuírem uma drenagem linfática disfuncional, o que auxilia na retenção das nanopartículas nos tumores. Desta maneira, as nanopartículas são capazes de extravasar dos vasos sanguíneos e acumulam-se nos tecidos tumorais, permanecendo retidas por tempo suficiente para sua desintegração e liberação do fármaco nas adjacências do tumor (BRANNON-PEPPAS & BLANCHETTE, 2004; WANG & THANAU, 2010; FANG, NAKAMURA, MAEDA, 2011).

Figura 2. Diferenças entre tecidos normais e tecidos tumorais que explicam a vetorização passiva das nanopartículas pelo efeito de permeação e retenção aumentadas. (A) Tecidos normais apresentam vasos sanguíneos lineares mantidos pelos pericitos; presença de fibras de colágeno, fibroblastos e macrófagos na matriz extracelular; presença de vasos linfáticos. (B) Tecidos tumorais apresentam vasos sanguíneos defeituosos com cavidades e fenestrações; matriz extracelular contém mais fibras de colágeno, fibroblastos e macrófagos que os tecidos normais; ausência de vasos linfáticos.

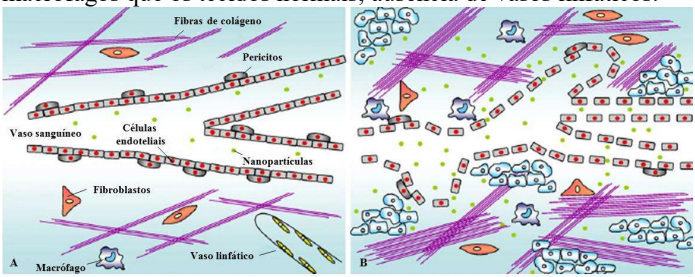

Fonte: Adaptado de Danhier, Feron, Préat (2010)

3.1 Nanopartículas de quitosana

3.1.1 Quitosana

Uma vasta gama de materiais tem sido empregada como carreadores de fármacos, dentre eles, os polissacarídeos têm recebido uma maior atenção devido a suas excelentes propriedades físico-químicas e biológicas (LIU et al., 2008). A quitosana é um héteropolímero constituído de unidades de N-acetil-2-amino-2-deoxi-D-glucopiranose e 2-amino-2-deoxi-D-glucopiranose unidas por ligações glicosídicas β-(1→4) (Figura 3). Este polímero é obtido pela desacetilação termoquímica da quitina, um polímero natural encontrado no exoesqueleto de crustáceos como camarões, lagostas e caranguejos, insetos e alguns fungos, na presença de álcalis (DASH et al., 2011). A diferença entre a quitosana e a quitina está no grau de desacetilação, o qual é definido como a razão molar de 2-amino-2-deoxi-D-glucopiranose (unidades deacetiladas) e indica o número de grupamentos amina ao longo da cadeia. Neste contexto, o termo quitosana corresponde a um grande grupo de quitinas contendo pelo menos 60% de resíduos de D-glucosamina (KUMAR et al., 2004; CROISIER & JÉRÔME, 2013; BALAN & VERESTIUC, 2014).

Figura 3. Estrutura química da unidade monomérica da quitosana.

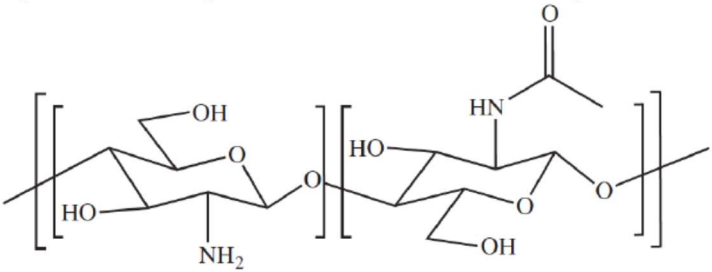

Fonte: Croisier & Jérôme (2013).

A quitosana é uma base fraca com valor de pK_a para o resíduo de D-glucosamina de cerca de 6,2 – 7,0 e, desta maneira, é insolúvel em pH neutro e alcalino. A solubilização da quitosana ocorre em soluções de ácidos diluídos devido a quartenização dos grupamentos amina. Em valores de pH superiores a 6,0 as aminas da quitosana são desprotonadas e o polímero torna-se insolúvel (HEZAJI & AMIJI, 2003; RINAUDO, 2006). Do ponto de vista químico, a quitosana é um polieletrólito catiônico (em meio ácido) com uma estrutura única, devido à presença de uma amina primária na posição C2 dos resíduos de glucosamina. Poucos polímeros biológicos possuem esta grande quantidade de aminas primárias. Estas aminas conferem propriedades funcionais importantes à quitosana que podem ser exploradas para aplicações farmacêuticas e biomédicas (NAGPAL, SINGH, MISHRA, 2010). Além disso, a quitosana possui uma abundante disponibilidade, mucoadesividade única, propriedades farmacológicas inerentes e outras propriedades biológicas benéficas como biocompatibilidade, biodegradabilidade, baixa toxicidade e imunogenicidade (AGRAWAL, STRIJKERS, NICOLAY, 2010; PARK et al., 2010; BALAN & VERESTIUC, 2014).

As propriedades mucoadesivas da quitosana são conferidas pela sua estrutura química catiônica que possui capacidade de interagir eletrostaticamente com as subestruturas aniônicas presentes no muco na forma de ácido siálico e ácido sulfônico. Além da alta densidade de cargas positivas, as propriedades mucoadesivas da quitosana podem ser atribuídas à presença de grupamentos com forte habilidade em formar ligações de hidrogênio como os grupos hidroxila e carboxila, alta massa molar, flexibilidade de cadeia e propriedades de energia de superfície que favorecem a sua difusão no muco. Desta maneira, sugere-se que a mucoadesividade apresentada pela quitosana seja capaz de prolongar o tempo de residência da forma farmacêutica no cólon (SINHA et al., 2004; GEORGE & ABRAHAM, 2006; BERNKOP-SCHNÜRCH & DÜNNHAUPT, 2012).

A quitosana é degradada *in vivo* por uma série de proteases e principalmente pela lisozima. Existem oito quitinases humanas identificadas e três delas possuem atividade enzimática em relação à quitosana. A biodegradação da quitosana leva à formação de oligossacarídeos atóxicos de comprimentos variados que são incorporados em vias metabólicas ou excretados. A taxa de degradação da quitosana é relacionada principalmente com o seu grau de deacetilação, porém a distribuição dos resíduos de N-acetil-D-glucosamina e a massa molar também afetam a taxa de degradação (CROISIER & JÉRÔME, 2013).

Além disso, sabe-se que as enzimas colônicas produzidas por bactérias anaeróbicas, principalmente *Bacteroides* e *Bifidobaterias*, são responsáveis pela hidrólise de dissacarídeos, oligossacarídeos e polissacarídeos. Os polissacarídeos não são digeridos no TGI superior, porém são degradados pelas suas polissacaridases correspondentes produzidas pelas bactérias existentes no cólon. Sendo assim, a degradação colônica da quitosana torna-se uma das mais importantes propriedades para a sua utilização na liberação colônica de fármacos (TOZAKI et al., 1997; ZHANG et al., 2002; ZHANG & NEAU, 2002).

3.1.2 Obtenção de nanopartículas de quitosana pelo método de interação iônica

Os diferentes métodos de preparo de nanopartículas permitem obter sistemas com propriedades adequadas para garantir a liberação apropriada do fármaco. A seleção do método depende de fatores como o tamanho de partícula desejado, a estabilidade térmica e química do fármaco, a reprodutibilidade dos perfis de liberação, a estabilidade e a toxicidade residual associada ao produto final (AGNIHOTRI, MALLIKARJUNA, AMINABHAVI, 2004).

A obtenção de nanopartículas pelo método de interação iônica tem recebido grande atenção nos últimos anos, pois é considerado um método simples e fácil de ser

realizado. Outras vantagens deste método incluem a proteção do fármaco devido à ausência de estresse físico e químico durante a fabricação, baixa toxicidade, uso de pouca energia e é adequado para a transposição de escala (AMIDI et al., 2010). A formação das nanopartículas envolve a mistura de soluções de polieletrólitos de cargas opostas, o que resulta numa associação espontânea devido à formação de ligações eletrostáticas fortes, porém reversíveis. A formação e estabilidade destas ligações eletrostáticas dependem de diversos fatores como o grau de ionização de cada polieletrólito, densidade das cargas, distribuição das cargas ao longo da cadeia polimérica, concentração dos polieletrólitos, razão da mistura, ordem da mistura, posição dos grupos iônicos nas cadeias poliméricas, massa molar dos polieletrólitos, flexibilidade das cadeias dos polímeros e também a temperatura, força iônica e pH do meio de reação (HAMMAM, 2010).

O policátion mais comumente empregado para esta finalidade é a quitosana, pois esta molécula possui grupamentos catiônicos capazes de interagir com uma série de poliânions, dentre eles o tripolifosfato (Figura 4). A formação de nanopartículas via interação iônica pode ser dividida em dois processos: (1) a mistura das soluções de polieletrólitos e a dispersão dos ânions do tripolifosfato dentro das moléculas de quitosana e (2) a interação entre grupamentos catiônicos da quitosana e aniônicos do tripolifosfato. Estes dois processos ocorrem inicialmente em sequência, porém, subsequentemente em paralelo visto que a complexação é quase instantânea e começa enquanto a mistura ainda está ocorrendo (DONG et al., 2013; FÀBREGAS et al., 2013).

Figura 4. Representação esquemática da interação entre quitosana e tripolifosfato para a obtenção de nanopartículas.

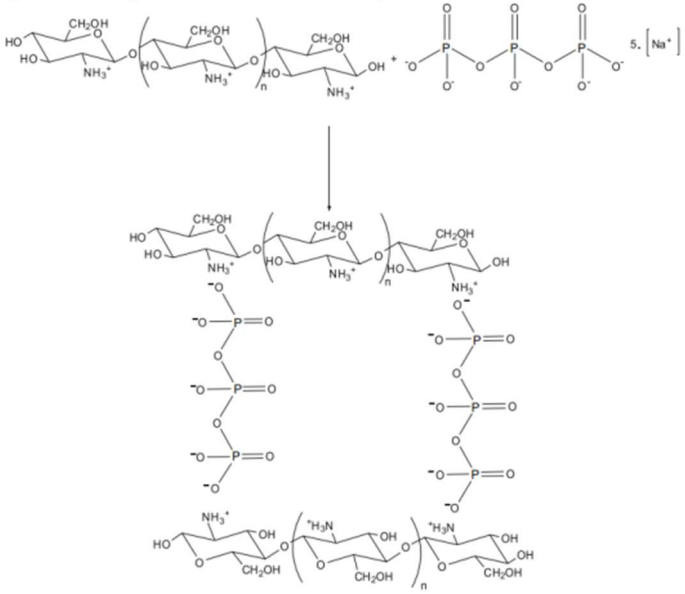

Fonte: Coelho et al. (2010)

Diversos estudos demonstram o emprego da quitosana na obtenção de nanopartículas pela técnica de interação iônica para a associação de fármacos tanto hidrofílicos quanto hidrofóbicos. Ji e colaboradores (2011) desenvolveram nanopartículas de quitosana/tripolifosfato encapsulando gentamicina e ácido salicílico. Diferentes valores de eficiência de encapsulação e teor dos fármacos foram obtidos variando a proporção entre quitosana e tripolifosfato, proporção entre fármacos e polímero, proporção entre gentamicina e ácido salicílico e o pH da solução de quitosana. As nanopartículas obtidas apresentaram teor de 24,67 ± 2,06 % para a gentamicina e de 26,64 ± 3,92 % para o ácido salicílico, eficiência de encapsulação entre

59,45 ± 3,02 % e 87,20 ± 3,09 %, diâmetro médio entre 148 ± 8,6 e 345 ± 12,9 nm e potencial zeta superiores à +30mV.

Hafner e colaboradores (2009) sintetizaram nanopartículas constituídas de quitosana/lecitina para a encapsulação da melatonina. O diâmetro, potencial zeta e teor de melatonina nas nanopartículas foram avaliados em relação ao tipo de lecitina utilizada (Lipoid S45, S75 e S100) e proporções de lecitina/quitosana de 5:1, 10:1 e 20:1. O tamanho e o potencial zeta aumentaram com o aumento da concentração de quitosana e da carga negativa das lecitinas utilizadas nas formulações, respectivamente. As nanopartículas de lecitina/quitosana apresentaram tamanhos entre 121,6 ± 2,8 e 347,5 ± 3,2 nm. A eficiência de encapsulação das nanopartículas variaram de 26 a 38,2 % e o teor de 4,9 a 7,1 %. Sonvico e colaboradores (2006) também desenvolveram nanopartículas de quitosana/lecitina utilizando diferentes tipos de quitosana e a lecitina S45 (Lipoid S45) para a encapsulação da progesterona. O diâmetro o potencial zeta das nanopartículas foram avaliados em função da proporção entre lecitina/quitosana (de 5:1 até 80:1), viscosidade da solução de quitosana e pH da suspensão coloidal. Foram obtidas nanopartículas com diâmetros inferiores a 280nm, índice de polidispersão abaixo de 0,2 e potencial zeta de +40mV. A eficiência de encapsulação e o teor de fármaco foram avaliados através da adição de concentrações crescentes de progesterona (2, 5, 10, 13, 15 e 20 mg/mL) nas formulações. Nas concentrações de 2, 5 e 10 mg/mL a eficiência de encapsulação foi maximizada (cerca de 60 %) com teor de fármaco de cerca de 3,5%.

4. SINVASTATINA

A sinvastatina (Figura 5) é um fármaco semi-sintético obtido a partir da adição de um grupamento metila à molécula de lovastatina, uma estatina natural obtida através da fermentação do *Aspergillus terréus* (WONG et al., 2002). Apresenta-se como um pó cristalino branco praticamente

insolúvel em água (0,03 mg/mL; log P = 4,68) e facilmente solúvel em clorofórmio, dimetilsulfóxido, metanol e etanol (AMBIKE, MAHADIK, PARADKA, 2005; OLIVEIRA et al., 2010). Bioquimicamente, a sinvastatina atua diretamente na via do mevalonato também conhecida como via da biossíntese do colesterol. A via do mevalonato inicia com a conversão enzimática da acetoacetil-CoA em 3-hidroxi-3-metilglutaril-CoA (HMG-CoA) catalisada pela HMG-CoA sintase. A HMG-CoA é então convertida em mevalonato numa reação catalisada pela HMG-CoA redutase, seguida de uma série de reações bioquímicas que levam a síntese de colesterol (GAUTHAMAN, FONG, BONGSO, 2009; CORCOS & JOSSIC-CORCOS, 2013).

Figura 5. Estrutura química da sinvastatina.

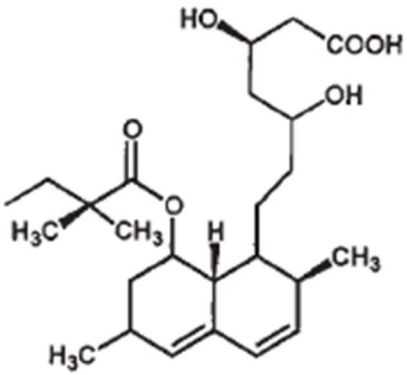

Fonte: Wong et al. (2002)

A sinvastatina é um inibidor competitivo efetivo da 3-hidroxi-3-metil-glutaril coenzima A redutase (HMG-CoA redutase) e possui aproximadamente 1.000 vezes mais afinidade pelo sítio ativo da enzima do que o seu substrato natural. A inibição da HMG-CoA redutase promove a redução da síntese de colesterol através da prevenção da conversão da 3-hidroxi-3-metil-glutaril coenzima A (HMG-

CoA) em mevalonato, um intermediário limitante na via da biossíntese de colesterol no corpo humano (WONG et al., 2002). Desta maneira, a sinvastatina é extensivamente utilizada na terapêutica para o tratamento da hipercolesterolemia. O colesterol é um importante componente estrutural das membranas celulares e a necessidade fisiológica diária do organismo é alcançada através da síntese endógena ou do suprimento exógeno. Níveis aumentados de colesterol levam a aterosclerose e ao estreitamento dos vasos sanguíneos, o que pode afetar o fornecimento de sangue para o coração, cérebro e circulação periférica levando a morbidade ou mortalidade (GAUTHAMAN, FONG, BONGSO, 2009).

Além do seu efeito redutor dos níveis de colesterol, evidências sugerem que a sinvastatina possui efeitos terapêuticos contra o câncer devido à sua interação com uma série de funções celulares essenciais (HINDLER et al., 2006; CHO et al., 2008; CHANG et al., 2013). A inibição da via do mevalonato inibe a síntese de moléculas importantes como os isoprenóides farnesil pirofosfato e geranil pirofosfato (Figura 6). Estes isoprenóides são responsáveis pela isoprenilação de várias proteínas celulares sinalizadoras, incluindo as pequenas GTPases das famílias Ras, RhoA e Rac. Estas proteínas possuem funções fisiológicas potencialmente envolvidas na carcinogênese, pois estão ligadas aos processos de crescimento celular, proliferação celular, migração celular e estresse oxidativo (BARDOU, BARKUN, MARTEL, 2014; PISANTI et al., 2014). O processo de isoprenilação permite que estas proteínas sejam corretamente ancoradas às membranas celulares e possam desempenhar suas atividades enzimáticas normais. A restrição da atividade da via do mevalonato pela interrupção das reações iniciais promovida pela sinvastatina resulta na deficiência de farnesil pirofosfato e geranilgeranil pirofosfato, impedindo que as GTPases obtenham suas atividades funcionais normais (BROWN, 2007; ACQUAVELLA et al., 2010; ALI et al., 2010).

Figura 6. Esquema simplificado da via do mevalonato. As enzimas iniciais estão demonstradas em verde e os metabólitos preniladores (farnesil pirofosfato e geranilgeranil pirofosfato) e as proteínas alvo estão demonstrados em azul.

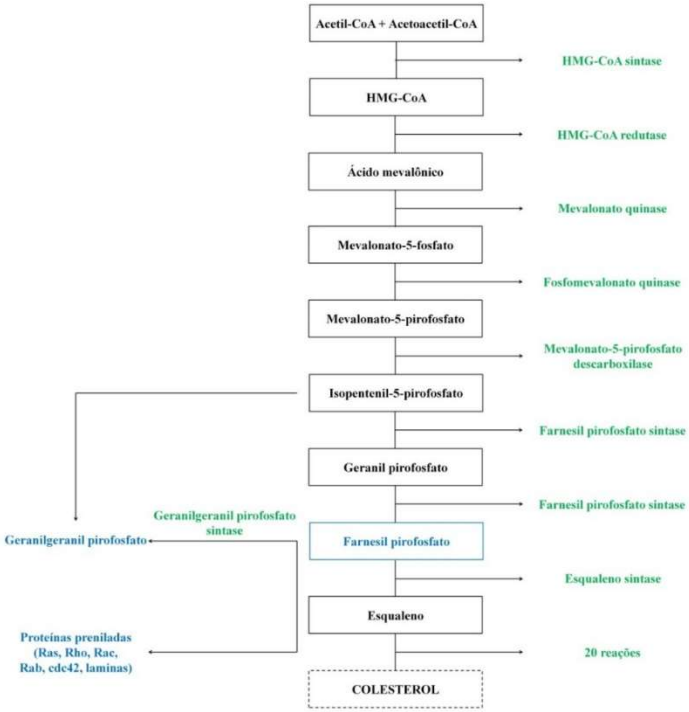

Fonte: Adaptado de Corcos & Jossic-Corcos (2013)

Diversos estudos demonstram os efeitos antitumorais da sinvastatina em vários tipos de câncer. Galopan e colaboradores (2013) demonstraram que a sinvastatina induz a apoptose em células de câncer de mama humano através da ativação da via pró-apoptótica DR5 de maneira dependente das proteínas quinases JNK e CHOP. Os resultados sugerem que o mevalonato e o geranilgeranil pirofosfato são

marcadores moleculares nas células de câncer de mama e a superexpressão de JNK/CHOP/DR5 são biomarcadores em potencial para o monitoramento da resposta ao tratamento com sinvastatina. Yu e colaboradores (2013) avaliaram a atividade antitumoral e quimiopreventiva da sinvastatina na linhagem celular A549 de câncer de pulmão. A sinvastatina inibiu o crescimento das células A549 de maneira dose dependente, promoveu um decréscimo na expressão da proteína Bcl-2 e aumentou a expressão da proteína Bax de maneira tempo e dose dependente. Além disso, a sinvastatina bloqueou a fase G_1 de crescimento celular, suprimiu a expressão da ciclina D1 e das proteínas CDKs, mediada pelo aumento da expressão das caspases 3, 8 e 9, levando as células à apoptose, e também diminuiu os níveis da metalopeptidase MMP-9, possivelmente através da inibição do NF-κB. Estes resultados demonstraram que a sinvastatina possui um efeito antitumoral em células A549 de câncer de pulmão através da inibição da proliferação celular, da influência no ciclo celular e indução da apoptose.

Os efeitos antitumorais da sinvastatina em diferentes linhagens celulares de câncer colorretal também tem sido estudados. CHO e colaboradores (2008) avaliaram o efeito da sinvastatina nas vias de apoptose relacionadas à sinalização do fator de transcrição nuclear ƙB (NF- ƙB) e os efeitos antitumorais em modelo animal. As linhagens celulares COLO205 e HCT116 foram tratadas com sinvastatina e a apoptose determinada através da análise do ciclo celular, coloração anexina V – FITC, atividade das caspase-3 e microscopia confocal. A expressão dos fatores anti-apoptóticos foi avaliada por técnicas de biologia molecular. No modelo *in vivo* de câncer colônico associado à colite ulcerativa, os tumores foram induzidos nos camundongos C57/BL6 através da administração de azoximetano e dextrana sulfato de sódio. O efeito da sinvastatina foi avaliado em relação ao crescimento do tumor. Em ambas as linhagens celulares a sinvastatina causou morte celular de maneira dose e tempo dependente, através do aumento da atividade da

capase-3 e supressão da expressão de proteínas anti-apoptóticas como Bcl-2, Bcl-xL, cIAP1 e cFLIP. No modelo *in vivo*, a sinvastatina reduziu significativamente o desenvolvimento do tumor. Os tumores apresentaram volumes reduzidos, maiores áreas necróticas, menor expressão do fator de crescimento endotelial vascular (VEGF) e altos escores apoptóticos. Como conclusão, este estudo demonstrou que a sinvastatina inibe o desenvolvimento do câncer de cólon através da indução da apoptose e da supressão da angiogênse *in vitro* e *in vivo*.

QI e colaboradores (2010) avaliaram o papel do estresse oxidativo na citotoxicidade da sinvastatina em células CT26 de carcinoma de cólon murino. Este estudo demonstrou que a exposição das células à sinvastatina interrompe o sistema de defesa antioxidante, gerando espécies reativas de oxigênio intracelular e promovendo a apoptose das células CT26. Além do mais, o aumento do estresse oxidativo e da morte celular foi suprimido pelos isoprenóides mevalolactona, farnesil pirofosfato, geranilgeranil pirofosfato, coenzima Q10 e antioxidantes como N-acetil cisteína, glutationa, superóxido desmutase e catalase.

CHANG e colaboradores (2013) avaliaram a indução da apoptose das células HCT116 de câncer colorretal humano pela sinvastatina através da cascata de sinalização da p38MAPK-p53-survivina. Elevados níveis de survivina, uma proteína inibidora da apoptose, são encontrados em diversos tumores humanos e esta proteína tem sido relacionada com a progressão da tumorigênese. Devido ao seu papel central na divisão celular e na atividade de supressão da apoptose, a survivina representa um potencial alvo molecular no manejo do câncer. Os resultados deste estudo demonstraram que a sinvastatina ativa o gene supressor de tumor p53, inibe a expressão de survivina e subsequentemente promove a apoptose das células HCT116 através da cascata de sinalização da proteína quinase ativada por mitógeno p38. Desta maneira, estes estudos sugerem que a sinvastatina pode

ser um potencial agente terapêutico no tratamento do câncer colorretal.

CAPÍTULO 1

A liberação colônica de fármacos após administração oral tem sido considerada uma estratégia promissora para o tratamento de diversas patologias locais, incluindo o câncer colorretal (CHOURASIA & JAIN, 2003). A sinvastatina é um fármaco inibidor competitivo da HMG-CoA reductase, enzima responsável pela conversão da HMG-CoA em mevalonato, o precursor do colesterol. Desta maneira, a sinvastatina é amplamente utilizada na terapêutica como um agente redutor dos níveis séricos de colesterol e redutor da progressão da aterosclerose (TIWARI & PATHAK, 2011). Entretanto, diversos estudos demonstram que a sinvastatina exerce uma série de outras atividades como anti-inflamatória, imunomodulatória e antitumoral (WANG et al., 2008).

Na primeira parte deste capítulo, foi realizado um estudo de formulação com o objetivo de aumentar a encapsulação da sinvastatina em nanopartículas de quitosana/tripolifosfato através da adição de diferentes concentrações de taurocolato de sódio, usando a técnica de interação iônica. A influência da concentração do taurocolato de sódio empregada na preparação das nanopartículas sobre as propriedades físico-químicas das partículas e sobre a capacidade de incorporar a sinvastatina foi avaliada. Em seguida, com o objetivo de proteger o fármaco durante a passagem da forma farmacêutica pelo trato gastrointestinal superior, as nanopartículas de quitosana foram encapsuladas em micropartículas entéricas de Eudragit® S100 pela técnica de interação iônica e os sistemas foram submetidos à secagem por aspersão. Diferentes proporções de nanopartículas/Eudragit® S100 foram testadas e os perfis de liberação da sinvastatina a partir das micropartículas foi avaliado em diferentes valores de pH. As nanopartículas e as micropartículas entéricas foram caracterizadas por diversas técnicas como espalhamento de luz dinâmico, microscopia eletrônica de transmissão, microscopia eletrônica de varredura, calorimetria exploratória diferencial, espectroscopia de infravermelho e difração de raios-x.

Diversos estudos *in vitro* demonstram que a sinvastatina apresenta atividade antitumoral em diferentes linhagens celulares de adenocarcinoma de cólon humano (COLO 205 e HCT 116) e de carcinoma de cólon murino (CT26) (CHO et al., 2008; QI et al., 2010; CHANG et al., 2013). Sendo assim, na segunda parte deste capítulo é descrita a avaliação antitumoral *in vitro* das nanopartículas de quitosana contendo sinvastatina em células de adenocarcinoma de cólon humano (HT-29).

Publicação 1. *Spray-Dried Enteric Microparticles Entrapping Chitosan Nanoparticles for Colonic Delivery of Simvastatin for the Treatment of the Colorectal Carcinoma*

Spray-Dried Enteric Microparticles Entrapping Chitosan Nanoparticles for Colonic Delivery of Simvastatin for the Treatment of the Colorectal Carcinoma

MARIANA DALAGNOL, ELENARA LEMOS-SENNA*
Pharmaceutical Technology Laboratory, Pharmaceutical Sciences Department, Federal University of Santa Catarina, Campus Universitário, Florianópolis, 88040-970, Brazil.

*Corresponding author: +55 48 3721 5067, Email address: lemos.senna@ufsc.br

ABSTRACT

In this study, spray-dried enteric microparticles (SDP) entrapping simvastatin (SIM)-loaded chitosan nanoparticles (CSNP) were developed with the aim of delivering this drug in the colon for the treatment of the colorectal cancer. The addition of sodium taurocholate (STC) to the nanoparticles was tested as a new strategy to increase the SIM loading. CSNPs displayed mean diameters ranging from 317.2 to 443.7 nm and a positively-charged surface. The addition of STC allowed a 3.3-fold increase in the drug loading, probably due to the formation of a more hydrophobic particle structure. SDPs were prepared by adding Eudragit® S100 to the external phase of CSNP. The spray-drying technique yielded SDPs with spherical shape, diameters around 3 µm and negative zeta potential values. The interactions between the components of the formulations and crystallinity properties of the particles in both CSNP and SDP were assessed by DSC, FT-IR, and XRD techniques. The release studies demonstrated that a small fraction of the drug was released in acidic medium, but sustained drug release occurred over 8 h in phosphate buffer solution at pH 7.2. These results indicated that this innovative hybrid drug delivery system could be promisor to deliver SIM in the colon.

Keywords: Simvastatin; Chitosan; Nanoparticles; Sodium Taurocholate; Enteric Microparticles; Spray-drying; Colonic Drug Delivery.

INTRODUCTION

Simvastatin (SIM) is a lipophilic drug, which is obtained synthetically through the methylation of lovastatin, a natural statin obtained as a fermentation product of *Aspergillus terreus*. This drug is a potent inhibitor of the 3-hydroxy-3-methyl-glutaryl-coenzyme A (HMG-CoA) reductase, which catalyzes the conversion of HMG-CoA to mevalonate, a precursor of cholesterol. Similarly to other statins, SIM is prescribed to reduce the serum cholesterol levels and slow the progression of atherosclerosis.[1] However, several studies have demonstrated that, besides their lipid-lowering effect, statins exert pleiotropic actions, including anti-inflammatory, immunomodulatory, and antitumor effects.[2] In particular, epidemiological studies have shown reductions in cancer recurrence or cancer-specific mortality in statin users with breast, prostate, and colorectal cancer.[3,4] The antitumor properties of SIM in relation to colorectal cancer have been also demonstrated in several *in vitro* and *in vivo* studies. SIM was able to induce apoptosis in murine CT26 and in human COLO 205 and HCT 116 colon cancer cells.[5-7] In animal studies, SIM was able to reduce the tumor development in a murine colitis-associated colon cancer model induced by azoxymethane and dextran sulfate sodium and, in a xenograft model, tumors treated with SIM had smaller volumes, larger necrotic areas, lower expression of VEGF and higher apoptotic scores.[5] These results suggest, therefore, that the colonic delivery of SIM may be a useful approach for the treatment of the colorectal cancer.

The release of drugs directly in the colon after oral administration has been considered a promising approach to

treating colon diseases, since it provides a high local concentration of drug at the site of action, with reduced incidence of systemic side effects. Nonetheless, the major challenge in relation to obtaining successful colonic delivery is to prevent drug release in the stomach and the small intestine and allow the release only in the colon. As a general rule, colonic delivery systems can be developed by making use of some specific conditions in the gastrointestinal tract (GIT), such as the intraluminal pH changes along the GIT, the gastrointestinal transit, the presence of peristaltic movements, and the presence of enzymes in the colonic microflora. Then, colonic formulations can be classified into (*i*) pH-dependent (delayed-release) systems, (*ii*) time-dependent systems, (*iii*) microbially-dependent systems, and (*iv*) luminal pressure-dependent systems. In general, colonic drug delivery systems are developed using a combination of two or more of the above-mentioned physiological characteristics.[8-12]

Chitosan (CS) is a natural polysaccharide obtained by the partial deacetylation of chitin found in the exoskeleton of crustaceans, insects, and some fungi.[13] CS is a nontoxic, biodegradable and biocompatible polymer, which has been considered a promising material for developing colonic drug delivery systems. Among its advantages, bioadhesiveness of the chitosan particles has played an important role in the development of successful colonic drug delivery systems, with electrostatic interactions of the cationic chitosan with the negatively-charged mucin being considered the main factor associated with its strong mucosal adhesion, alongside minor contributions from hydrogen bonding and hydrophobic effects.[14] Besides its mucoadhesion properties, on reaching the colon chitosan undergoes degradation by enzymes or the breaking down of the polymer backbone, leading to a subsequent reduction in its molecular weight and thereby a loss of mechanical strength, which may contribute to the release of the encapsulated drug.[15] In addition, regarding the treatment of colon cancer, nanoparticles could reach the tumor passively through the leaky vasculature surrounding the

tumors through enhanced permeability and retention effect, releasing the drug directly at the site of action.[16,17]

On the other hand, to obtain particulate drug delivery systems, chitosan should be cross-linked to avoid its dissolution in the gastrointestinal (GI) fluids. In aqueous acidic solutions, CS becomes a polyelectrolyte due to the protonation of the $–NH_2$ groups, which are readily available for crosslinking with multivalent anions.[18,19] Among the various polyanions, tripolyphosphate (TPP) has been the most investigated in relation to obtaining CS nanoparticles, due to its quick-gelling capability and nontoxic property.[19,20] However, the nanoparticulate drug delivery systems produced from ionic gelation between CS and TPP are not appropriate for the loading of poorly water-soluble compounds. Conversely, recent studies have demonstrated that self-organized structures, resulting from the electrostatic interaction between chitosan and lecithin, were able to encapsulate hydrophobic drugs with high encapsulation efficiencies.[21-24] In our study, the addition of the anionic surfactant sodium taurocholate (STC) was proposed as a new strategy to increase the simvastatin loading in chitosan nanoparticles. Yet, in order to avoid the release of SIM in the upper GIT and the proximal portion of the small intestine, CS nanoparticles were microencapsulated into enteric microparticles. Then, in this study, we describe the development of spray-dried enteric microparticles containing chitosan nanoparticles as an innovative system to deliver simvastatin in the colon for the treatment of colorectal cancer.

MATERIALS AND METHODS

Materials

Simvastatin (SIM) was purchased from Pharma Nostra® (Rio de Janeiro, Brazil). Chitosan (CS) (MW 50-190 kDa; deacetylation degree between 75% and 85%; viscosity 20-300 cP) and sodium taurocholate (STC) were purchased

from Sigma-Aldrich (St. Louis, MO, USA). Sodium tripolyphosphate (TPP) was donated by Plury Química (São Paulo, Brazil). Poly(methacylic acid-co-methyl methacrylate) 1:2 (Eudragit® S100) was donated by Rohm Pharma (Germany). All other chemicals were of analytical grade.

Methods

Preparation of chitosan nanoparticles

The chitosan nanoparticles (CSNP) were prepared using the ionic gelation technique.[25] Briefly, 10 mL of an ethanol:water solution (40:60 v/v) containing SIM (10 mg), TPP (9.16 mg) and STC (20, 30, 40, 50, 60, 70 or 80 mg) was prepared. This hydroalcoholic solution was then slowly poured using a glass Pasteur pipette into 10 mL of a 0.55% (w/v) CS solution under magnetic stirring. The CS solution was previously prepared by dissolving CS in 1% (w/v) acetic acid. The resulting colloidal suspension was evaporated under reduced pressure to remove the organic solvent and adjust the final volume to 10 mL. The formulations were prepared in triplicate.

Physicochemical and morphology characterization of chitosan nanoparticles

The mean particle size and zeta potential of the CSNPs were determined by dynamic light scattering and laser Doppler anemometry, respectively, using a Zetasizer Nano Series (Malvern Instruments, UK). The nanoparticles were diluted in ultrapure water at appropriate concentrations. Size analysis was performed at a fixed scattering angle of 173º. For measurements of the zeta potential, samples were placed in an electrophoretical cell, where a potential of ±150 mV was established. The zeta potential values were calculated from mean electrophoretic mobility values using Smoluchowski´s equation. The morphology of the CSNPs was examined by

transmission electron microscopy (TEM) using a JEOL JEM-1011 microscope (Tokyo, Japan), with an acceleration voltage of 100 kV. The nanoparticles suspensions were dropped onto carbon-coated copper grids and visualized without staining.

Determination of simvastatin content and entrapment efficiency in nanoparticles

The SIM content and entrapment efficiency were determined by UV spectroscopy using a UV-1800 Shimadzu spectrophotometer at 237 nm. The analytical method was previously validated according to the ICH guideline.[26] The calibration curve for SIM in methanol was linear over the range of 4 to 16 μg/mL, with a correlation coefficient of 0.999. The detection and quantification limits were 0.238 μg/mL and 0.792 μg/mL, respectively, indicating that the method was sufficiently sensitive to determine the SIM content in the nanoparticles. The specificity of the method was confirmed after the analysis of unloaded nanoparticles. The precision of the method was evaluated and all relative standard deviation (RSD) values were below 2%, indicating an acceptable intra-day and inter-day variability of the SIM content. The recovery values ranged from 97% to 99%, satisfying the acceptance criteria for accuracy in this study.

The drug content was determined in the solutions obtained after complete dissolution of the nanoparticles in methanol and the results were expressed as μg of SIM per mL of CSNP suspensions. The entrapment efficiency (EE%) was estimated as the percent difference between the total concentration of SIM in the CSNP suspensions and the concentration found in the supernatant obtained after ultrafiltration/centrifugation of the nanosuspensions using Microcon Centrifugal Filter Devices with Ultracel YM-100 (100.000 NMWL, Millipore, USA). All analyses were carried out in triplicate.

Preparation of enteric spray-dried microparticles containing nanoparticles

Spray drying was performed using a Büchi 290 Mini Spray Drier (Büchi Labortechnik AG, Flawil, Switzerland). Drying conditions are given as follows for all samples prepared: the inlet air temperature was 120 °C, the outlet temperature was 65∼70°C, the pump flow rate was 5 mL/min, and the aspirator setting was 100%. Prior to the spray-drying procedure, 50 mL of a SIM-loaded CS nanoparticle suspension ($CSNP_{70}$) was added to 100 mL of an aqueous solution containing 2.88 g, 4.32 g or 5.76 g of Eudragit® S100 adjusted to pH 7.2 in order to obtain nanoparticle/Eudragit® S100 ratios of 1:4, 1:6 and 1:8 (w/w), respectively. The spray-dried powders (SDP) were collected and stored in tightly-sealed glass bottles until analysis. The yield (%) of the spray-drying process was estimated considering the theoretical amount of solid in the feed solutions.

Physicochemical characterization and morphology evaluation of spray-dried powders

The residual moisture content of the spray-dried powders was obtained using the Ohaus MB25 Halogen Moisture Analyser (Ohaus®, New Jersey, USA). Around 600 mg of the samples were weighted in aluminum dishes and heated until 105 °C by an integral halogen dryer allowing the moisture to vaporize. This temperature was held constant and the results were expressed as percent moisture content. All analyses were carried out in triplicate.

The morphology of the particles was examined using a Jeol JSM-6390LV (Jeol Inc., USA) scanning electron microscope, operated under high vacuum conditions with an acceleration voltage of 10 kV. The samples were mounted onto aluminum pin stubs using double-sided tape and sputter-coated with gold in a Leica EM SCD500 coater unit (Leica Microsystems, USA). The mean particle size of the samples

was determined after the analysis of SEM images using the SizeMeter® software. The Martin's diameter of 200 randomly selected particles was determined in a fixed direction from the field of view of the SEM images. The zeta potential of the particles was determined by laser Doppler anemometry using a Zetasizer Nano Series (Malvern Instruments, UK), as described above.

The SIM content in the spray-dried powders was determined by UV spectroscopy using a UV-1800 Shimadzu spectrophotometer at 237 nm after complete dissolution of the particles in methanol. The results were expressed as percent weight (wt%) of SIM in the spray-dried powders. All analyses were carried out in triplicate.

Differential Scanning Calorimetry (DSC)

The thermal behavior of the raw materials, freeze-dried CSNPs, and SDPs were obtained using a DSC-60 instrument (Shimadzu, Japan). For the measurements, approximately 2 mg of the samples were accurately weighted in aluminum pans, sealed, and heated from 30 to 300 ºC under nitrogen atmosphere, with a heating rate of 10 °C/min.

Fourier Transform Infrared Spectroscopy (FT-IR)

The FT-IR spectra were obtained using a PerkinElmer Frontier spectrophotometer (PerkinElmer®, Massachusetts, USA). The raw materials, freeze-dried CSNPs, and SDPs were recorded in the wavenumber ranging from 4000 to 650 cm^{-1}.

X-ray diffraction analysis (XRD)

The X-ray diffraction patterns of the raw materials, freeze-dried CSNPs, and SPDs were recorded on a Philips X'Pert X-ray diffractometer (Philips, Netherlands), using CuKα radiation at 40 kV and 40 mA. Measurements were

carried out at 2θ angles ranging from 5 to 45° with a step size of 5° and a scan step time of 5 s.

In vitro SIM release studies

The *in vitro* release of SIM from SDPs was assessed on an Erweka BioDis RRT 10 dissolution tester (Erweka®, Germany) using the United States Pharmacopoeia (USP) apparatus III (reciprocating cylinders). The dissolution conditions were established according to a modified European Pharmacopeia method: 1 h in 250 mL of hydrochloric acid solution at pH 1.2, 3 h in 250 mL of phosphate buffer solution at pH 4.5, and 8 h in 250 mL of phosphate buffer solution at pH 7.2.[27] The samples were accurately weighted (230 mg, 300 mg, and 280 mg for SDP prepared with nanoparticles/Eudragit® S100 ratios of 1:4, 1:6, and 1:8, respectively) and filled into transparent capsules which were placed in the dissolution station where the temperature was kept at 37 ± 0.5 °C. The dip speed was set at 20 cycles/min when dissolution was carried out in hydrochloric acid at pH 1.2 and phosphate buffer at pH 4.5, and at 8 cycles/min when the dissolution was carried out in phosphate buffer at pH 7.2. At specific intervals aliquots of the dissolution medium were withdrawn without replacement. The SIM released from the particles was according to previously described methdo. Curves for the cumulative amounts of SIM released (%) versus time (h) were plotted. The dissolution efficiency (DE%) was determined for each release profile, as the area under the release curve obtained for the different release media, expressed as a percentage of the area of the rectangle described by 100% dissolution within the same period of time. All of the experiments were carried out with six replicates. The results were statistically analyzed by ANOVA followed by the Tukey´s multiple comparisons test. In order to evaluate the redispersion ability of the chitosan nanoparticles during the SIM release studies, samples of spray-dried powders were dispersed in water adjusted to pH 7.2 and maintained under

magnetic stirring for 5 h. The samples were then appropriately diluted in ultrapure water and the particle size was determined by dynamic light scattering in a Zetasizer Nano Series (Malvern Instruments, UK), as described above.

RESULTS

Preparation and characterization of SIM-loaded chitosan nanoparticles

In this study, we firstly evaluated the effect of STC addition on the physicochemical properties of chitosan nanoparticles and on the simvastatin-loading capacity. SIM-loaded CS nanoparticles were prepared by ionic gelation, in which the CS to TPP ratio was maintained unchanged (6:1), while increasing amounts of STC were added to the formulations. The physicochemical properties and SIM loading obtained for the nanoparticle formulations are summarized in Table 1. By adding the TPP and STC solution, the initially clear CS solution spontaneously changed to an opalescent dispersion, indicating the formation of the nanoparticles.[28] The mean particle diameter ranged from 317.2 nm to 442.7 nm with polydispersity index (PDI) values ranging from 0.34 to 0.51. The nanoparticles exhibited a positively-charged surface with zeta potential values ranging from +40.0 mV to +47.27 mV, reflecting the predominance of the amino groups of CS at the surface of the particles.[28] A slight decrease in the zeta potential was verified with the addition of STC, but the concentrations tested were not high enough to neutralize the CS charge.

Table 1 clearly shows that the SIM content increased with the presence of STC in the nanoparticles. The nanoparticle suspension prepared without the addition of STC ($CSNP_0$) presented a drug content of only 66.91 μg/mL, whereas nanoparticles prepared with the addition of 70 mg of STC ($CSNP_{70}$) reached a maximum drug content of 225.14 μg/mL, that is, an approximately 3.3-fold increase. The

encapsulation efficiency values were above 91%, indicating that SIM is found preferentially associated to the nanoparticles, probably through hydrophobic interactions, since this drug exhibits poor water solubility.

The addition of STC affected the morphology of the particles, as observed in the TEM micrographs of the SIM-loaded CS nanoparticles obtained using STC amounts of 20, 40, and 70 mg ($CSNP_{20}$, $CSNP_{40}$, and $CSNP_{70}$, respectively) (Figure 1). Both $CSNP_{20}$ and $CSNP_{40}$ (Figs. 1a and 1b, respectively) had a spherical shape, but $CSNP_{20}$ exhibited a more compact structure, as indicated by the deeper color contrast obtained for these nanoparticles, while $CSNP_{40}$ appeared to have a less dense structure. On the contrary, the nanoparticles prepared with 70 mg of STC ($CSNP_{70}$) (Fig. 1c) displayed an irregular morphology, with a compact core surrounding by a less dense corona, probably due to the hydrophilic characteristic of STC, which may be located at the surface of the particles.

Table 1. Physicochemical characteristics of the SIM-loaded CS nanoparticles (Mean ± SD, n = 3).

Formulation[1]	CS/TPP/STC[2]	SIM content (μg/mL)	Encapsulation efficiency (%)	Mean diameter (nm)	PDI	Zeta potential (mV)
$CSNP_0$	6/1/0	66.9 ± 17.0	93.4 ± 0.5	338.9 ± 20.3	0.51 ± 0.07	+47.2 ± 1.9
$CSNP_{20}$	6/1/2.18	83.6 ± 1.9	92.1 ± 0.2	576.3 ± 73.2	0.45 ± 0.12	+43.2 ± 0.7
$CSNP_{30}$	6/1/3.27	152.8 ± 2.5	92.4 ± 0.6	457.9 ± 15.5	0.35 ± 0.09	+42.3 ± 0.5
$CSNP_{40}$	6/1/4.36	136.3 ± 10.0	91.1 ± 0.4	410.0 ± 68.4	0.38 ± 0.12	+41.2 ± 1.1
$CSNP_{50}$	6/1/5.45	120.3 ± 21.0	92.9 ± 2.6	374.4 ± 11.3	0.30 ± 0.06	+42.5 ± 0.4
$CSNP_{60}$	6/1/6.45	204.6 ± 23.7	96.4 ± 0.3	368.8 ± 6.1	0.42 ± 0.06	+40.9 ± 1.4
$CSNP_{70}$	6/1/7.63	225.1 ± 23.7	97.2 ± 0.1	386.1 ± 39.1	0.40 ± 0.06	+41.4 ± 0.1
$CSNP_{80}$	6/1/8.70	169.6 ± 3.5	92.9 ± 2.3	440.0 ± 17.3	0.35 ± 0.09	+40.0 ± 0.4

[1]CSNP was used to denote chitosan nanoparticles, in which the subscripted numbers corresponds to the amount (mg) of sodium taurocholate added to the formulations. [2]CS/TPP/STC corresponds to the ratio between chitosan (CS), tripolyphosphate (TPP) and sodium taurocholate (STC) in the nanoparticles.

Figure 1. TEM micrographs of the chitosan nanoparticles: (a) $CSNP_{20}$; (b) $CSNP_{40}$; and (c) $CSNP_{70}$.

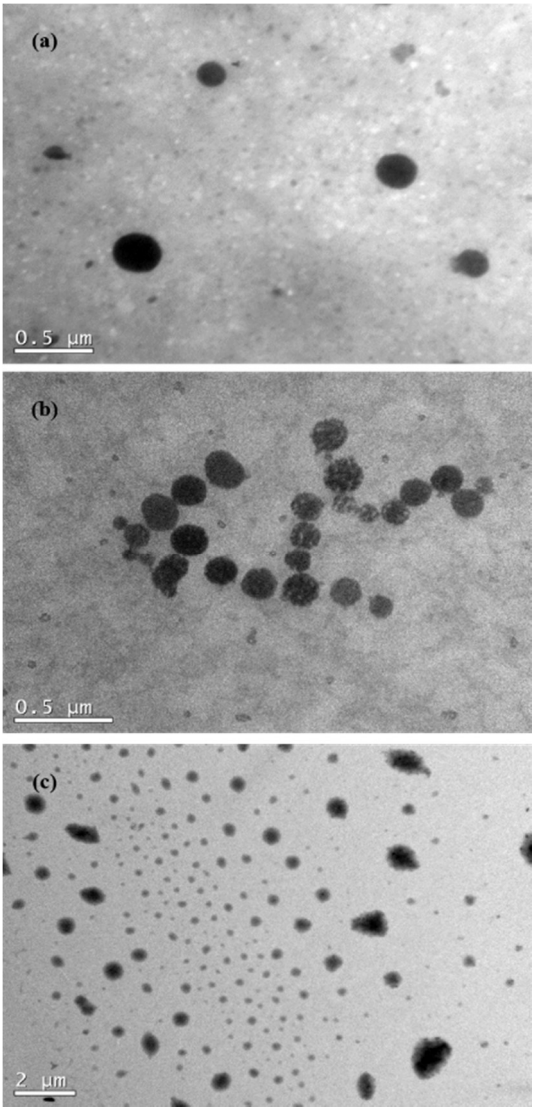

Preparation and characterization of spray-dried powders

The physicochemical properties of the spray-dried powders prepared from dispersions containing different chitosan nanoparticles/Eudragit® S100 ratios of 1:4, 1:6, and 1:8 ($SDP_{1:4}$, $SDP_{1:6}$, and $SDP_{1:8}$, respectively) are shown in Table 2. The process yield, calculated considering the total solids content of the feed dispersions, and the residual moisture of SDP varied from 80.2 to 87.0% and 5.1 to 5.7%, respectively, indicating that the spray-drying process was successful. The SIM contents were found to be 1.05, 0.88, and 0.92 % for $SDP_{1:4}$, $SDP_{1:6}$, and $SDP_{1:8}$, respectively. The spray-drying turned the nanoparticle dispersions into microparticles, as expected, with particles displaying mean diameters of around 3 μm. The spray-dried powders exhibited negative zeta potential values, which were -44.17, -48.27, and -49.30 for $SDP_{1:4}$, $SDP_{1:6}$, and $SDP_{1:8}$, respectively. These negative charges may be attributed to the carboxylic groups of the methacrylic acid residues in the Eudragit® S100 backbone. The microparticles presented spherical shape with smooth surfaces. Collapsed regions due to the spray-drying process can be noted in some particles (Figure 2).

Figure 2. SEM micrographs of the SDP prepared with chitosan nanoparticles to Eudragit® S100 ratios of (a) 1:4; (b) 1:6; and (c) 1:8.

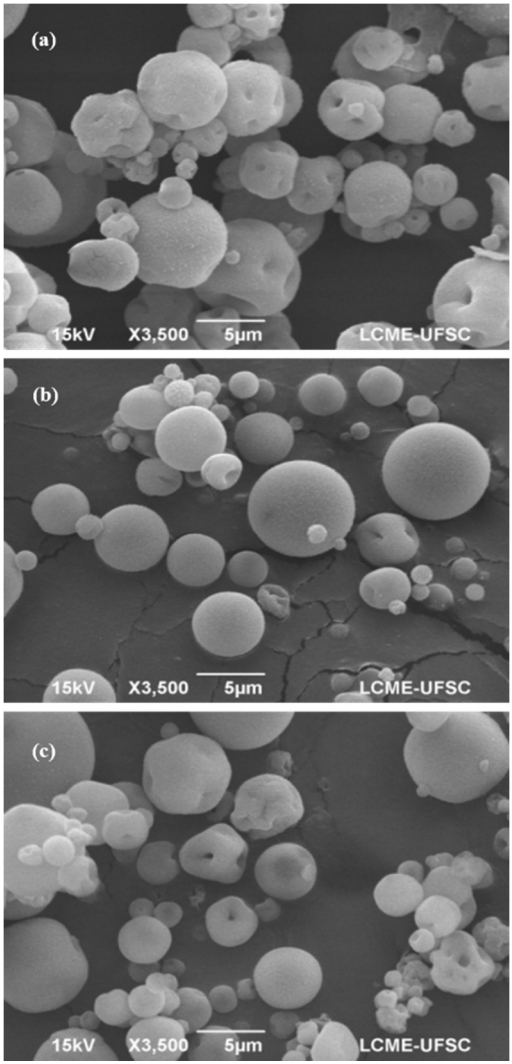

Table 2. Physicochemical characteristics of spray-dried enteric microparticles containing chitosan nanoparticles (Mean ± SD, n = 3).

Formulation[1]	Yield (%)	Moisture Content (%)	Mean diameter (μm)	Zeta Potential (mV)	SIM content (wt%)
$SDP_{1:4}$	82.4 ± 3.1	5.7 ± 0.6	3.3 ± 2.6	-44.17 ± 0.85	1.05 ± 0.10
$SDP_{1:6}$	87.0 ± 2.3	5.1 ± 0.2	3.1 ± 1.7	-48.27 ± 0.51	0.88 ± 0.02
$SDP_{1:8}$	80.2 ± 2.3	5.3 ± 0.3	3.4 ± 1.9	-49.30 ± 0.21	0.92 ± 0.10

[1]SDP denotes spray-dried powders, in which the subscripted numbers corresponds to the chitosan nanoparticles to Eudragit® S100 ratio in the feed dispersions.

DSC analysis

The thermal behavior of the raw materials, chitosan nanoparticles, and spray-dried powders obtained by DSC are shown in Figure 3. The DSC curve for SIM exhibited an endothermic peak at 136.17 °C (Fig. 3a), corresponding to the melting of the drug.[29] CS exhibited an endothermic peak at 77.68 °C (Fig. 3b), corresponding to the loss of crystallization water associated to the hydrophilic groups of this polymer.[30] The DSC curve obtained for TPP showed no thermal events between 30 and 300 ºC (Fig. 3c), since it melts at temperatures above 600 °C.[31] STC displayed endothermic peaks at 86.90 °C and 105.03 °C, corresponding to the loss of water, and an endothermic peak at 239.59 °C, which corresponds to the melting of this surfactant (Fig. 3d). Finally, the DSC curve obtained for Eudragit® S100 exhibited an endothermic peak at 207.25 °C (Fig. 3e), corresponding to the glass transition temperature of this polymer.[32] The DSC analysis of chitosan nanoparticles prepared without STC ($CSNP_0$) revealed the presence of an endothermic peak at 55.31 °C, which corresponds to the loss of water, and a second endothermic peak at 127.4 °C corresponding to SIM (Fig. 3f). When STC was added to the nanoparticle formulation ($CSNP_{70}$; Fig. 3g) this endothermic peak disappeared and only the endothermic peak at 52.35 °C, corresponding to water loss, was observed. Spray-dried microparticles containing chitosan nanoparticles ($SDP_{1:8}$) displayed a similar profile with only an endothermic peak at 76.24 °C, representative of water loss (Fig. 3h).

Figure 3. DSC curves of (a) SIM; (b) CS; (c) TPP; (d) STC; (e) Eudragit® S100; (f) $CSNP_0$; (g) $CSNP_{70}$; and (h) $SDP_{1:8}$.

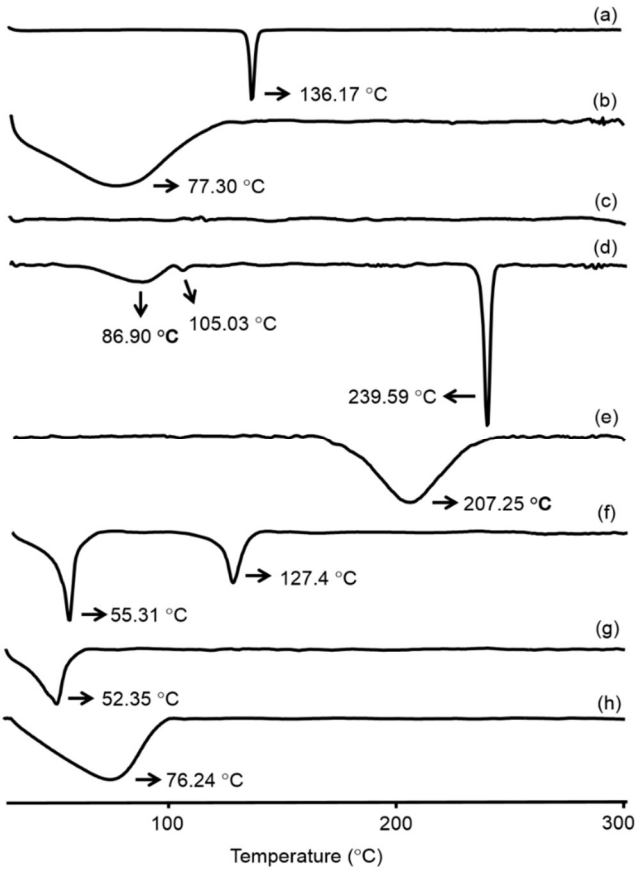

FT-IR analysis

Figure 4 shows the FT-IR absorption bands for the raw materials, chitosan nanoparticles and spray-dried powders. The FT-IR spectrum for the pure SIM (Fig. 4a)

exhibited characteristic bands at 3553.9 cm^{-1}, corresponding to free O-H stretching vibrations; 3011.6 cm^{-1}, 2959.7 cm^{-1}, and 2872.7 cm^{-1}, corresponding at C-H stretching vibrations; and 1695.8 cm^{-1}, corresponding to the stretching vibrations of the ester and the lactone carbonyl functional group.[29] The FT-IR spectrum for CS (Fig. 4b) showed a band of amide bond at 1651.0 cm^{-1} and a protonated amine band at 1586.9 cm^{-1}, since CS is obtained from the partial N-deacetylation of chitin.[33] The TPP spectrum (Fig. 4c) showed bands at 1133.9 cm^{-1} and 882.4 cm^{-1}, corresponding to the stretching vibrations of P=O and P–O groups, respectively.[34] The STC spectrum (Fig. 4d) presented bands at 1187 cm^{-1} and 1374.6 cm^{-1}, corresponding to the symmetric and asymmetric S=O stretching vibrations.[34] The Eudragit® S100 spectrum (Fig. 4e) exhibited a characteristic absorption band at 1727.7 cm^{-1}, corresponding to the symmetrical vibration of the carbonyl group.[35] The FT-IR spectrum of $CSNP_{70}$ (Fig. 4f) revealed the presence of amide and protonated amine bands of CS shifted to 1640.1 cm^{-1} and 1544.5 cm^{-1}, respectively, P=O and P–O bands of TPP shifted to 1152.4 cm^{-1} and 890.5 cm^{-1}, respectively, and the S=O bands of STC shifted to 1404.7 cm^{-1} and 1204.6 cm^{-1}. These results indicated that effective interactions between the anionic groups of TPP and STC with the cationic groups of CS occurred, suggesting that both compounds are involved in the formation of the nanoparticle structure. Finally, the spectrum obtained for $SDP_{1:8}$ (Fig. 4g) showed the protonated amino band of CS shifted from 1544.5 cm^{-1} to 1561.4 cm^{-1}, and the carbonyl group band of Eudragit® S100 shifted from 1727.7 cm^{-1} to 1718.8 cm^{-1}. These results suggest that, besides the previously reported ionic interaction between TPP, STC and CS, interactions between the positive charges of the chitosan nanoparticles and the negative charges of Eudragit® S100 also occurred.

Figure 4. Infrared spectra of (a) SIM; (b) CS; (c) TPP; (d) STC; (e) Eudragit® S100; (f) $CSNP_{70}$; and (g) $SDP_{1:8}$.

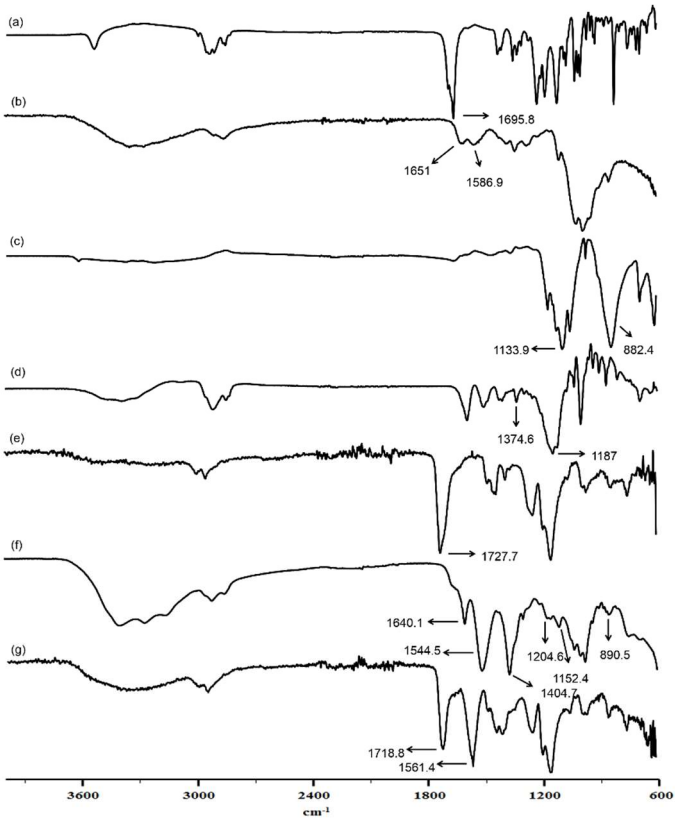

X-Ray Powder Diffraction

The X-ray diffraction patterns for the raw materials, chitosan nanoparticles and enteric spray-dried microparticles are shown in Figure 5. SIM displayed peaks at 7.83°, 9.37°, 10.91°, 14.91°, 15.63°, 16.56°, 17.17°, 18.81°, 19.42°, 21.99°, and 22.50° 2θ (Fig. 5a), evidencing the crystalline structure of this drug.[36] CS and Eudragit® S100 (Fig. 5b and 5e, respectively) did not exhibited diffraction peaks, revealing their amorphous property. TPP exhibited the most intense peaks at 18.71°, 19.33°, 33.16°, 33.88°, and 34.40° 2θ (Fig. 5c), while a broad peak at 14.81° 2θ was observed for STC (Fig. 5d). Chitosan nanoparticles prepared without STC ($CSNP_0$) exhibited diffraction peaks at 8.86°, 11.53°, 17.07°, 19.22° 22.71°, and 29.78° 2θ (Fig. 5f), indicating that the CS/TPP nanoparticles have a crystalline structure. In contrast, the addition of STC to the formulations rendered more amorphous particles (Fig. 5g), which is in agreement with the results obtained by DSC. The enteric spray-dried microparticles ($SDP_{1:8}$) did not display any crystallinity peaks, as expected, since this technique is generally applied to the production of amorphous powders.

Figure 5. X-Ray diffractograms of (a) SIM; (b) CS; (c) TPP; (d) STC; (e) Eudragit® S100; (f) $CSNP_0$; (g) $CSNP_{70}$; and (h) $SDP_{1:8}$.

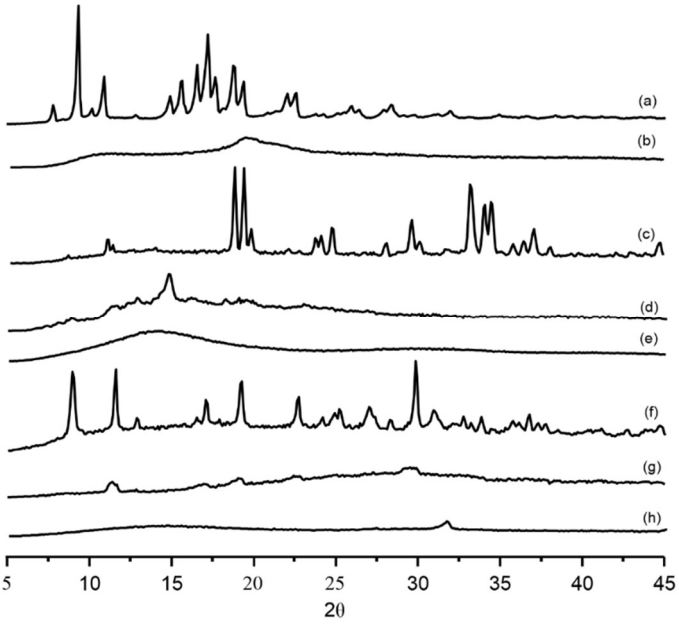

In vitro release studies

The *in vitro* release of SIM from the enteric spray-dried microparticles (SDP) was investigated in media with gradually changing pH conditions and the results are shown in Figure 6. As can be observed, SIM exhibited a pH-dependent release profile. In the first hour, in the hydrochloric acid solution at pH 1.2, which would correspond to the time for gastric emptying , the values for SIM release were 13.49, 12.64, and 7.88 % for $SDP_{1:4}$, $SDP_{1:6,}$ and $SDP_{1:8}$, respectively. The release of SIM did not occur in the subsequent 3 h in phosphate buffer solution at pH 4.5,

indicating that this initial release corresponds to the fraction of the drug adsorbed at the surface of the spray-dried microparticles. When the medium was changed to phosphate buffer at pH 7.2, which corresponds to the pH of the ileocecal region of the GIT, the remaining drug was released from the microparticles at a controlled rate. After 12 h, the values for the SIM released from $SDP_{1:4}$, $SDP_{1:6,}$ and $SDP_{1:8}$ were 98.06, 96.77, and 95.67 %, respectively. In order to identify statistical differences between the release profiles in relation to the amount of enteric polymer added, the dissolution efficiency (DE) values were calculated for each dissolution media (Table 3). The analysis of variance revealed that DE was significantly affect by the amount of enteric polymer added to the formulations, with a slower release occurring when a higher amount of Eudragit® S100 ($SDP_{1:8}$) was employed.

Figure 6. SIM release profiles from the SDP prepared with chitosan nanoparticles to Eudragit® S100 ratios of (♦) 1:4; (■) 1:6; and (▲) 1:8.

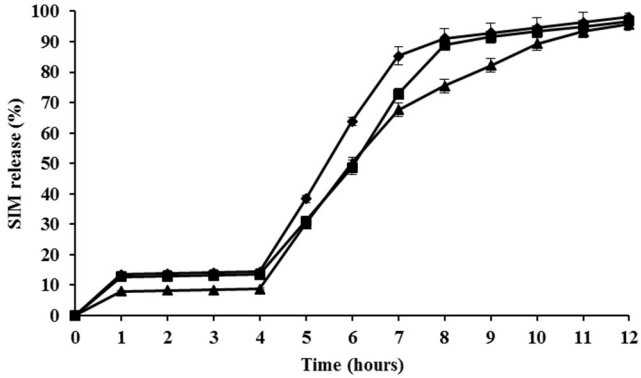

Table 3. Dissolution efficiency (DE).

Formulation	Dissolution Efficiency (%)[1] (Mean ± SD, n = 6)		
	pH 1.2	pH 4.5	pH 7.2
$SDP_{1:4}$	6.7 ± 0.5^{a}	7.1 ± 1.0^{c}	70.2 ± 1.8^{e}
$SDP_{1:6}$	6.3 ± 0.3^{a}	6.72 ± 0.5^{c}	65.3 ± 0.9^{f}
$SDP_{1:8}$	3.9 ± 0.1^{b}	4.2 ± 0.2^{d}	63.2 ± 1.4^{f}

[1]Equal letters indicate no statistical significance between the values. F_{cal} pH 1.2 = 96.16; F_{cal} pH 4.5 = 56.22; F_{cal} pH 7.2 = 22.57; $F_{critical}$ = 3.682. Significance level of 5%.

The mean diameters of the particles measured after 5 h of magnetic stirring in water adjusted to pH 7.2 were 562.37, 723.70, and 569 nm, with PDI values of 0.45, 0.36, and 0.27, for formulations prepared with nanoparticles/Eudragit® S100 ratios of 1:4, 1:6, and 1:8, respectively. This result indicated that after this period of time the enteric polymer was quite dissolved, rendering a redispersed colloidal suspension.

DISCUSSION

The application of the ionic gelation method in the preparation of nanoparticles has received increased attention in recent years, since this method is simple, involves mild conditions, does not require heating, toxic organic solvents or chemical crosslinkers, and is suitable for scaling up.[37-39] The most common polymer employed to obtain nanoparticles using the ionic gelation method is chitosan, which is a positively-charged polysaccharide, with weak basic groups capable of interacting with several polyanions, such as tripolyphosphate, resulting in their self-assembly through the formation of strong, but reversible electrostatic links.[40,41] Studies have demonstrated that the loading of lipophilic drugs

into chitosan nanoparticles can be greatly improved through either the chemical modification of the chitosan or the introduction of molecules into the chitosan nanoparticles, which are able to create hydrophobic domains in the nanoparticle structure.[21,24,42-45] In our study, we modified the ionic gelation method with the addition of sodium taurocholate to produce chitosan nanoparticles with higher loadings of simvastatin. Sodium taurocholate is a conjugated primary bile salt which can interact with chitosan, yielding a water-insoluble, poorly crystalline, hydrophobic chitosan salt.[46,47] As we had hypothesized, the addition of this anionic surfactant promoted an increase in the drug loading, probably due to the previously hydrophilic structure of the nanoparticles becoming more hydrophobic, while maintaining the particle size in the nanometric range (Table 1).

Meyerhoffer and McGown (1989)[48] reported that the critical micellar concentration (c.m.c) of STC in water ranges between 8 mM and 12 mM and, with the exception of $CSNP_{70}$ and $CSNP_{80}$, the concentrations of STC in the formulations were below its c.m.c. However, the morphology of the nanoparticles appeared to be affected by the concentration of STC added to the formulations (Fig. 1). Structures that are more compact were observed for $CSNP_{20}$ and $CSNP_{40}$, prepared with the lower concentrations of STC, whereas a less dense corona surrounding a denser nanoparticle core was observed when STC was used at a higher concentration ($CSNP_{70}$). These results suggest that at higher concentrations this surfactant is also found adsorbed at the surface of the nanoparticles. Both the interactions between CS and STC and the formation of more amorphous particles, as reported elsewhere[46], were demonstrated by DSC, FT-IR, and XRD techniques (Figs. 3-5).

Colonic drug delivery after oral administration has gained increased attention for the treatment of several colon diseases, including colorectal cancer. In the treatment of these diseases, high local concentrations can be achieved while

minimizing the side effects that occur due to the drug release in the upper GIT or unnecessary systemic absorption.[10,49] A major challenge in the development of colonic delivery systems is therefore to prevent drug release and/or absorption during its passage through the stomach and the small intestine.[8] The most common physiological factor considered in the design of a successful colonic delivery system is the pH gradient throughout the GIT tract. In normal healthy subjects, the pH increases progressively from 1-2 in the stomach (reaching pH 4 during digestion) to pH 6-7 in the small intestine, and to 7-8 in the distal ileum.[49] The pH decreases in the cecum (pH 6.4 ± 0.4) and then rises from the right to the left colon with a final value of 7.0 ± 0.7.[50] Colonic delivery systems are, therefore, pH-dependent delayed-release dosage forms. However, the residence time of the dosage form in the several segments of the GIT and the extent to which the drug delivery system undergoes degradation by the colonic enzymes are other important parameters for colon-targeted drug delivery systems. Thus, combining pH-dependent release, prolonged release, and microbially-dependent approaches to the development of drug delivery systems would allow a better distribution of the drug throughout the large intestine, improving the potential of the drug delivery in the colon. In this study, to reach this goal, SIM-loaded chitosan nanoparticles were encapsulated into Eudragit® S100 microparticles using the spray-drying technique, generating a hybrid drug delivery system. Eudragit® S100 is an anionic methacrylic acid–methyl methacrylate copolymer (1:2), which is reportedly appropriate for the development of colonic drug delivery systems, since it has a threshold pH for dissolution of 7.0.[51] The encapsulation of nanoparticles into microparticles has been described for the delivery of proteins in the lungs and the administration of corticoids for the treatment of posterior segment eye diseases.[52,53] However, the use of this strategy to deliver a drug to the colon has not previously been reported in the literature.

The spray-drying technique yielded microparticles with spherical shape (Fig. 2), diameters around 3 μm and negative zeta potential values, which indicated the complete masking of the positively-charged surface of the chitosan (Table 1) due to the entrapment of the nanoparticles inside microparticles. The amorphous property and the presence of interactions between CS and Eudragit® S100 were evidenced in the DSC, FT-IR, and XRD studies (Figs. 3-5). The release studies indicated that only a small fraction of the drug would be released in the acidic medium of the stomach. At pH 7.0, which corresponds the pH of the terminal ileum, the release of the drug was dependent on the nanoparticles/Eudragit® S100 ratio; the higher the Eudragit® S100 concentration the slower the drug release was. In this case, the microencapsulated chitosan nanoparticles prepared with a nanoparticles/Eudragit® S100 ratio of 1:8 seems to be the most promising formulation to deliver SIM in the colon.

CONCLUSIONS

In this study, we demonstrated that higher loadings of the hydrophobic drug SIM in chitosan/tripolyphosphate nanoparticles can be achieved through the addition of STC, probably due to the formation of a more hydrophobic particle structure. Furthermore, the nanoparticles were successful incorporated into Eudragit® S100 microparticles using the spray-drying technique, resulting in a new hybrid enteric drug delivery system. This system could be suitable for the colonic delivery of SIM to treat colorectal carcinoma, since this innovative strategy allowed the properties of delayed-release systems to be combined with the targeting and bioadhesiveness of the chitosan nanoparticles.

ACKNOWLEDGEMENTS

This research was supported by the Coordination for the Improvement of Higher Education Personnel Superior

(CAPES, Ministry of Education, Brazil), which granted a scholarship to one of the authors.

DECLARATION OF INTEREST

The authors report no conflicts of interest.

REFERENCES

1. Tiwari R, Pathak K 2011. Nanostructured lipid carrier versus lipid nanoparticles of simvastatin: Comparative analysis of characteristics, pharmacokinetics and tissue uptake. Int. J. Pharm. 415:232-243.

2. Wang C-Y, Liu P-Y, Liao JK 2008. Pleiotropic effects of statin therapy: molecular mechanisms and clinical results. Trends Mol. Med. 14:37-44.

3. Cardwell CR, Hicks BM, Hughes C, Murray LJ 2014. Statin use after cancer diagnosis and survival: a population-based cohort study. J. Clin. Oncol. 32:3177-3183.

4. Bardou A, Barkun A, Martel M. effect of statin therapy on colorectal cancer 2010. Gut 59:1572-1585.

5. Cho S-J, Kim JS, Kim JM, Lee JY, Jung HC, Song IS 2008. Simvastatin induces apoptosis in human colon cancer cells and in tumor xenografts, and attenuates colitis-associated colon cancer in mice. Int. J. Cancer 123:951-957.

6. Qi X-F, Kim D-H, Yoon Y-S, Kim S-K, Cai D-Q, Teng Y-C, Shim K-Y, Lee K-J 2010. Involvement of oxidative stress in simvastatin-induced apoptosis of murine CT26 colon carcinoma cells. Toxicol. Lett. 199:277-287.

7. Chang H-L, Chen C-Y, Hsu Y-F, Kuo W-S, Ou G, Chiu P-T, Huang Y-H, Hsu M-J 2013. Simvastatin induced HCT116 clorectal cancer cell apoptosis through p38MAPK-p53-Survivin signaling cascade. Biochim. Biophys. Acta 1830: 4053-4064.

8. Ashgar LFA, Chandran S 2006. Multiparticulate formulation approach to colon specific drug delivery: current perspectives. J. Pharm. Pharm. Sci. 9:327-338.

9. Singh B 2007. Modified-release solid formulations for colonic delivery. Recent Pat. Drug Deliv. Formul. 1:53-63.
10. Pinto JF 2010. Site-specific drug delivery systems within the gastro-intestinal tract: From the mouth to the colon. Int. J. Pharm. 395:44 – 52.
11. Maroni A, Del Curto MD, Zema L, Foppoli A, Gazzaniga A 2013. Film coatings for oral colon delivery. Int. J. Pharm. 457:372 – 394.
12. Palugan L, Cerea M, Zema L, Gazzaniga A, Maroni A 2015. Coated pellets for oral colon delivery. J. Drug Deliv. Sci. Tec 25:1 – 15.
13. Dash M, Chiellini F, Ottenbrite RM, Chiellini E 2011. Chitosan – A versatile semi-synthetic polymer in biomedical applications. Prog. Polym. Sci. 36:981-1014.
14. Sogias AY, Williams AC, Khutoryanskiy VV 2008. Why is Chitosan Mucoadhesive? Biomacromolecules 9:1837–1842.
15. Saboktakina MR, Tabatabaiea RM, Maharramovb A, Ramazanovb ML 2011. Synthesis and in vitro evaluation of carboxymethyl starch–chitosan nanoparticles as drug delivery system to the colon. Int. J. Biol. Macromol. 48: 381-385.
16. Danhier F, Feron O, Préat V 2010. To exploit the tumor microenviroment: Passive and active tumor targeting of nanocarriers for the ant-cancer drug delivery. J. Control. Rel. 148:135-146.
17. Acharya S, Sahoo SK 2011. PLGA nanoparticles containing various anticancer agents and tumor delivery by EPR effect. Adv. Drug Deliver. Rev. 63:170-183.
18. Agnihotri SA, Mallikarjuna NN, Aminabhavi TM 2004. Recent advances on chitosan-based micro- and nanoparticles in drug delivery. J. Control. Rel. 100:5-28.
19. Rinaudo M 2006. Chitin and chitosan: properties and applications. Prog. Polym. Sci. 31:603- 632.
20. Luo Y, Zhang B, Cheng WH, Wang Q 2010. Preparation, characterization and evaluation of selenite-loaded chitosan/TPP nanoparticles with or without zein coating. Carbohydr. Pol. 82:942-951.

21. Sonvico F, Cagnani A, Rossi A, Motta S, Di Bari MT, Cavatorta F, Alonso MJ, Deriu A, Colombo P 2006. Formation of self-organized nanoparticles by lecithin/chitosan ionic interaction. Int. J. Pharm. 324:67-73.
22. Senyigit T, Sonvico F, Barbieri S, Ozer O, Santi P, Colombo P 2010. Lecithin/chitosan nanoparticles of clobetasol-17-propionate capable of accumulation in pig skin. J. Control. Rel. 142:368-373.
23. Barbieri S, Sonvico F, Como C, Colombo G, Zani F, Buttini F, Bettini R, Rossi A, Colombo P 2013. Lecithin/chitosan controlled release nanopreparations of tamoxifen citrate: loading, enzyme-trigger release and cell uptake. J. Control. Rel. 167:276-283.
24. Chhonker YS, Prasada, YD, Chandasanaa H, Vishvkarmaa A, Mitrab K, Shuklac PK, Bhattaa RS 2015. Amphotericin-B entrapped lecithin/chitosan nanoparticles for prolonged ocular application. Int. J. Biol. Macromol. 72:1451 – 1458.
25. Fan W, Yan W, Xu Z, Ni H 2012. Formation mechanism of monodisperse, low molecular weight chitosan nanoparticles by ionic gelation technique. Colloids Surf. B 90:21-27.
26. ICH 2005. Harmonised tripartite guideline: validation of analytical procedures: text and methodology Q2 (R1).
27. European Pharmacopoeia 2008, 6th ed., Council of Europe: Strasbourg. p 266 – 274.
28. Gan Q, Wang T, Cochrane C, McCarron P 2005. Modulation of surface charge, particle size and morphological properties of chitosan-TPP based nanoparticles intended for gene delivery. Colloids Surf. B 44:65 – 73.
29. Ambike AA, Mahadik KR, Paradkar A 2005. Spray-dried amorphous solid dispersions of simvastatin, a low T_g drug: *in vitro* and *in vivo* evaluations. Pharm. Res. 22:990 – 998.
30. Sarmento B, Martins S, Ribeiro A, Veiga F, Neufeld R, Ferreira D 2006. Development and comparison of different nanoparticulate polyelectrolyte complexes as insulin carriers. Int. J. Pept. Res. Ther. 12:131 – 138.

31. Gierszewka-Druzynska M, Ostrowska-Czubenko J 2010. The effect of ionic crosslinking on thermal properties of hydrogel chitosan membranes. PCACD 15:25 – 32.
32. Hu D, Liu L, Chen W, Li S, Zhao Y 2012. A novel preparation method for 5-aminosalicylic acid loaded Eudragit S100 nanoparticles. Int. J. Mol. Sci. 13:6454 – 6468.
33. Sarmento B, Ferreira D, Veiga F, Ribeiro A 2006. Characterization of insulin-loaded alginate nanoparticles produced by ionotropic pre-gelation through DCS and FTIR studies. Carbohydr. Pol. 66:1 – 7.
34. Silverstein R, Webster FX, Kiemle D. 2005. Spectrometric Identification of Organic Compounds, 7th ed., New York. p 71 – 109.
35. Cilurzo F, Minghetti P, Selmin F, Casiraghi A, Montanari L 2003. Polymethacrylate salts as new low-swellable mucoadhesive materials. J. Control. Rel. 88:43–53.
36. Pandya P, Gattani S, Jain P, Khirwal L, Surana S 2008. Co-solvent evaporation method for enhancement of solubility and dissolution rate of poorly aqueous soluble drug simvastatin: *in vitro-in vivo* evaluation. AAPS Pharm. Sci. Tech. 9:1247 – 1252.
37. Mao S, Bakowsky U, Jintapattanakit A, Kissel T 2006. Self-Assembled Polyelectrolyte Nanocomplexes between Chitosan Derivatives and Insulin. J. Phar. Sci. 95(5)1035 – 1048.
38. Amidi M, Mastrobattista E, Jiskoot W, Hennink WE 2010. Chitosan-based delivery systems for protein therapeutics and antigens. Adv. Drug Deliver. Rev. 62:59 – 82.
39. Dong Y, Ng WK, Shen S, Kim S, Tan RBH 2013. Scalable ionic gelation synthesis of chitosan nanoparticles for drug delivery in static mixers. Carbohyd. Pol. 94:940 – 945.
40. López-León T, Carvalho ELS, Seijo B, Ortega-Vinuesa JL, Bastos-González D 2005. Physicochemical characterization of chitosan nanoparticles: electrokinetic and stability behavior. J. Colloid. Interf. Sci. 283:244 – 351.

41. Hamman JH 2010. Chitosan Based Polyelectrolyte Complexes as Potential Carrier Materials in Drug Delivery Systems. Mar. Drugs 8:1305 – 1322.
42. Zhang J, Chen XG, Li YY, LIU CS 2007. Self-assembled nanoparticles based on hydrophobically modified chitosan as carriers for doxorubicin. Nanomedicine: NBM 3:258 – 265.
43. Bhattaa RS, Chandasanab H, Chhonkera YS, Rathib C, Kumara D, Mitrac K, Shuklad PK 2012. Mucoadhesive nanoparticles for prolonged ocular delivery of natamycin: In vitro and pharmacokinetics studies. Int. J. Pharm. 432:105 – 112.
44. Hafner A, Lovric J, Voinovich D, Filipovic-Grcic 2009. Melatonin-loaded lecithin/chitosan nanoparticles: Physicochemical characterization and permeability through Caco-2 cell monolayers. Int. J. Pharm. 381:205 – 213.
45. Mahamoud AA, El-Fekya GS, Kamela R, Awadb GEA 2001. Chitosan/sulfobutylether-β-cyclodextrin nanoparticles as a potential approach for ocular drug delivery. Int. J. Pharm. 413:229 – 236.
46. Muzzarelli RAA, Orlandini F, Pacetti D, Boselli E, Frega NGc, Tosi G, Muzzarelli C 2006. Chitosan taurocholate capacity to bind lipids and to undergo enzymatic hydrolysis: An *in vitro* model. Carbohyd. Pol. 66:363 – 371.
47. Thongngam M, McClements DJ 2006. Isothermal titration calorimetry study of the interactions between chitosan and a bile salt (sodium taurocholate). Food Hydrocolloid. 19:813–819.
48. Meyerhoffer SM, McGown LB 1989. Critical Micelle Concentration Behavior of Sodium Taurocholate in Water. Langmuir 6(1):187 – 191.
49. Chourasia MK, Jain SK 2003. Pharmaceutical approaches to colon targeted drug delivery systems. J. Pharm. Pharmaceut. Sci. 6(1):33 – 66.
50. Singh BN 2007. Modified-Release Solid Formulations for Colonic Delivery. Recent Pat. Drug Deliv. Formul. 1:53 – 63.
51. Wang XQ, Zhang Q 2012. pH-sensitive polymeric nanoparticles to improve oral bioavailability of

peptide/protein drugs and poorly water-soluble drugs. Eur. J. Pharm. Biopharm. 82:219 – 229.
52. Grenha A, Begoña S, Remuñán-Lópoez, C 2005. Microencapsulated chitosan nanoparticles for lung protein delivery. Eur. J. Pharm. Biopharm. 25:427 – 437.
53. Gómez-Gaete C, Fattal E, Silva L, Besnard M, Tsapis N 2008. Dexamethasone acetate encapsulation into Trojan particles. J. Control. Rel. 128:41 – 49.

Publicação 2. *Evaluation of In Vitro Cytotoxic Activity of Simvastatin-loaded Chitosan Nanoparticles Against HT-29 Human Cancer Carcinoma Cells*

Evaluation of *in vitro* cytotoxic activity of simvastatin-loaded chitosan nanoparticles against HT-29 human cancer carcinoma cells

MARIANA DALAGNOL[a], LORENA SANTOS-BUBNIAK[b], MARIA CLÁUDIA SANTOS-SILVA[b], ELENARA LEMOS SENNA[a,*]

[a]Departamento de Ciências Farmacêuticas, Universidade Federal de Santa Catarina, Campus Trindade, CEP 88040-970, Florianópolis, Santa Catarina, Brasil.
[b]Departamento de Análises Clínicas, Universidade Federal de Santa Catarina, Campus Trindade, CEP 88040-970, Florianópolis, Santa Catarina, Brasil.

[*]Corresponding author: +55 48 3721 5067, Email address: lemos.senna@ufsc.br

ABSTRACT

Simvastatin is a potent inhibitor of the 3-hydroxy-3-methyl-glutaryl coenzyme A reductase, which action encloses the reduction of the cholesterol synthesis by preventing the conversion of 3-hydroxy-3-methyl-glutaryl coenzyme A to mevalonate. Besides its lipid lowering effect, evidences have suggested that this drug may be helpful for the treatment of a variety of diseases, including cancer. On the other hand, chitosan nanoparticles has been considered promisor drug carriers due to its biocompatibility, biodegradable, and mucoadhesive properties, besides its ability of releasing the drug directly in the site of action, increasing the therapeutic efficacy, while minimizing the adverse effects. So, the aim of this study was to evaluate and compare the cytotoxic activity of free simvastatin and simvastatin-loaded chitosan nanoparticles in HT-29 human colon carcinoma cells. The nanoparticles were prepared using the ionic interaction technique and characterized according to the drug loading,

encapsulation efficiency, particle size and zeta potential. *In vitro* studies revealed that both free simvastatin and simvastatin-loaded chitosan nanoparticles were cytotoxic against HT-29 cells, exhibiting IC_{50} values smaller than those obtained for 5-fluoruracil after 24 h and 48 h of incubation. Also, both free and encapsulated drug caused programmed cell death (apoptosis), inhibited cell migration, and reduced the ability of HT-29 cells to form colonies. Our findings evidenced the antitumor properties of simvastatin-loaded nanoparticles, but further *in vivo* studies should still be carried out to demonstrate the interest of this drug delivery system in the colorectal cancer treatment.

Keywords: Simvastatin; Chitosan; Nanoparticles; Sodium Taurocholate; Colonic Drug Delivery; *In vitro* models; HT-29 cells; Colorectal Cancer.

INTRODUCTION

Simvastatin (SIM) is a drug widely prescribed to reduce the levels of serum cholesterol, whose action encloses the inhibition of the 3-hydroxy-3-methyl-glutaryl coenzyme A (HMG-CoA) reductase, which catalyzes conversion of HMG-CoA to mevalonate, a precursor of cholesterol.[1] Besides its lipid lowering effect, several studies have demonstrated that SIM exerts pleiotropic actions, including anti-inflammatory, immunomodulatory, and antitumor effects. The inhibition of the mevalonate pathway also inhibits the synthesis of other important molecules as the isoprenoids farnesyl pyrophosphate and geranylgeranyl pyrophosphate. These molecules are responsible for the isoprenylation of many cellular proteins that are responsible for physiological functions potentially involved in carcinogenesis, as cellular growth, proliferation and migration, and also oxidative stress.[2,3]

Many studies have demonstrated the antitumor effects of SIM in various types of colon cancer cells. Qi *et al.*

(2010) investigated the SIM-induced cytotoxicity in murine CT26 colon cancer cells and showed that this drug is capable of inducing significant cytotoxicity by breaking down the antioxidant defense system and inducing apoptosis. Cho *et al.* (2008) evaluated the effect of SIM on the apoptosis of COLO 205 and HCT 116 cells and proved that this drug can inhibit colon cancer development by induction of apoptosis as well as suppression of angiogenesis *in vitro* and *in vivo*.[4,5] So, these studies suggest that SIM could be a potential therapeutic agent for the treatment of the colorectal cancer.

In the last decades there has been increased interest in the development of biodegradable nanoparticles (NP) as drug delivery systems. These systems have several advantages as (1) the capacity of releasing the drug directly in the site of action, increasing the therapeutic efficacy while minimizing the adverse effects, (2) the subcellular size of the NP allows a higher intracellular phagocytosis in comparison with other delivery systems, (3) the capacity of improve the stability of the drug, and (4) can be synthesized from materials that are either biocompatible or biodegradable.[6,7]

A wide range of materials have been employed in the development of nanoparticles, such as natural or synthetic polymers, lipids, surfactants and dendrimers. Among these, the polysaccharides has gained major attention due to their excellent biological and physicochemical properties.[8] Chitosan (CS) is a linear aminopolysaccharide composed by randomly distributed D-glucosamine and N-acetyl-D-glucosamine units obtained by the deacetylation of chitin, a polysaccharide extensively found in the exoskeletons of crustacean like shrimps and crabs, and some fungi.[9,10] CS is a weak base with pKa values for the D-glucosamine residue between 6.2 – 7.0, being insoluble in neutral and alkaline pH. In acid medium, the amino groups of CS are protonated resulting in a soluble and positive charged polysaccharide.[11] This cationic polysaccharide has been largely used for colonic delivery of drugs owing to its properties of mucoadhesivity, degradability by the colonic microflora and an absorption

enhancing activity due to the increase of the tight junctions permeability of epithelial cells.[12,13] In a previous study, we developed a new nanoparticulate delivery system made from chitosan, sodium tripolyphosphate and sodium taurocholate, with the aim to deliver simvastatin in the colon for the treatment of the colorectal cancer. In this study, we aimed to evaluate and compare the cytotoxic activity of free simvastatin and simvastatin-loaded chitosan nanoparticles in HT-29 human colon adenocarcinoma cells.

MATERIALS AND METHODS

Materials

Simvastatin (SIM) was purchased from Pharma Nostra® (Rio de Janeiro, Brazil). Chitosan (CS) (MW 50-190 kDa; deacetylation degree between 75% and 85%; viscosity 20-300 cP) and sodium taurocholate (STC) were purchased from Sigma-Aldrich (St. Louis, MO, USA). Sodium tripolyphosphate (TPP) was a gift from Plury Química (São Paulo, Brazil).

HT-29 human colon carcinoma cells were acquired from Banco de Células do Rio de Janeiro (BCRJ, Brazil). Acridine orange (AO), ethidium bromide (EB), and dimethyl sulfoxide (DMSO) were purchased from Sigma–Aldrich (USA). RPMI medium, fetal bovine serum (FBS), 4-(2-hydroxyethyl)-1-piperazineethanesulfonic acid (HEPES, 10 mM), penicillin, and streptomycin were purchased from Invitrogen Corporation Manufactured (GIBCO, São Paulo, SP, Brazil). Phosphate buffered saline (PBS) was purchased from Laborclin (Pinhais, PR, Brazil), trypan blue was purchased from Biosystems (VETEC; Rio de Janeiro, RJ, Brazil), and 3-(4,5-dimethyl-2-thiazolyl)-2,5-diphenyl-2H-tetrazolium bromide (MTT) were obtained from AMRESCO (Solon, Ohio). All other chemicals were of analytical grade.

Methods

Nanoparticles preparation

The nanoparticles were prepared using the ionic gelation technique.[14] Briefly, a ethanol:water solution (40:60 v/v) containing 10 mg of SIM, TPP, and 70 mg of STC was prepared. Separately, CS was dissolved in acetic acid 1% (v/v) solution at a concentration of 0.55% (w/v). The nanoparticles were spontaneously obtained by injection of 10 mL of the hydroalcoholic solution into 10 mL of CS solution under magnetic stirring. The organic solvent was eliminated by evaporation under reduced pressure and the final volume was adjusted to 10 mL.

Characterization of the nanoparticles

Drug loading and entrapment efficiency

The simvastatin loading and the entrapment efficiency were assessed after determination of the drug content in the nanoparticles suspensions by ultraviolet absorption spectroscopy (UV) at a wavelength of 237 nm. The drug content was determined in the solutions obtained after complete dissolution of the nanoparticles in methanol and the results were expressed as μg of SIM per mL of nanoparticles suspension. The entrapment efficiency (EE) was estimated as being the percent difference between the total concentration of SIM in the chitosan nanoparticles suspensions and the concentration found in the supernatant obtained after ultrafiltration/centrifugation procedure of nanosuspensions using Microcon Centrifugal Filter Devices with Ultracel YM-100 (100.000 NMWL, Millipore, USA). The analyses were carried out in triplicate.

Particle size and zeta potential determination

The mean particle size and zeta potential of the nanoparticles were determined by dynamic light scattering and laser Doppler anemometry, respectively, using a Zetasizer Nano Series (Malvern Instruments, UK). The nanoparticles were diluted in ultrapure water at appropriate concentrations. Size analysis were performed at fixed scattering angle of 173º. For measurements of zeta potential (ζ), samples were placed in an electrophoretic cell, where a potential of ±150 mV was established. The zeta potential values were calculated from mean electrophoretic mobility values using Smoluchowski´s equation.

Evaluation of *in vitro* cytotoxicity

HT-29 human colon carcinoma cells were cultured in RPMI medium and were supplemented with 10 % fetal bovine serum, 100 U/mL penicillin, 100 µg/mL streptomycin and 10 mM HEPES, pH 7.4 at 37 °C in a 5 % CO_2 humidified atmosphere in plastic culture flasks. Free simvastatin (free SIM), 5-fluorouracil (5-FU), unloaded nanoparticles (unloaded-NP) and simvastatin-loaded nanoparticles (SIM-NP) were added to cells (2.5×10^5 cells/mL, 1.25×10^5 cells/mL, 6.25×10^4 cells/mL) and incubated at 37 °C for 24, 48 or 72 hours, respectively. *In vitro* cell viability was assessed using MTT (3-(4,5-dimethiazol-zyl)-2-5-diphenyltetrazolium bromide) assay.[15] The initial screening of free SIM, SIM-NP, and 5-FU at 100 µM concentration was performed to identify the cytotoxic effectiveness against HT-29 cells. Subsequently, cells were incubated in the presence of different concentrations of free SIM, SIM-NP, and 5-FU (1 - 100 µM) for 24, 48 and 72 hours, in order to calculate the IC_{50} (50 % inhibitory concentration) values. Control group was only plated with cell culture medium and MTT reagent. All assays were performed in triplicate.

Assessment of apoptosis

Apoptotic death was verified as described by Geng *et al.* (2003).[16] HT-29 cells (5×10^5 cells/mL) were incubated with free SIM and SIM-NP at their respective IC_{50} values and with unloaded-NP (maintaining the same volume of treatment with SIM-NP), for 24 h. Then, the coverslips covering the bottom of the plate were removed, washed with PBS and treated with 40 µL of acridine orange (10 µg/mL) and ethidium bromide (5 µg/mL) solution. Cells were examined under a fluorescence microscope (Olympus BX-FLA) and representative fields were photographed using a digital camera (Olympus BX40, Japan). Viable cells exhibited green fluorescence (acridine orange staining) whereas apoptotic cells exhibited an orange-red nuclear fluorescence (ethidium bromide staining).

Colony Assay

The HT-29 cells (1×10^3 cells/dish) in 2 mL of RPMI containing 10% FBS were seeded in culture dishes (60 mm x 15 mm, surface area size 22.1 cm^2) and incubated at 37°C with 5% CO_2 for 24 hours. After this time, the cells were treated with free SIM, SIM-NP, and 5-FU at their respective IC_{50}, unloaded-NP (maintaining the same volume of treatment with SIM-NP) and another group with RPMI without sample, which served as a control. Then, the cells were incubated at 37°C with 5% CO_2 for 24 hours. Treatments were removed, the cells were washed twice with PBS, 2 mL of RPMI were added, and again incubated at 37°C with 5% CO_2 for more six days. The HT-29 colonies were fixed for 30 min by adding 1 mL of 4% paraformaldehyde directly to each dish and stained with 1 mL of 0.5% trypan blue. The number of HT-29 cells constituting a colony ranged from 25 to 50, and the considered colony size was ≥ 0.2 mm. The photographs were taken with Sony Cyber Shot DSC-W620 14.1.

Scratching assay

The HT-29 cells (1×10^6 cells/dish) in RPMI containing 10% FBS were seeded in a culture dishes (60 mm x 15 mm, surface area size 22.1 cm^2). Once the confluent monolayer was formed, a linear scratch was generated in the monolayer with a sterile pipette tip. Cellular debris (if any) was removed by washing with phosphate buffer saline (PBS). The medium was then replaced with 2 mL of RPMI containing free SIM, 5-FU and SIM-NP at their respective IC_{50}, unloaded-NP (maintaining the same volume of treatment with SIM-NP) and RPMI without sample served as a control. Photographs were taken at a 40 times magnification using a microphotograph (Olympus BX40, Japan) on day 0, then plates were incubated at 37°C with 5% CO_2 and photographs were taken at day 1 and 4. The images acquired for each sample were further analyzed quantitatively by using computing software *ImageJ*. By comparing the images from day 0 to 4, the distance of each scratch closure was determined and the percentage migration rate was calculated. In each well two scratches were made (left and right) and three points per scratch were considered. Average of left and right scratch were taken separately. The distance of each scratch closure was determined, and percentage of migration rate was calculated using the comparison of the images from day 0 with those obtained on day 1 (24 h) or 4 (96 h). Samples were prepared in triplicate. Percent rate of migration obtained from all four wells were averaged and recorded.

Statistical analysis

The *in vitro* cytotoxic results have been presented as means ± SEM, except for the mean IC_{50} values (i.e. the concentration of drugs or compounds reducing the cell viability by 50% relative to the control value) which have been reported as geometric means accompanied by their respective 95 % confidence limits. The statistical significance

between the groups has been determined by analysis of variance followed by Bonferroni's multiple comparison test or by Student's t Test for paired samples. *P*-values of less 0.05 have been considered indicative of significance. The IC_{50} values have been determined by graphical interpolation from the individual experiments.

RESULTS AND DISCUSSION

An ideal chemotherapeutic agent must have comproved efficacy, convenient dosing schedule and minimal side effects or an acceptable toxicity profile.[17] However, the present chemotherapy is tipically accompained by severe side effects mainly due to the toxicity of the anticancer drugs to the normal tissues. Therefore, the amount of drug that can be given to a patient is limited and as a result the tumor tissue may not be exposed to an ideal dose.[18,19] It is well known that cancer erradication by chemotherapy is achieved by triggering tumor cells to undergo programmed cell death (apoptosis), though the stimuli need to be modified to target these cells in a more specific and consequently less toxic manner.[20] Today, there is a strong focus on nanotechnology application in cancer treatment. Nanoparticles confer several advantages over that of free drugs such as protect the drug from premature degradation, prevent drugs from prematurely interacting with the biological environment, enhance absorption of the drugs into a selected tissue, control the pharmacokinetic, the distribution profile of drugs in tissues, and improve intracellular penetration.[21]

Simvastatin is an extensively prescribed drug that reduces serum cholesterol levels by competitively inhibiting hydroxymethylglutaryl coenzyme A (HMG-CoA) reductase, the rate-limiting enzyme in the mevalonate pathway.[22,2] However, the role of this drug extends beyond its lipid-lowering effect. The mevalonate pathway for cholesterol biosynthesis has been implicated in various aspects of cancer development. The end products of this pathway are required

for a number of essential functions and may explain the antitumor effects of this drug. Although the mechanism of simvastatin-induced apoptosis is not completely elucidated, it appears to me mediated predominantly through depletion of prenilated proteins.[23,24] Protein prenilation is the enzymatic transfer of farnesyl- or geranylgeranyl moieties to proteins that enables these proteins to attach to cell membranes and carry out their biological functions.[25] Interestingly, several *in vitro* studies have demonstrated that most normal cell types are largely unaffected by simvastatin. On the contrary, simvastatin induced strong toxicity in many cancer cells, and quite often results in apoptosis. This preferential activity towards cancer cells makes this drug a good candidate to target these cells and drive them to undergo programmed cell death.[26,27]

Thus, considering the potential antitumor properties of simvastatin and the potential of nanoparticles in cancer treatment, the present work aimed to assess the citotoxic effect of simvastatin-loaded chitosan nanoparticles in HT-29 human adenocarcinoma cells. The nanoparticles were prepared by the ionic gelation technique between the positive charges of CS and the negative charges of TPP and STC. The nanoparticles were characterized according to their mean particle size, polidispersity index (PDI), zeta potential, SIM content and encapsulation efficiency (Table 1). Unloaded nanoparticles and SIM-loaded nanoparticles displayed mean particle sizes of 344.9 nm and 368.2 nm, and zeta potential values of +38.8 mV and +39.0 mV, respectively. The zeta potential was positive for both samples, reflecting the presence of the positively charged amino groups of CS at the particle surface.[28] The SIM content in the nanoparticle suspension was 223.4 μg/mL, and the encapsulation efficiency was 97.5%, indicating that most of the drug is associated to the nanoparticles, probably by hydrophobic interactions.

Table 1. Physicochemical properties of the unloaded-chitosan nanoparticles and simvastatin-loaded chitosan nanoparticles (Mean ± SD, n = 3).

	Unloaded-NP	SIM-NP
Size (nm)	344.9 ± 12.6	368.2 ± 10.5
Polidispersity index	0.22 ± 0.04	0.32 ± 0.03
Zeta potential (mV)	+38.8 ± 1.1	+39.0 ± 1.3
SIM content (μg/mL)	-	223.4 ± 9.1
EE (%)	-	97.5 ± 0.9

Cytotoxic effects of free SIM, SIM-NP, unloaded-NP, and 5-FU at different concentrations were analyzed in HT-29 human colon carcinoma cells by MTT assay for 24, 48, and 72 h. Incubation of HT-29 cells with free SIM, SIM-NP, and 5-FU caused significant reduction of cell viability (Figure 1). The incubation of HT-29 cells with unloaded-NP caused no significant reduction of viable cells, when compared to the control group after 24 h of treatment. However after 48 and 72 h it was observed an increase of cytotoxicity, that can be explained by the presence of chitosan in the nanoparticles.[29] Almost all works related to chitosan application refer to this polysaccharide as being a non-toxic, biologically compatible material and, therefore, suitable to be used in the development of drug delivery systems.[30] Despite this information, it is possible to say that in many cases chitosan exhibits a certain degree of toxicity that is mostly dependent on the dose, but also conditioned by the polymer characteristics, such as molecular weight, degree of deacetylation (higher degree of deacetylation provides higher density of positively charged amino groups available that are capable of reducing cell viability), pH of the incubation medium and time of incubation.[30-33] Several studies have demonstrated that chitosan displays some cytotoxicity in many cancer cells lines as CCRF-CEM (human lymphoblastic leukaemia), B16F10 (murine melanoma), SW 480 (human colon adenocarcinoma), HeLa (human cervical carcinoma) and Hep3B (human hepatoma).[34-36,31] Regardless of the decrease in the cell

viability displayed by the unloaded-NP in 48 and 72 h, the cytotoxic effects of free SIM, SIM-NP, and 5-FU against HT-29 cells were significantly higher at all exposure times. The IC_{50} calculated for free SIM, SIM-NP, and 5-FU are listed in Table 2. Free SIM exhibited the higher cytotoxic effect against HT-29 cells, as demonstrated by the smaller IC_{50} values in 24 and 48 h of incubation. The lower cytotoxic activity exhibited for SIM-NP, when compared with free SIM, may be related to the drug encapsulation, which made it less available in the cell culture medium when it was administered at the same dose as its free form. On the other hand, 5-FU also exhibited lower cytotoxic effect against HT-29 cell, when compared with both free SIM and SIM-NP after 24 h and 48 h of incubation. This result may be related to the fact that 5-FU is an antimetabolite, which inhibits the biosynthesis of DNA and RNA by fluoronucleotides erroneous incorporation during DNA synthesis, which may make its action at the cell duplication time.[37,38] As can be seen in Table 2, the higher cytotoxic effect was verified for 5-FU only after 72 h of treatment, since the doubling time of HT-29 cells is 40-60 hours.

Figure 1. Cytotoxic effect of free SIM, unloaded-NP, SIM-NP, and 5-FU on HT-29 human colon carcinoma cells after 24, 48, and 72 hours of incubation. Samples were added to cells at 100 µM concentration. Optical density of control was taking as 100 % of cell viability. The results are the mean ± SEM of at least three independent experiments. $^{*}P < 0.001$ compared with control group; $^{\#}P < 0.001$ compared with free SIM; $^{a}P < 0.001$ compared between unloaded-NP and SIM-NP groups at the same concentration, using one-way ANOVA followed by Bonferroni's test.

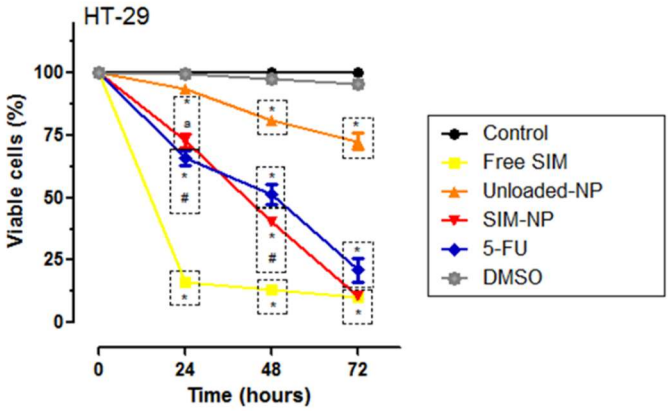

Table 2. IC_{50} values of free SIM, SIM-NP, and 5-FU for cell viability on HT-29. Free SIM, SIM-NP, and 5-FU were added to HT-29 at different concentration (1-100 µM) and incubated for 24, 48, and 72 hours.

	IC_{50} (µM)		
	24 h	**48 h**	**72 h**
Free SIM	31.76 ± 1.23	22.76 ± 1.24	17.59 ± 1.93
SIM-NP	112.80 ± 2.93*	42.23 ± 0.68*	7.76 ± 0.22$^{\#}$
5-FU	148.40 ± 4.58*	72.83 ± 2.81*	17.15 ± 0.87

The cell viability was monitored through the MTT assay. Optical density of control was taken as 100 % of cell viability. Data are presented as mean ± SEM of at least three independent experiments. $^{*}P < 0.001$ and $^{\#}P < 0.01$ represents significant difference compared to treatment with free SIM (Student's t Test for paired samples).

Apoptosis is the programmed cell death process induced by intrinsic and extrinsic stimuli which triggers a cascade of intracelular molecules that initiate the cell death program. This process is mediated by caspases, a family of cysteine proteases, and is morphologically characterized by shrinking and fragmentation of cells and their nuclei.[39,40] The ability of free SIM and SIM-NP to induce apoptosis on HT-29 colon carcinoma cells was investigated using acridine orange/ethidium bromide (AO/EB) staining (Figure 2). In the AO/EB staining assay, the control group (not treated cells) showed bright green nuclei with uniform intensity, evidencing the cell viability. After free SIM and SIM-NP treatment for 24 h, HT-29 cells shrank and adhered together. Moreover, detached condensed nuclei or apoptotic bodies were clearly shown in the apoptotic cells after staining with ethidium bromide (red fluorescence). This red dye is membrane-impermeable owing to two positive charges in its structure, but it enters the cells when membrane damage occurs. Ethidium bromide has a strong ability to intercalate DNA because it binds to nucleic acids and the fluorescence change is proportional to the number of apoptotic cells.[36,41] The treatment of HT-29 cells with both free SIM and SIM-NP for 24 h increased the number of apoptotic cells, when compared with control group (Figure 2). The apoptotic effect exhibited by SIM-NP treatment may be attributed to the action of SIM, since unloaded nanoparticles were not able to induce apoptosis cell death. This result is in agreement with the literature, since simvastatin exposure to COLO 205 and HCT 116 human colon carcinoma cells proved to induce apoptosis.[5,42]

The effect of free SIM and SIM-NP on the proliferation of HT-29 human colon carcinoma cells was carried out by the colony assay. This assay tests every cell in the population for its ability to undergo “unlimited” division and it integrates all forms of cell death, being the method of choice to determine the effectiveness of cytotoxic agents. Therefore, this methodology evaluates cell survival in the

course of time.[43,44] Interestingly, 6 days of exposure to free SIM treatment was enough to cause an expressive decrease of HT-29 cell colonies (about 98%), while treatment with SIM-NP and 5-FU reduced about 79% and 85%, respectively. It is important to mention that the size of colonies was smaller in the presence of free SIM and 5-FU (Figure 3). As already mentioned before, the unloaded-NP presented some cytotoxicity after 48 and 72 h of treatment. The results obtained in the colony assay corroborate the MTT assay results, since after 6 days of treatment the unloaded-NP nanoparticles reduced about 53% the number of colonies. However, it is possible to observe that there was no change in the size of the colonies. The antiproliferative effects of simvastatin were previously demonstrated in a wide range of cancer cell lines.[45-47]

Figure 2. Detection of apoptotic effects of free SIM, SIM-NP, and unloaded-NP on HT-29 human colon carcinoma cells by acridine orange/ethidium bromide method. Cells were incubated with free SIM, unloaded-NP, and SIM-NP at their respective IC_{50} values for 24 hours. Viable cells exhibited green fluorescence (acridine orange staining) whereas apoptotic cells exhibited orange-red nuclear fluorescence (ethidium bromide staining). The group without treatment was taken as control group. The slides were viewed with an increase of 40x. The analysis was performed using ImageJ software. Statistically significant differences compared to the control group (*P <0.001), the SIM-NP group (^{a}P < 0.001) and the group treated with free SIM ($^{\#}$P < 0.001), using one-way ANOVA followed by Bonferroni's test.

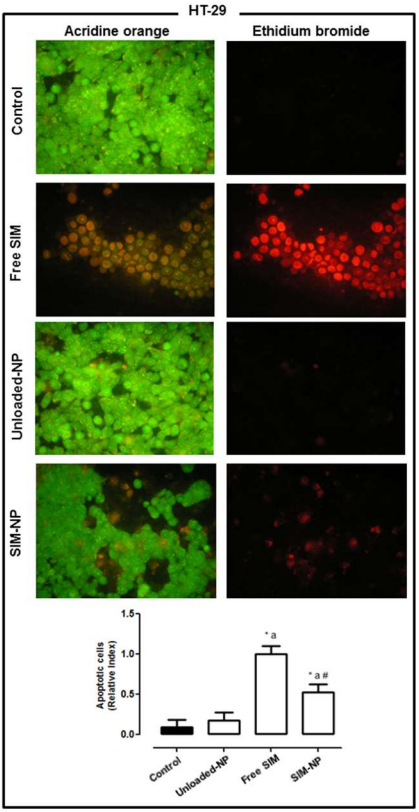

Figure 3. Effect of free SIM, SIM-NP, unloaded-NP, and 5-FU on HT-29 cell proliferation. HT-29 human colon adenocarcinona cells (1.0×10^3) were cultured in different concentration of free SIM, SIM-NP, unloaded-NP, and 5-FU for 24 hours. Macroscopy images are representative of HT-29 cells upon 10 days incubation (37ºC, 5% CO_2). Stained cells indicate the viable cells. The group without treatment was taken as control group. Statistically significant differences compared to the control group (* $P < 0.001$), the SIM-NP group (^{a} $P < 0.001$) and the group treated with free SIM ($^{\#}$ $P < 0.001$), using one-way ANOVA followed by Bonferroni's test.

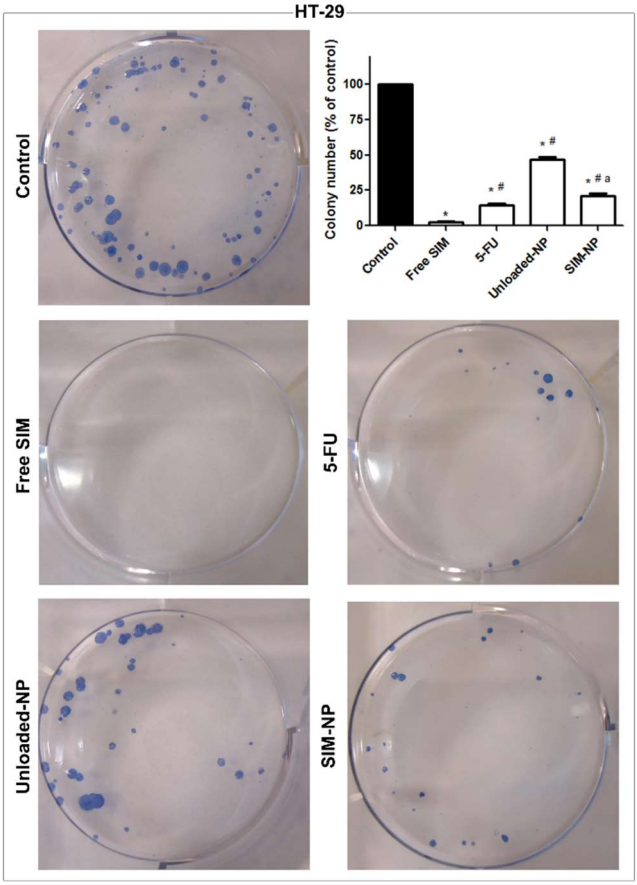

One parameter of aggressiveness of HT-29 human colon carcinoma cells is its capacity for migration. The scratch assay, an *in vitro* wound healing assay, was used to assess the effect of free SIM and SIM-NP on HT-29 cells migration. This method is based on the creation of an artificial gap called "scratch" on the confluent cell monolayer. When wounded or scratched, cell monolayers respond to the disruption of cell-cell contacts and then the cells polarize toward the wound, initiate protrusion, migrate, and close the wound.[48,49] To enable wound healing, free SIM, SIM-NP and 5-FU were used in their respective IC_{50} dose. The scratch assay (Figure 4) revealed that free SIM and SIM-NP inhibits HT-29 cells migration when compared with non-treated control group. The inhibition of HT-29 migration by SIM-NP may be attributed to the action of SIM, since unloaded-NP were not able to reduce the wound area. Besides that, the reduction of the cells that were able to migrate after the treatment with free SIM and SIM-NP can be partially due to the inhibition of cell proliferation and induction of apoptosis.

Figure 4. Effect of free SIM, SIM-NP, and unloaded-NP on HT-29 cell migration in *in vitro* scratching assay. HT-29 human colon adenocarcinoma cells (1.0 x 10^6) were treated with free SIM, SIM-NP, unloaded-NP, and 5-FU in their respective IC_{50} values and incubated for 24 hours. The group without treatment was taken as control group. (**Panel A**) Microscopy images were acquired at 40 x magnification using a phase contrast microscope (Olympus BX40, Japan), at days 0, 1, and 4 after incubation in scratch assay. (**Panel B**) The mean area was measured by quantifying the total distance that the cells moved from the edge of the scratch toward the center (*ImageJ* software). (**Panel C**) Percentage of migration rate was calculated using the comparison of the images from day 0 with those obtained on day 1 or 4. Significant differences compared to the control groups: 0 h group (* $P < 0.001$), 24 h group ($^{\#}P < 0.001$) and 96 h group (^{a} $P < 0.001$), using one-way ANOVA followed by Bonferroni's test.

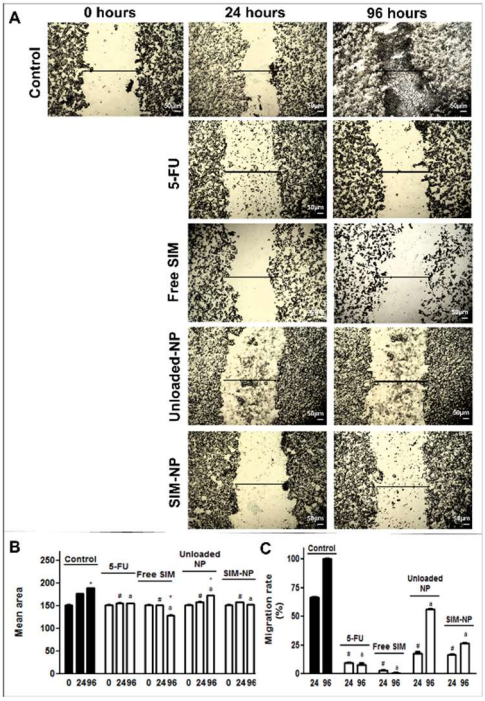

CONCLUSIONS

In this study, we reported the antitumor activity of SIM-loaded chitosan nanoparticles against the HT-29 human colon carcinoma cells. Both free and encapsulated drug exhibited cytotoxic effect, besides to cause programmed cell death (apoptosis), inhibit cell migration, and reduce the ability of HT-29 cells to form colonies. However, *in vivo* studies should still be carried out to demonstrate the interest of this drug delivery system in the colorectal cancer treatment.

ACKNOWLEDGEMENTS

This research was supported by the Coordination for the Improvement of Higher Education Personnel Superior (CAPES, Ministry of Education, Brazil), which granted a scholarship to one of the authors.

REFERENCES

1. Sassano A, Platanias LC 2008. Statins in tumor suppression. Cancer Lett. 260:11 – 19.
2. Bardou M, Barkun A, Martel M 2010. Effect of statin therapy on colorectal cancer. Gut. 59:1572 – 1585.
3. Brown JA 2007. Cholesterol, statins and cancer. Clin. Exp. Pharmacol. Physiol. 34:135 – 141.
4. Qi XF, Kim DH, Yoon YS, Kim SK, Cai DQ, Teng YC, Shim KY, Lee KJ 2010. Involvement of oxidative stress in simvastatin-induced apoptosis of murine CT26 colon carcinoma cells. Toxicol. Lett. 199:277 – 287.
5. Cho SJ, Kim JS, Kim JM, Lee JY, Jung HC, Song IS 2008. Simvastatin induces apoptosis in human colon cancer cells and in tumor xenografts, and attenuates colitis-associated colon cancer in mice. Int. J. Cancer 123:951 – 957 (2008).
6. Soppimath KS, Aminabhavi TM, Kulkarni AR, Rudzinski WE 2001. Biodegradable polymeric nanoparticles as drug delivery devices. J. Control. Release 70:1 – 20.

7. Mora-Huertas E, Fessi H, Elaissari A 2010. Polymer-based nanocapsules for drug delivery. Int. J. Pharm. 385:113 – 142.
8. Liu Z, Jiao Y, Wang Y, Zhou C, Zhang Z 2008. Polysaccharides-based nanoparticles as drug delivery systems. Adv. Drug Deliv. Rev. 60:1650 – 1662.
9. Kumar MNVR, Muzzarelli RAA, Muzzarelli C, Sashiwa H, Domb AJ 2004. Chitosan Chemistry and Pharmaceutical Perspectives Chem. Rev. 104:6017 – 6084.
10. Dash M, Chiellini F, Ottenbrite RM, Chiellini E 2001. Chitosan—A versatile semi-synthetic polymer in biomedical applications. Prog. Polym. Sci. 36:981 – 1014.
11. Hejazi R, Amiji M 2003. Chitosan-based gastrointestinal delivery systems. Control. Release. 89:151 – 165.
12. Park JH, Saravanakumar G, Kim K, Kwon IC 2010. Targeted delivery of low molecular drugs using chitosan and its derivatives. Adv. Drug Del. Rev. 61:28 – 41.
13. Zhang H, Alsarra IA, Neau SH 2002. An *in vitro* evaluation of a chitosan-containing multiparticulate system for macromolecule delivery to the colon. Int. J. Pharm. 239:197 – 205.
14. Fan W, Yan W, Xu Z, Ni H 2012. Formation mechanism of monodisperse, low molecular weight chitosan nanoparticles by ionic gelation technique. Colloids Surf. B 90:21 – 27.
15. Mosmann, T. 1983. Rapid colorimetric assay for cellular growth and survival: application to proliferation and cytotoxicity assays. J. Immunolog. Methods. 65(1-2): 55-63.
16. Geng X, Zeng ZC, Wang JY 2003. Docetaxel inhibits SMMC-7721 human hepatocellular carcinoma cells growth and induces apoptosis. World J. Gastroenterol. 9:696 – 700.
17. Half E, Arber N 2009. Colon cancer: preventive agents and the presente status of chemoprevention. Expert Opin. Pharmacother. 10(2):211 – 219.
18. Jain A, Jain SK, Ganesh N, Barve J, Beg AM 2010. Design and development of ligand-appended polysaccharidic nanoparticles for the delivery of oxaliplatin in colorectal cancer. Nanomedicine: NBM 6:179 – 190.

19. Khan DR 2010. The Use of Nanocarriers for Drug Delivery in Cancer Therapy. J. Cancer Sci. Ther. 2(3):58 – 62.
20. Wong WWL, Dimitroulakos J, Minden MD, Penn LZ 2002. HMG-CoA reductase inhibitors and the malignant cell: the statin family of drugs as triggers of tumor-specific apoptosis. Leukemia 16:508 – 519.
21. Peer D, Karp JM, Hong S, Farokhzad OC, Margalit R, Langer R 2007. Nanocarriers as an emerging platform for cancer therapy. Nat. Nanotechnol. 2:751 – 760.
22. Gauthaman K, Fong CY, Bongso A 2009. Statins, Stem Cells, and Cancer. J. Cell. Biochem. 106:975 – 983.
23. Chan KKW, Oza AM, Siu LL 2003. The Statins as Anticancer Agents. Clin. Cancer Res. 9:10 – 19.
24. Osmak M 2012. Statins and cancer: Current and future prospects. Cancer Lett. 324:1 – 12.
25. Gruenbacher G, Thurnher M 2015. Mevalonate metabolism in cancer. Cancer Lett. 356:192 – 196.
26. Gauthaman K, Richards M, Wong J, Bongso A 2007. Comparative evaluation of the efects of statins on human stem and cancer cells in vitro. Reprod. Biomed. Online 15(5):566 – 581.
27. Kotamraju S, Williams CL, Kalyanaraman B 2007. Statin-Induced Breast Cancer Cell Death: Role of Inducible Nitric Oxide and Arginase-Dependent Pathways. Cancer Res. 67(15):7386 – 8973.
28. Gan Q, Wang T, Cochrane C, McCarron P 2005. Modulation of surface charge, particle size and morphological properties of chitosan–TPP nanoparticles intended for gene delivery. Colloids Surf. B 44:65 – 73.
29. Huang M, Khor E, Lim LY 2004. Uptake and Cytotoxicity of Chitosan Molecules and Nanoparticles: Effects of Molecular Weight and Degree of Deacetylation. Pharm. Res. 21(2):344 – 353.
30. Rodrigues S, Dionísio, M, López, CR, Grenha, A 2012. Biocompatibility of Chitosan Carriers with Application in Drug Delivery. J. Funct. Biomat. 3:615 – 641.

31. Huang R, Mendis E, Rajapakse N, Kim SK 2006. Strong electronic charge as an important factor for anticancer activity of chitooligosaccharides (COS). Life Sci. 78:2399 – 2408.
32. Kowapradit J, Opanasopit P, Ngawhirunpat T, Apirakaramwong A, Rojanarata T, Ruktanonchai U, Sajomsang W 2010. *In vitro* Permeability Enhancement in Intestinal Epithelial Cells (Caco-2) Monolayer of Water Soluble Quaternary Ammonium Chitosan Derivatives. AAPS PharmSciTech. 11(2):497 – 508.
33. Loh JW, Yeoh G, Saunders M, Lim LY 2010. Uptake and cytotoxicity of chitosan nanoparticles in human liver cells. Toxicol. Appl. Phar. 249:148–157.
34. Carreño-Gómez B, Duncan R 1997. Evaluation of the biological properties of soluble chitosan and chitosan microspheres. Int. J. Pharm. 148:231 – 240.
35. Richardson SC, Kolbe HV, Duncan R 1999. Potential of low molecular mass chitosan as a DNA delivery system: biocompatibility, body distribution and ability to complex and protect DNA. Int. J. Pharm. 178: 231 – 243.
36. King MA 2000. Detection of dead cells and measurement of cell killing by flow cytometry. J. Immunol. Methods. 243: 155 – 166.
37. Longley DB, Harkin P, Johnston PG 2003. 5-Fluorouracil: mechanisms of action and clinical strategies. Nature Reviews 3:330 – 338.
38. Rich TA, Shepard RC, Mosley ST 2004. Four Decades of Continuing Innovation With Fluorouracil: Current and Future Approaches to Fluorouracil Chemoradiation Therapy. J. Clin. Oncol. 22:2214 – 2232.
39. Nagata S 2005. DNA degradation in development and programmed cell death. Annu. Rev. Immunol. 23:853 – 875.
40. Acquavella N, Quiroga MF, Wittig O, Cardier JE 2009. Effect of simvastatin on endothelial cell apoptosis mediated by Fas and TNF-α. Cytokine 49:45 – 50.
41. Lewinski N, Colvin V, Drezek R 2008. Cytotoxicity of Nanoparticles. Small. 4(1):26 – 49.

42. Chang HL, Chen CY, Hsu YF, Kuo WS, Ou G, Chiu PT, Huang YH, Hsu MJ. 2013. Simvastatin induced HCT166 colorectal cancer cell apoptosis through p38MAPK-p53-*survivin* signaling cascade. Biochim Biophys Acta, 1830:4053 – 4064.
43. Brown JM, Attardi LD 2005. The role of apoptosis in cancer development and treatment response. Nat. Rev. Cancer 5:231–237.
44. Franken NA, Rodermond HM, Stap J, Haveman J, Van Bree C 2006. Clonogenic assay of cells *in vitro*. Nat. Protoc. 1:2315–2319.
45. Seeger H, Wallwiener D, Mueck AO 2003. Statins Can Inhibit Proliferation of Human Breast Cancer Cells in Vitro. Exp. Clin. Endocrinol. Diabetes 111:47 – 48.
46. Wu H, Jiang H, Lu D, Xiong Y, Qu C, Zhao D, Mahmood A, Chopp M 2009. Effect of Simvastatin on Glioma Cell Proliferation, Migration and Apoptosis. Neurosurgery 65(6): 1087 – 1097.
47. Schointuch MN, Gilliam TP, Stine JE, Han X, Zhou C, Gehrig PA, Kim K, Bae-Jump BL 2014. Simvastatin, an HMG-CoA reductase inhibitor, exhibits anti-metastatic and anti-tumorigenic effects in endometrial cancer. Gynecol. Oncol. 134:346 – 355.
48. Yarrow JC, Perlman ZE, Westwood NJ, Mitchison TJ 2004. A high-throughput cell migration assay using scratch wound healing, a comparison of image-based readout methods. BMC Biotechnol. 4(21):1 – 9.
49. Liang CC, Park AY, Guan JL 2007. *In vitro* scratch assay: a convenient and inexpensive method for analysis of cell migration *in vitro*. Nat. Protoc. 2(2):329 – 333.

CAPÍTULO 2

No capítulo 2 estudos de formulação foram realizados utilizando a sulfobutiléter-β-ciclodextrina, uma ciclodextrina aniônica, como uma segunda estratégia para aumentar a associação da sinvastatina nas nanopartículas de quitosana. As ciclodextrinas tem sido utilizadas como poliânions para formar nanopartículas de quitosana pela técnica de interação iônica. Além disso, as ciclodextrinas possuem a habilidade de formar complexos de inclusão com fármacos hidrofóbicos e, desta maneira, são capazes de aumentar a associação dos mesmos às nanopartículas (MAHMOUD et al., 2011; WU, SHEN, FANG, 2012). Primeiramente, um estudo de solubilidade de fases foi realizado para avaliar a formação de complexos de inclusão entre sinvastatina e sulfobutiléter-β-ciclodextrina. Em seguida, nanopartículas foram obtidas pela da técnica de interação iônica através da adição diferentes concentrações de sulfobutiléter-β-ciclodextrina às nanopartículas de quitosana/tripolifosfato e também foram desenvolvidas nanopartículas constituídas apenas de quitosana/sulfobutiléter-β-ciclodextrina. A influência da concentração de ciclodextrina adicionada às formulações sobre as propriedades físico-químicas das partículas e sobre a capacidade de incorporar a sinvastatina foi avaliada. A encapsulação das nanopartículas em micropartículas de Eudragit® S100, bem como a caracterização dos complexos de inclusão, nanopartículas e micropartículas entéricas foram realizadas conforme descrito no capítulo 1.

Publicação 1. *Spray-Dried Enteric Microparticles Entrapping Sulfobutylether-β-Cyclodextrin/Chitosan Nanoparticles as a New Approach to Deliver Simvastatin in The Colon Aiming the Treatment of the Colorectal Cancer*

Spray-Dried Enteric Microparticles Entrapping Sulfobutylether-β-Cyclodextrin/Chitosan Nanoparticles as a New Approach to Deliver Simvastatin in the Colon Aiming the Treatment of the Colorectal Cancer

MARIANA DALAGNOL[1], HELENA MARIA CABRAL MARQUES[2], ELENARA LEMOS-SENNA[1*]

[1]Pharmaceutical Technology Laboratory, Pharmaceutical Sciences Department, Federal University of Santa Catarina, Campus Universitário, Florianópolis, 88040-970, Brazil.
[2]IMed.UL (Research Institute for Medicines and Pharmaceutical Sciences), Faculty of Pharmacy, University of Lisbon, Lisbon, 1649-003, Portugal.

[*]Corresponding author: +55 48 3721 5067, Email address: lemos.senna@ufsc.br

ABSTRACT

In this study, spray-dried enteric microparticles (SDP) entrapping simvastatin (SIM)-loaded chitosan nanoparticles (CSNP) were developed aiming the delivery of this drug in the colon for the treatment of colorectal cancer. The addition of sulfobutylether-β-cyclodextrin (SBE-β-CD) to the chitosan/tripolyphosphate nanoparticles ($CSNP_{TPP/CD}$) and the formulation of chitosan/sulfobutylether-β-cyclodextrin nanoparticles ($CSNP_{CD}$) were tested as strategies to increase SIM loading. $CSNP_{CD}$ displayed mean diameters ranging from 345.8 to 406.9 nm, and $CSNP_{TPP/CD}$ displayed mean diameters between 319.6 and 549.5 nm. All formulations exhibited positively charged surface. $CSNP_{CD}$ showed SIM content varying from 160.38 µg/mL to 634.62 µg/mL and the addition of SBE-β-CD in the nanoparticles allowed and increasing of drug loading up to 13 times. SDPs were prepared by adding Eudragit® S100 in the external phase of CSNP. The spray-drying technique yielded SDP displaying

spherical shape, sizes around 5 μm, and negative zeta potential values. The interactions between the components of the formulations and crystallinity properties of the particles were assessed by DSC, FT-IR, and DRX techniques. The release studies demonstrated that a small fraction of the drug was released in acidic medium, but the drug release occurred in a sustained way over 8 hours in pH 7.2 phosphate buffer solution. These results indicated that this innovative drug delivery system could be promising to deliver SIM in the colon.

Keywords: Simvastatin; Chitosan; Nanoparticles; Sulfobutylether-β-cyclodextrin; Enteric Microparticles; Spray-drying; Colonic Drug Delivery.

INTRODUCTION

Simvastatin (SIM) is a lipophilic drug derived from the fermentation of *Aspergillus terreus* and acts as a lipid-lowering agent by inhibiting hydroxy-3-methylglutaryl coenzyme A (HMG-CoA) reductase. HMG-CoA reductase catalyzes the conversion of HMG-CoA into mevalonate and is the rate-limiting step in the cholesterol biosynthesis.[1,2] However, the role of SIM extends beyond its lipid-lowering effects, since this drug has been proven to possess a wide variety of therapeutic properties, including antitumor activity. Several studies have demonstrated that SIM is able to induce the apoptosis in murine CT26 colon cancer cells and in COLO 205, HCT 116 and HT-29 human colon cancer cells.[3-5] Also, SIM was able to reduce the tumor development in the murine colitis-associated colon cancer model.[3] These findings suggest that SIM may constitute a potential therapeutic agent and/or may be used in combined interventions against colorectal cancer.

The colonic delivery of drugs after oral administration is a promising strategy for the treatment of several colonic diseases, such as colorectal cancer. In the local

treatment of these diseases, high local drug concentration can be achieve, while minimizing side effects that occur when the drug is released in the upper gastrointestinal tract (GIT) or unnecessary systemic absorption.[6,7] Due to the distal location of the colon in the GIT, an ideal colonic delivery system should prevent drug release in the stomach and small intestine and affect an abrupt onset of drug release upon entry into the colon.[8] The most common pharmaceutical strategies used to achieve a colon-specific drug delivery either utilize a single or a combination of two or more physiological characteristics of the colon, which includes pH, transit time, colonic microflora and luminal pressure.[9-11]

In particular, chitosan (CS) nanoparticles have been considered a promising material for the development of colonic drug delivery systems. Chitosan is a linear copolymer of β-(1-4) linked 2-acetoamido-2-deoxy-β-D-glucopyranose and 2-amino-2-deoxy-β-D-glycopyranose units obtained by deacetylation of chitin, a polysaccharide widely distributed in the exoskeleton of crustaceans, insects and certain fungi.[12] Besides its abundant availability, unique mucoadhesivity, biocompatibility, biodegradability, non-toxicity and low-immunogenicity, CS undergoes degradation of the glycosidic linkages by the colonic microflora, which may contribute for the control of the drug release rate.[13,14] Colonic delivery of drugs, peptides, proteins, and genes have been achieved by using different chitosan formulations, including chitosan-coated tablets, capsules, beads, microparticles, and nanoparticles.[15]

CS nanoparticles can be prepared by several techniques, but the ionotropic gelation has been by far the most reported in the literature. The solubilization of CS occurs by protonation of the $–NH_2$ function on the C-2 position of the D-glucosamine repeat unit, whereby it is converted to a positively charged polysaccharide in acidic media.[16,17] The cationic amino groups of CS can interact electrostatically with oppositely charged polyelectrolytes to form nanoparticles.[18,19] Usually, tripolyphosphate (TPP) is employed as the anionic

polyelectrolyte, however, the nanoparticles made from ionic gelation between CS and TPP are not suitable to load poorly water-soluble drugs as SIM. Some studies have demonstrated that self-organized structures, resulting from the electrostatic interaction chitosan and lecithin, were able to encapsulate hydrophobic drugs with high encapsulation efficiencies.[20-21] Similarly, in our previous studies, the use of the anionic surfactant sodium taurocholate was proposed as a new strategy to increase the simvastatin loading into chitosan nanoparticles (results not published). Also, anionic cyclodextrins as sulfobutylether-β-cyclodextrin or carboxymethyl-β-cyclodextrin have been used as a source of polyanions to form CS nanoparticles. The main advantage lies in the ability of these excipients to include hydrophobic drugs inside their cavity, improving the association of poorly water-soluble drugs into CS nanoparticles.[22-25]

Sulfobutylether-β-cyclodextrin (SBE-β-CD) is a negatively charged β-cyclodextrin derivative, which has a sodium sulfonate salt separated from the lipophilic cavity by a butyl ether spacer group. SBE-β-CD has an average of 6.8 substituents per cyclodextrin and therefore about seven negative charges associated with it. The SBE-β-CD, being a polyanionic and complexing agent, has been considered as a versatile substance to form nanoparticles with CS by the ionic gelation technique. Drugs as econazole nitrate, methotrexate and calcium folinate, glutathione, and docetaxel have been successfully loaded into CS/SBE-β-CD nanoparticles.[22,26,27,23] In this study, we propose to combine the advantages of CS nanoparticles together with the favorable properties of SBE-β-CD in a unique drug delivery system to delivery of SIM for the treatment of the colorectal cancer. However, to preserve the formulation during its passage through the stomach and upper part of the small intestine, the chitosan nanoparticles were entrapped into Eudragit® S100 microparticles, using the spray-drying technique. Eudragit® S100 is an anionic copolymer based on methacrylic acid and methacrylate, which dissolves at pH higher than pH 7.0. This approach was

used to deliver the caspase 3 activator and 5-fluorouracil in the colon, but is the first time tested to deliver simvastatin as a promising drug to be used in the adjuvant therapy to treat the colorectal cancer.[28,29]

MATERIALS AND METHODS

Materials

Simvastatin (SIM) was purchased from Pharma Nostra® (Rio de Janeiro, Brazil). Chitosan (CS) (MW 50 – 190 KDa; 75 – 85% deacetylated; viscosity 20 – 300 cP) was purchased from Sigma-Aldrich (St. Louis, MO, USA). Sodium tripolyphosphate (TPP) was a gift from Plury Química (São Paulo, Brazil). Sulfobutylether-β-ether cyclodextrin (SBE-β-CD) (CAPTISOL®, average substitution degrees of sulfobutyl group: 6.6, MW 2163) was a gift from by CyDex Pharmaceuticals (Lawrence, Kansas, USA). Poly(methacrylic acid-co-methyl metacrylate) 1:2 (Eudragit® S100) was a gift from Rohm Pharma (Germany). All other chemicals were of analytical grade.

Methods

Phase-solubility

Phase-solubility studies were performed using the method described by Higuchi and Connors (1965)[30]. An amount of SIM exceeding its solubility was added to unbuffered aqueous solutions of SBE-β-CD (0, 2, 4, 6, 8, and 10 mM) in 10 mL capped tubes. The flasks were sealed to avoid changes due to evaporation and stirred for 48 hours at 25 ± 0.5 °C on rotatory shaker. Preliminary "time-dependence" experiments were performed which showed that the equilibrium was reached after 48 h stirring period. After equilibrium, the samples were filtered, suitably diluted with methanol, and analyzed by UV spectroscopy at wavelength of

237 nm to determine SIM concentration. The apparent stability constant ($K_{1:1}$) and the complexation efficiency (CE) were determined from the slope of the linear phase-solubility diagram (the total drug solubility versus total SBE-β-CD concentration in millimolar[31]:

$$K_{1:1} = \frac{\text{slope}}{S_0(1 - \text{slope})} \quad \text{(Eq. 1)}$$

$$\text{CE} = \frac{\text{slope}}{1 - \text{slope}} = \frac{[\text{D/CD}\,[\text{complex}]}{\text{CD}} = K_{1:1} \times S_0 \quad \text{(Eq. 2)}$$

where S_0 is the intrinsic solubility of the drug.

Nanoparticles preparation

The chitosan nanoparticles (CSNP) were prepared using the ionic gelation technique, which was modified to allow the incorporation of SBE-β-CD.[32,33] Briefly, 10 mL of an ethanol:water solution (40:60 v/v) containing SIM (10 mg), TPP (0 or 4.58 mg), and SBE-β-CD (25, 35, 45, 55, or 65 mg) was prepared. Following, the hydroalcoholic solution was slowly poured using a glass Pasteur pipette into 10 mL of a 0.55 % (w/v) CS solution in 1% (v/v) acetic acid, under magnetic stirring. The resulting colloidal suspension was evaporated under reduced pressure to remove the organic solvent and adjust the final volume to 10 mL. The formulations were prepared in triplicate. In order to evaluate the formation of inclusion complexes, the hydroalcoholic solutions containing SIM/SBE-β-CD and SIM/SBE-β-CD/TPP were evaporated under reduced pressure, filtered, freeze-dried, and characterized.

Physicochemical and morphology characterization of chitosan nanoparticles

The mean diameter and zeta potential of the CSNPs were determined by dynamic light scattering and laser Doppler anemometry, respectively, using a Zetasizer Nano Series (Malvern Instruments, UK). The nanoparticles were dispersed in ultrapure water at appropriate concentrations. Size analysis were performed at fixed scattering angle of 173°. For measurements of zeta potential (ζ), samples were placed in an electrophoretical cell, where a potential of ±150 mV was established. The zeta potential values were calculated from mean electrophoretic mobility values using Smoluchowski's equation. The morphology of the CSNPs was examined by transmission electron microscopy (TEM) using a H-8100 Hitachi with high brightness LaB6 electron source microscope (Schaumburg, Illinois, USA) and acceleration voltage of 200 kV. The nanoparticles suspensions were dropped onto a carbon-coated copper grids and were visualized without staining.

Determination of simvastatin content and entrapment efficiency in nanoparticles

The SIM content and entrapment efficiency were determined by UV spectroscopy using a Hitachi U-1900 spectrophotometer (Tokyo, Japan) at 237 nm. The analytical method was previously validated according to ICH.[34] The calibration curve for SIM in methanol was linear over the range of 4 to 16 μg/mL with a correlation coefficient of 0.999. The detection and quantification limits were 0.223 μg/mL and 0.744 μg/mL, respectively, indicating that the method was sufficiently sensitive to determine SIM content in the nanoparticles. The specificity of the method was confirmed after analysis of unloaded nanoparticles. The precision of the method was evaluated and all relative standard deviation values (RSD) were below 2%, indicating an acceptable intra-

day and inter-day variability of SIM content. The recovery values were ranged from 99% to 101%, satisfying the acceptance criteria for accuracy in this study.

The drug content was determined in the solutions after complete dissolution of the nanoparticles in methanol and the results were expressed as µg of SIM per mL of CSNP suspensions. The entrapment efficiency (EE) was estimated as being the percent difference between the total concentration of SIM in the CSNP suspensions and the concentration found in the supernatant that was assessed by ultrafiltration/centrifugation procedure using Microcon Centrifugal Filter Devices with Ultracel YM-100 (100.000 NMWL, Millipore, EUA). All the analyses were carried out in triplicate.

Preparation of enteric spray-dried microparticles entrapping chitosan nanoparticles

Spray drying was performed using a Büchi Mini Spray Dryer Model B-290 (Büchi Labortechnik AG, Flawil, Switzerland). Drying conditions are given as follows for all prepared samples: the inlet temperature was 120 °C, outlet temperature was 65~75 °C, the pump flow rate was 5 mL/min, and the aspiration setting was 100%[35]. Previously to spray drying procedure, 50 mL of a SIM-loaded CS nanoparticle suspension ($CSNP_{CD65}$ and $CSNP_{TPP/CD45}$) was added to 100 mL of an aqueous solution (pH 7.2) containing 3.20 g, 4.55 g or 5.85 g of Eudragit® S100 for $CSNP_{CD65}$, and 2.86 g, 4.01 g, and 5.15 g of Eudragit® S100 for $CSNP_{TPP/CD45}$ in order to obtain nanoparticle/Eudragit® S100 ratios of 1:4, 1:6, and 1:8 (w/w), respectively. The spray-dried powders (SDP) were collected and stored in glass bottles tightly until analyses. The yield (%) of the spray-drying process was estimated considering the theoretical amount of solid in the feed solutions.

Physicochemical and morphology characterization of spray-dried powders

The residual moisture content of the spray-dried powders was obtained using the Ohaus MB25 Halogen Moisture Analyser (Ohaus®, New Jersey, USA). About 600 mg of the SDP were weighted in an aluminum dish and heated until 105 °C by the integral halogen dryer allowing the moisture to vaporize. This temperature was held constant and the results were displayed as % of moisture content. All the analyses were carried out in triplicate.

The morphology of the particles was examined using a Jeol JSM-6390LV (Jeol Inc., USA) scanning electron microscope, operated under high vacuum conditions with an acceleration voltage of 100 kV. The samples were mounted onto aluminum pin stubs using double-sided tape and sputter-coated with gold in a Leica EM SCD500 (Leica Microsystems, USA) coater unit. The mean particle size of the samples was determined after analysis of SEM images using the SizeMeter® software. The Martin's diameter of 200 randomly selected particles was determined in a fixed direction from the field of view of the SEM images. The zeta potential of the particles was determined by laser Doppler anemometry using a Zetasizer Nano Series (Malvern Instruments, UK), as described above.

The SIM content in the SDP was determined by UV spectroscopy using a UV-1800 Shimadzu spectrophotometer at 237 nm after complete dissolution of the particles in methanol. The results were expressed as weight percent (wt%) of SIM in the spray-dried powders. All analyzes were carried out in triplicate.

Differential Scanning Calorimetry (DSC)

The thermal behavior of the raw materials, SIM/SBE-β-CD and SIM/TPP/SBE-β-CD complexes, freeze-dried chitosan nanoparticles, and spray-dried powders were

obtained using a DSC Q200 (TA Instruments, USA). For the measurements, approximately 2 mg of the sample were accurately weighted in aluminum pans, sealed, and heated from 30 to 300 °C under nitrogen atmosphere, with a heating rate of 10 °C/min.

Fourier Transform Infrared Spectroscopy (FT-IR)

The FT-IR spectra were obtained using an IR Affinity-1 Shimadzu (Shimadzu®, Japan). The spectra of the raw materials, SIM/SBE-β-CD and SIM/TPP/SBE-β-CD complexes, freeze-dried chitosan nanoparticles, and spray-dried powders were recorded in the wavenumber ranging from 4000 to 650 cm^{-1}.

X-ray diffraction analysis (XRD)

The X-ray diffraction patterns of the raw materials, freeze-dried chitosan nanoparticles, and spray-dried powders were recorded using a Rigaku MiniFlex II diffractometer (Tokyo, Japan), using a CuKα radiation at 30 kV and 15 mA. Measurements were carried out at 2θ angles range from 5 to 45° with a step size of 5° and a scan step time of 5 s.

In vitro SIM release studies

The *in vitro* release of SIM from SDPs was assessed on an Erweka BioDis RRT 10 dissolution tester (Erweka®, Germany) using the United States Pharmacopoeia (USP) apparatus III of reciprocate cylinders. The dissolution conditions were established according to a modified European Pharmacopeia method: one hour in 250 mL of pH 1.2 hydrochloric acid solution, 3 hours in 250 mL of pH 4.5 phosphate buffer solution, and 8 hours in 250 mL of pH 7.2 phosphate buffer solution.[35] The samples were accurately weighted (130 mg, 150 mg, and 170 mg for SDP_{CD65} and 170

mg, 180 mg, and 190 mg for $SDP_{TPP/CD45}$ prepared with the nanoparticle/Eudragit® S100 ratios of 1:4, 1:6, and 1:8, respectively), filled into transparent capsules and placed in the dissolution station where the temperature was kept at 37 ± 0.5 °C. The dip speed was set at 20 cycles/minutes when dissolution was carried out in pH 1.2 hydrochloric acid and pH 4.5 phosphate buffer solutions, and at 8 cycles/minute when dissolution was carried out in pH 7.2 phosphate buffer solution. At specific intervals of time, aliquots of the dissolution medium were withdrawn without replacement. The SIM released from the particles was determined by an UV spectrophotometric method at 237 nm. Cumulative amounts of SIM released (%) versus time (h) curves were plotted. The dissolution efficiency (DE %) was determined for each release profile, as the area under the release curve obtained for the different release media, expressed as a percentage of the area of the rectangle described by 100% dissolution in the same time. All the experiments were carried out with six replicates. The results were statistically analyzed by ANOVA followed by the Tukey´s multiple comparisons test. In order to evaluate the redispersion ability of chitosan nanoparticles during the SIM release studies, samples of spray-dried powders were dispersed in water adjusted to pH 7.2 and maintained under magnetic stirring during 5 h. Then, the samples were adequately diluted in ultrapure water and analyzed according their particles sizes by dynamic light scattering in a Zetasizer Nano Series (Malvern Instruments, UK), as described above.

RESULTS AND DISCUSSION

Phase-solubility

Phase-solubility studies were previously carried out in order to investigate the interaction between SIM and SBE-β-CD. The solubility of SIM increased linearly as a function of SBE-β-CD concentration, giving an A_L-type phase

solubility diagram, indicating the 1:1 SIM-SBE-β-CD complex was formed in solution over the SBE-β-CD concentration range of 0 to 10 mM (Figure 1). The solubility of SIM in aqueous solution at 25 °C increased up to 7.62 fold at 10 mM/L of SBE-β-CD concentration. The intrinsic solubility (S_0), the apparent stability constant ($K_{1:1}$) and the complexation efficiency (CE) were 0.015 mM, 900.94 M^{-1}, and 0.014, respectively. It has been reported that drug/cyclodextrin inclusion complexes with stability constant values ranging from 200 to 5,000 M^{-1} yield improvement in drug solubility. However**,** the complexation efficiency has been reported to be a more accurate method for determination of the solubilizing efficiency of cyclodextrin and it expresses the concentration ratio between cyclodextrin in a complex and free cyclodextrin. A CE of 0.018 indicated that 1 out of every 140 molecules of SBE-β-CD forms a complex with SIM.[31] The formation of complexes between SIM and hydroxypropyl-β-cyclodextrin[36], α-cyclodextrin and β-cyclodextrin[37], and randomly methylated β-cyclodextrin[38] has been described in the literature, and the apparent stability constant ($K_{1:1}$) values obtained were quite similar to that obtain for SBE-β-CD.

Figure 1. Phase-solubility diagram of SIM as a function of SBE-β-CD concentration at 25 ± 0.5 °C.

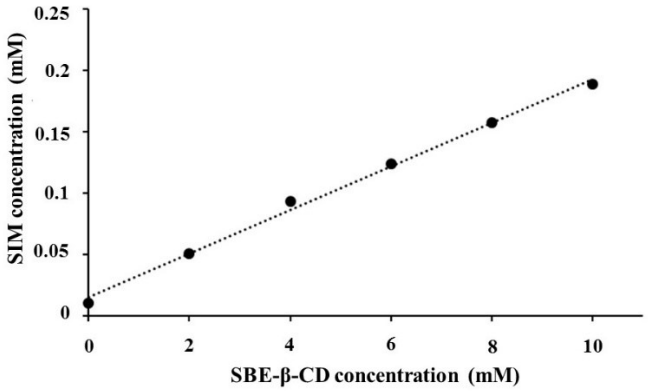

Preparation and characterization of SIM-loaded chitosan nanoparticles

The nanoparticles were prepared using the ionic gelation technique, which has attracted much attention because it is a very mild and simple process. In this study, we evaluated the effect of SBE-β-CD addition on the physicochemical properties of chitosan nanoparticles and on its ability to improve SIM loading in CS nanoparticles. Not only the incorporation of the negatively charged SBE-β-CD and TPP mixture to the CS solution led the formation of nanoparticle colloidal dispersions, but also nanoparticles could be obtained by using only SBE-β-CD as polyanion. The physicochemical properties and SIM loading obtained for the nanoparticle formulations are summarized in Table 1. The mean particle diameter for $CSNP_{CD}$ ranged from 345.8 nm to 406.9 nm with polidispersity index (PDI) values ranging from 0.11 to 0.31, and for $CSNP_{TPP/CD}$ the diameters varied from 319.6 to 549.5 nm with PDI values varying from 0.26 to 0.38. The $CSNP_{CD}$ and $CSNP_{TPP/CD}$ showed positive charges with zeta potential values ranging between +46.8 and +21.4 mV,

reflecting the presence of the amino groups of CS on the surface of the nanoparticles.[39] This net of positive charges of the nanoparticles is desirable to prevent particle aggregation and also to promote the subsequently electrostatic interaction with the negatively charged enteric polymer. Moreover, it was observed a decrease in the zeta potential values with the increase of SBE-β-CD concentration. This can be explained by an increase masking of the free positively charged amino groups of CS by the anionic groups in the SBE-β-CD structure.[33]

Table 1 shows that the SIM content in the nanoparticles depended upon the concentration of SBE-β-CD added to the formulations. It was observed an increase in the SIM content from 160.3 μg/mL to 634.6 μg/mL with the increase of the SBE-β-CD from 25 to 65 mg in the formulations. This effect was also observed in the formulations studies carried out by Mahmoud et al. (2011)[22] to encapsulate the econazole nitrate into chitosan/ SBE-β-CD nanoparticles and it also may be attributed to the increase in the amount of formed nanoparticles due to the greater concentration of the SBE-β-CD available to form nanoparticles and to encapsulate the drug. On the other hand, when nanoparticles were prepared in the presence of TPP, the SIM content values found in the colloidal dispersions were lower than those obtained when only SBE-β-CD was used to form the chitosan nanoparticles. In this case, the higher SIM content obtained was 476.1 μg/mL for $CSNP_{TPP/CD45}$ (CS/TPP/SBE-β-CD ratio of 6/0.5/4.9). However, this value was about 13 times higher than that obtained when chitosan nanoparticles were prepared only with TPP as polyanion. When SBE-β-CD amounts of 55 and 65 mg were tested (CS/TPP/SBE-β-CD ratios of 6/0.5/6 and 6/0.5/7.1), the SIM content values were reduced to 146 and 121 μg/mL, respectively. This decrease on SIM content may be explained by the excess of negative charges when SBE-β-CD was used in higher concentrations, promoting a destabilization of the nanoparticles and consequent decrease on SIM content. The

encapsulation efficiency values were above 93%, showing that SIM is found preferentially associated to the nanoparticles, probably due to the presence of interactions with the SBE-β-CD, since this drug exhibits a poor water solubility.

The TEM micrographs of the $CSNP_{CD}$ and $CSNP_{TPP/CD}$ are shown in Figure 2. The nanoparticles presented spherical shape with an irregular surface. It can be also noted that nanoparticles exhibit a deeper color in the core and lower electron density distribution on the surface. As SBE-β-CD contains sulphur element and TPP contains phosphorus, both having higher electron density than those elements of CS, it may be suggested that CS has a higher degree of cross-linking with SBE-β-CD and TPP in the nanoparticle core than the particle surface.[32]

Table 1. Physicochemical characteristics of the SIM-loaded CS nanoparticles (Mean ± SD, n = 3).

Formulation[1]	CS/CD (w/w) or CS/TPP/CD (w/w/w) ratio[2]	Mean diameter (nm)	PDI	Zeta potential (mV)	SIM content (μg/mL)	Encapsulation efficiency (%)
$CSNP_{CD25}$	6/2.7	345.8 ± 10.4	0.31 ± 0.02	+39.8 ± 0.3	160.3 ± 9.2	97.0 ± 0.1
$CSNP_{CD35}$	6/3.8	389.2 ± 16.8	0.22 ± 0.03	+35.9 ± 1.1	266.6 ± 35.9	98.2 ± 0.2
$CSNP_{CD45}$	6/4.9	395.1 ± 9.9	0.17 ± 0.01	+33.9 ± 0.8	308.4 ± 37.8	96.8 ± 0.5
$CSNP_{CD55}$	6/6	406.9 ± 14.4	0.11 ± 0.04	+32.5 ± 1.1	428.2 ± 13.6	98.4 ± 0.2
$CSNP_{CD65}$	6/7.1	403.1 ± 21.5	0.18 ± 0.04	+29.1 ± 0.3	634.6 ± 10.1	97.0 ± 0.1
$CSNP_{TPP/CD0}$	6/0.5/0	319.6 ± 6.0	0.26 ± 0.02	+46.8 ± 0.8	36.2 ± 7.1	94.5 ± 0.5
$CSNP_{TPP/CD25}$	6/0.5/2.7	321.0 ± 11.0	0.32 ± 0.04	+36.3 ± 0.8	239.4 ± 8.6	94.7 ± 0.3
$CSNP_{TPP/CD35}$	6/0.5/3.8	408.1 ± 16.9	0.36 ± 0.03	+34.7 ± 0.9	361.2 ± 10.7	96.5 ± 0.3
$CSNP_{TPP/CD45}$	6/0.5/4.9	479.3 ± 14.4	0.37 ± 0.04	+29.4 ± 0.7	476.1 ± 25.7	96.9 ± 0.2
$CSNP_{TPP/CD55}$	6/0.5/6	478.8 ± 11.8	0.34 ± 0.01	+22.9 ± 0.8	146.0 ± 3.8	93.3 ± 0.3
$CSNP_{TPP/CD65}$	6/0.5/7.1	549.5 ± 43.0	0.38 ± 0,08	+21.4 ± 0.8	121.4 ± 14.1	94.4 ± 0.3

[1]CSNP was used to denote chitosan nanoparticles. [2]CS/TTP/CD and CS/CD corresponds to the chitosan (CS)/tripolyphosphate (TPP)/SBE-β-CD (CD) and chitosan (CS)/SBE-β-CD (CD) ratio, for nanoparticles prepared with and without tripolyphosphate, respectively. The subscript number together CD denotes the SBE-β-CD amount (mg) added to the formulations.

Figure 2. TEM micrographs of: (A) $CSNP_{CD65}$; and (B) $CSNP_{TPP/CD45}$.

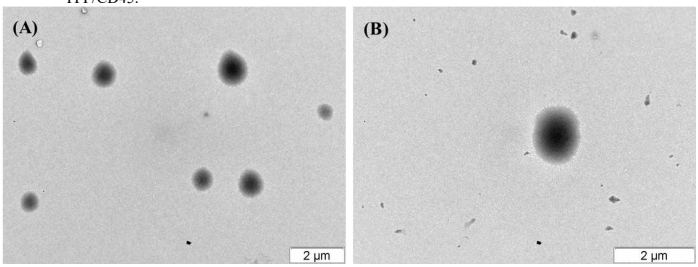

Preparation and characterization of spray-dried powders

The physicochemical properties of spray-dried powders prepared from dispersions containing chitosan nanoparticles/Eudragit® S100 ratios of 1:4, 1:6, and 1:8 are shown in Table 2. The process yield, calculated considering the total amount of solids presents in the feed dispersions, and residual moisture of SDPs varied from 72.9 to 75.8 % and from 5.3 to 6.4%, respectively, indicating that the spray-drying process was successful. The SIM content was found to be 1.5 %, 1.2 %, and 1.2 % (w/w) for SPD_{CD} and 1.1, 1.0, and 0.9 % (w/w) for the $SPD_{TPP/CD}$ for the nanoparticle/Eudragit® S100 ratios of 1:4, 1:6, and 1:8, respectively. The spray-drying powder turned the nanoparticle dispersions into microparticles as it was expected, with particles displaying mean sizes of about 5 µm. The SDPs exhibited negative zeta potential values, which it may be attributed to the carboxylic groups of the methacrylic acid residues in the Eudragit® S100 backbone. The microparticles presented spherical shape with smooth surface (Figure 3). Some collapsed regions can be noticed and this morphology was probably developed during the spray drying process.[40]

Table 2. Physicochemical characteristics of spray-dried enteric microparticles containing chitosan nanoparticles.

Formulation[1]	Physicochemical characteristics (Mean ± SD, n = 3)				
	Yield (%)	Moisture Content (%)	Mean diameter (µm)	Zeta Potential (mV)	SIM content (%, w/w)
SDP_{CD65} 1:4	74.9 ± 1.1	6.2 ± 0.1	5.3 ± 2.5	-48.30 ± 0.44	1.52 ± 0.07
SDP_{CD65} 1:6	73.6 ± 3.3	6.2 ± 0.2	5.7 ± 2.7	-46.33 ± 1.78	1.27 ± 0.05
SDP_{CD65} 1:8	75.8 ± 3.1	6.4 ± 0.1	5.3 ± 2.8	-46.20 ± 1.57	1.27 ± 0.12
$SDP_{TPP/CD45}$ 1:4	72.9 ± 0.7	6.1 ± 0.1	5.7 ± 3.1	-46.83 ± 1.42	1.15 ± 0.13
$SDP_{TPP/CD45}$ 1:6	73.7 ± 2.1	6.1 ± 0.1	5.6 ± 2.8	-45.18 ± 0.64	1.03 ± 0.17
$SDP_{TPP/CD45}$ 1:8	74.2 ± 3.3	5.3 ± 0.1	5.4 ± 2.4	-45.63 ± 1.33	0.91 ± 0.03

[1]SDP denotes spray-dried powders, in which the numbers corresponds to the chitosan nanoparticles to Eudragit® S100 ratio in the feed dispersions.

Figure 3. SEM micrographs of: (A) SPD_{CD65} 1:4; (B) SPD_{CD65} 1:6; (C) SPD_{CD65} 1:8; (D) $SPD_{TPP/CD45}$ 1:4; (E) $SPD_{TPP/CD45}$ 1:6; and (F) $SPD_{TPP/CD45}$ 1:8.

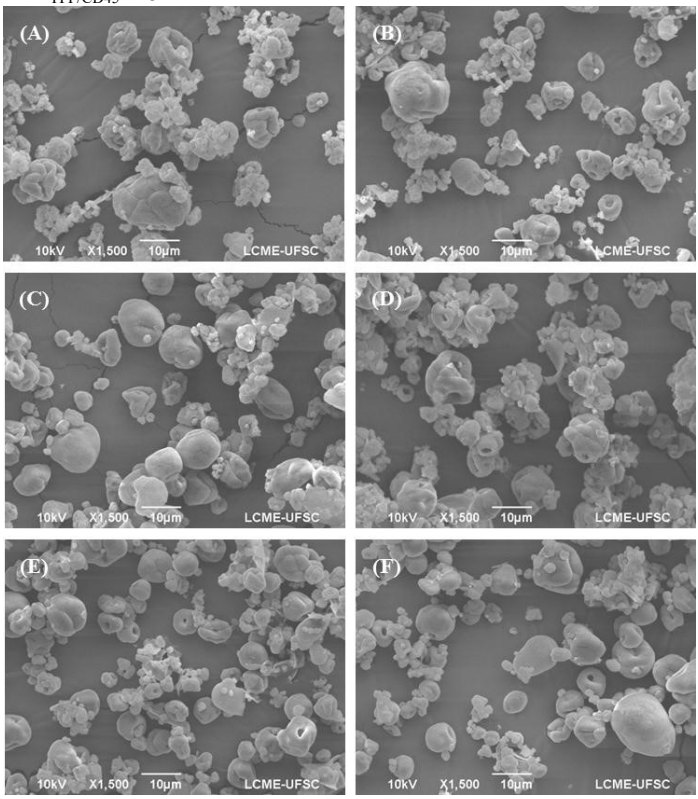

Differential scanning calorimetry

The thermal behavior of raw materials, inclusion complexes, chitosan nanoparticles, and spray-dried powders are showed in Figure 4 and 5. The DSC curve of SIM (Fig. 4a) displayed an endothermic peak at 139.77 °C, corresponding to the melting point of the drug.[41] CS displayed a broad endothermic peak between 80 and 100 °C (Fig. 4b),

due to the loss of moisture content of this polysaccharide.[42] SBE-β-CD (Fig. 4c) also exhibited an endothermic peak indicating loss of moisture between 80 and 100 ºC, and a endotherm peak at 269.92 °C corresponding to the melting point.[43] The DSC curve of TPP (Fig. 4d) did not display thermal events at the temperature ranging from 30 to 300 °C, since it melts at temperature above 600 °C.[44] The DSC curve of Eudragit® S100 (Fig. 4e) displayed an endothermic peak at 202.61 °C, corresponding to the glass transition temperature of this polymer.[45]

In order to verify the presence of interactions between the SIM and SBE-β-CD before the formation of the chitosan nanoparticles, SIM/SBE-β-CD complexes were prepared at conditions similar to that used in the preparation of the nanoparticles. The DSC curves obtained for SIM/SBE-β-CD and SIM/SBE-β-CD/TPP complexes (Fig. 5a and Fig. 5b) showed peaks corresponding to water loss at 92.48 °C and 90.74 °C, respectively, and the endothermic peak in both samples of SIM was absent. This complete disappearance of the crystalline SIM melting peak can be assumed as an evidence of the insertion of the drug inside the SBE-β-CD cavity, as reported elsewhere.[46,47] Although, the disappereance of the endothermic peak of SIM can also be due to the sample amorphization during the freeze drying process, and not be related to the formation of an inclusion complex. DSC curves obtained for $CSNP_{CD65}$ and $CSNP_{TPP/CD45}$ (Fig. 5c and 5d) exhibited peaks corresponding to the water loss at 109.12 °C and 98.23 °C, respectively. A second endothermic event was observed at 126.53 °C and 128.03 °C, respectively, probably due to the presence of SIM in a more crystalline form, in these samples. The reduction in the SIM melting point could indicate the presence of interaction between the drug and the excipients of the formulations. The DSC curves obtained for the spray-dried powders (SPD_{CD65} and $SPD_{TPP/CD45}$) displayed only endothermic peaks corresponding to the water loss from the samples (72.79 °C and 101.45 °C, respectively) (Figs. 5e and 5f).

Figure 4. DSC curves of (a) SIM; (b) CS; (c) SBE-β-CD; (d) TPP; and (e) Eudragit® S100.

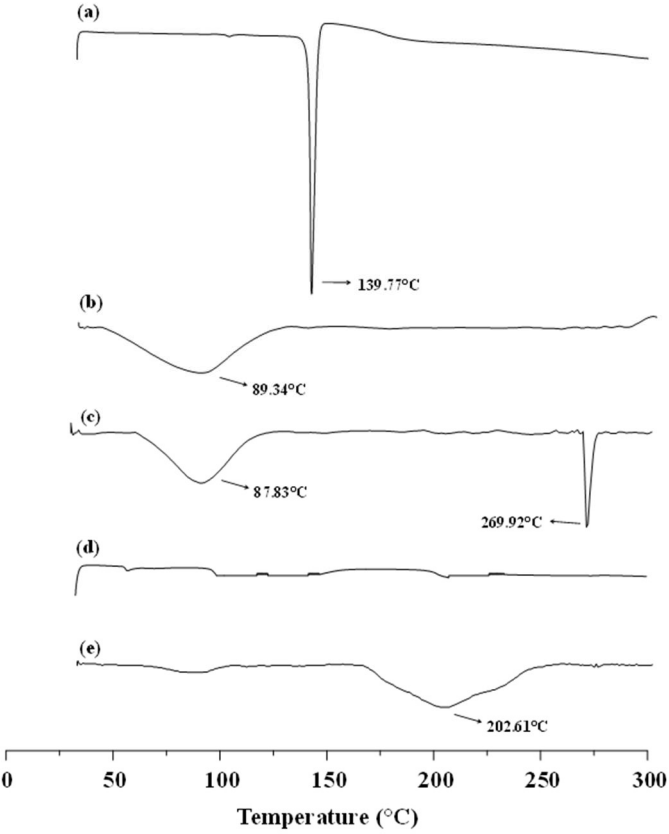

Figure 5. DSC curves of (a) SIM/SBE-β-CD; (b) SIM/SBE-β-CD/TPP; (c) $CSNP_{CD65}$; (d) $CSNP_{TPP/CD45}$; (e) SPD_{CD65} 1:6; and (f) $SPD_{TPP/CD45}$ 1:6.

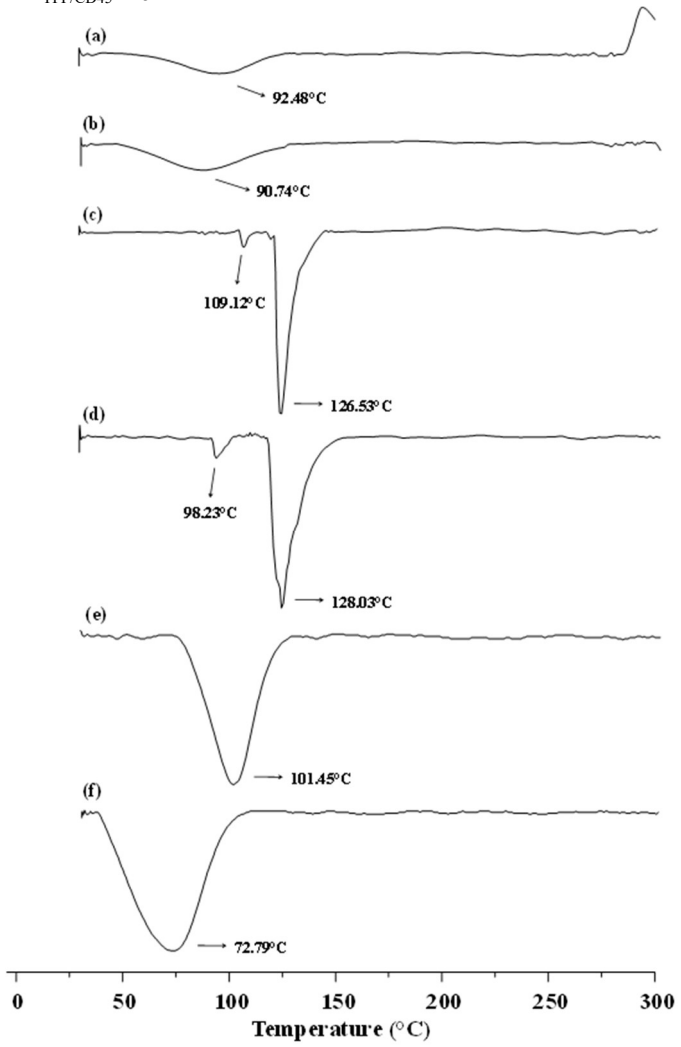

FT-IR analysis

The interactions between the formulations components were studied by FT-IR and the spectra are shown in the Figures 6 and 7. The IR spectrum of SIM (Fig. 6a) exhibited a characteristic band of free O–H strechinng vibrations at 3549.2 cm^{-1}, C–H streching vibrations at 2963.6 and 2872.3 cm^{-1}, and a characteristic band at 1713.2 cm^{-1}, corresponding to the stretching vibrations of the ester and lactone carbonyl functional group.[41] The CS spectrum (Fig. 6b) displayed a strong band at 3426.3 cm^{-1} that corresponds to combined bands of O–H stretching and intermolecular hydrogen bonding; the symmetric stretching of C–O–C was found around 1075.4 cm^{-1}, and the band at 1418.4 cm^{-1} belongs to the C–N stretching.[22] CS also exhibited a band of the amide bond at 1663.1 cm^{-1} and a protonated amino bond at 1586.9 cm^{-1}.[48] The IR spectrum of SBE-β-CD (Fig. 6c) is characterized by an intense band at 3414.4 cm^{-1} corresponding to O–H stretching vibrations and bands at 2937.5 and 2877.8 cm^{-1}, corresponding to the vibration of the CH and CH_2 groups. The band at 1646.8 cm^{-1} reflects the δ-HOH bending of water molecules attached to the cyclodextrin and the band at 1040.4 cm^{-1} corresponds to the stretching vibrations of the sulfoxide group.[22,49] The TPP spectrum (Fig. 6d) showed bands in 1143.6 cm^{-1} and 896.7 cm^{-1} corresponding to the stretching vibrations of P=O and P–O groups, respectively.[50] The spectrum of Eudragit® S100 showed a band at 1734.0 cm^{-1} that correponds to the streching vibrations of the carboxilic acid groups.[51]

The presence of interactions between the SIM and SBE-β-CD before the formation of the chitosan nanoparticles was also verified by FT-IR. The spectra of the SIM/SBE-β-CD and SIM/TPP/SBE-β-CD complexes (Figs. 7a and 7b) showed the displacement of the characteristic bands of SBE-β-CD to 1654.6 cm^{-1} and 1049.4 cm^{-1} and the stretching vibrations of the ester and lactone carbonyl functional group of SIM at 1713.2 cm^{-1} was absent. The disappearance of SIM

characteristic band can be an indicative of the inclusion complexation of SIM into the SBE-β-CD cavity. A similar result was observed by Jun et al. (2007)[36], where an inclusion complex of hydroxypropyl-β-cyclodextrin and SIM was prepared by supercritical antisolvent process. The absence of SIM characteristic band indicated the C=O group of lactone ring of SIM could be involed in the inclusion complexation.

$CSNP_{CD65}$ spectrum (Fig. 7c) showed that the protonated amino band of CS was shifted to 1552.2 cm^{-1} and the sulfoxide band of SBE-β-CD was shifted to 1049.4 cm^{-1}. Moreover, it was observed a single band at 1637.8 cm^{-1} that can be attributed to the overlapping of the amide group of CS and the δ-HOH bending of water molecules attached to the cyclodextrin. $CSNP_{TPP/CD45}$ spectrum (Fig. 7d) showed that the protonated amino band of CS was shifted to 1552.2 cm^{-1}, the sulfoxide band of SBE-β-CD was shifted to 1049.4 cm^{-1}, and the P=O and P-O bands of TPP were absent. Similarly as found for $CSNP_{CD65}$, the bands corresponding to the amide group of CS and the δ-HOH bending of water molecules attached to the cyclodextrin were overlapped at 1637.8 cm^{-1}. These spectral changes may be attributed to the electrostatic interactions between the CS cationic groups and the SBE-β-CD and TPP anionic groups, allowing the formation of the nanoparticles. The spectra of both SDP_{CD65} and $SDP_{TPP/CD45}$ with nanoparticle/Eudragit® S100 ratio of 1:6 (Fig. 7e and Fig. 7f) displayed the protonated amino band of CS shifted from 1586.9 cm^{-1} to 1562.5 cm^{-1} , and the band of the carbonyl groups of Eudragit® S100 shifted from 1734.0 cm^{-1} to 1714.2 cm^{-1}. These results suggest that, besides the ionic interaction between CS, TPP, and SBE-β-CD previously reported, interactions between the positive charges of chitosan nanoparticle and the negative charges of Eudragit® S100 also occurred.

Figure 6. FT-IR spectra of (a) SIM; (b) CS; (c) SBE-β-CD; (d) TPP; and (e) Eudragit® S100.

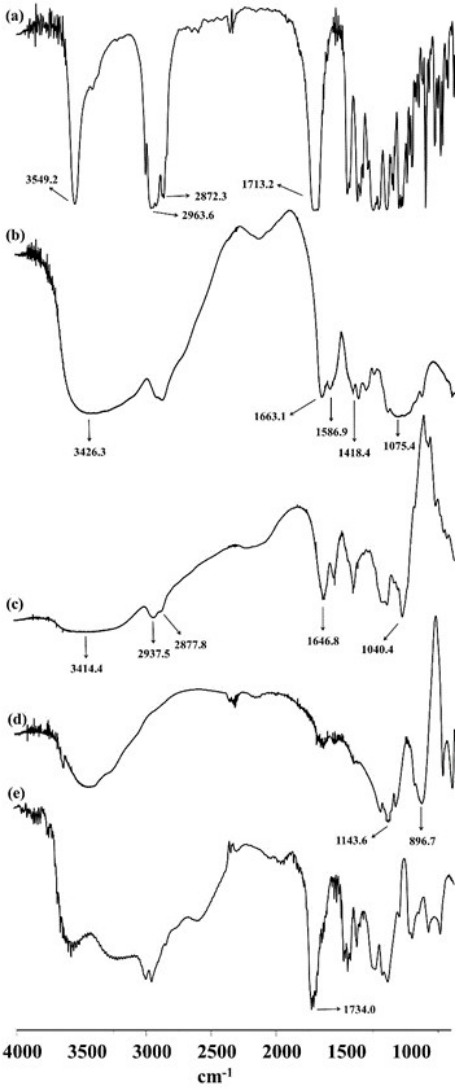

Figure 7. FT-IR spectra of (a) SIM/SBE-β-CD complex; (b) SIM/SBE-β-CD/TPP complex; (c) $CSNP_{CD65}$; (d) $CSNP_{TPP/CD45}$ 1:6; (e) SDP_{CD65} 1:6, and (f) $SDP_{TPP/CD45}$ 1:6.

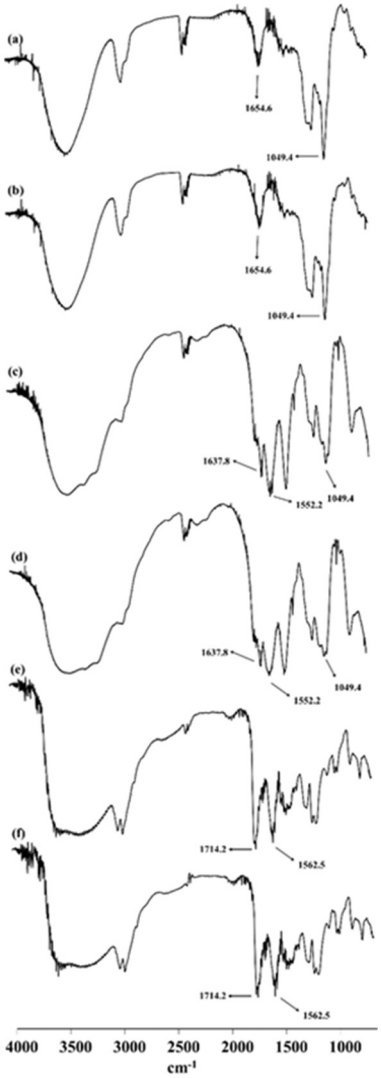

X-ray diffractometry

The X-ray diffraction patterns of raw materials, chitosan nanoparticles, and spray-dried powders are showed in Figures 8. SIM displayed peaks at 8.01°, 9.62°, 11.10°, 15.12°, 15.80°, 16.83°, 17.40°, 19.00°, 19.58°, 22.68°, and 28.52° 2θ (Fig. 8a), evidencing the crystalline structure of this drug.[52] CS, SBE-β-CD, and Eudragit® S100 (Fig. 8b, Fig. 8c and Fig. 8e, respectively) did not exhibited diffraction peaks, revealing their amorphous property. TPP exhibited the most intense peaks at 18.71°, 19.33°, 33.16°, 33.88°, and 34.40° 2θ (Fig. 8d). The diffractograms of $CSNP_{CD65}$ and $CSNP_{TPP/CD45}$ (Fig. 8f and Fig. 8g) showed a single crystalline peak in 8.81° and 8.92°, respectively, corresponding to SIM. SDP_{CD65} and $SPD_{TPP/CD45}$ with nanoparticle/Eudragit® S100 ratio of 1:6 (Fig. 8h and Fig. 8i) did not present any cristallinity peaks as it was expected, since the spray-dryer technique is generally applied in the manufacture of amorphous powders.

Figure 8. Diffractograms of (a) SIM; (b) CS; (c) SBE-β-CD; (d) TPP; and (e) Eudragit® S100; (f) $CSNP_{CD65}$; (g) $CSNP_{TPP/CD45}$; (h) SPD_{CD65} 1:6; and (i) $SPD_{TPP/CD45}$ 1:6.

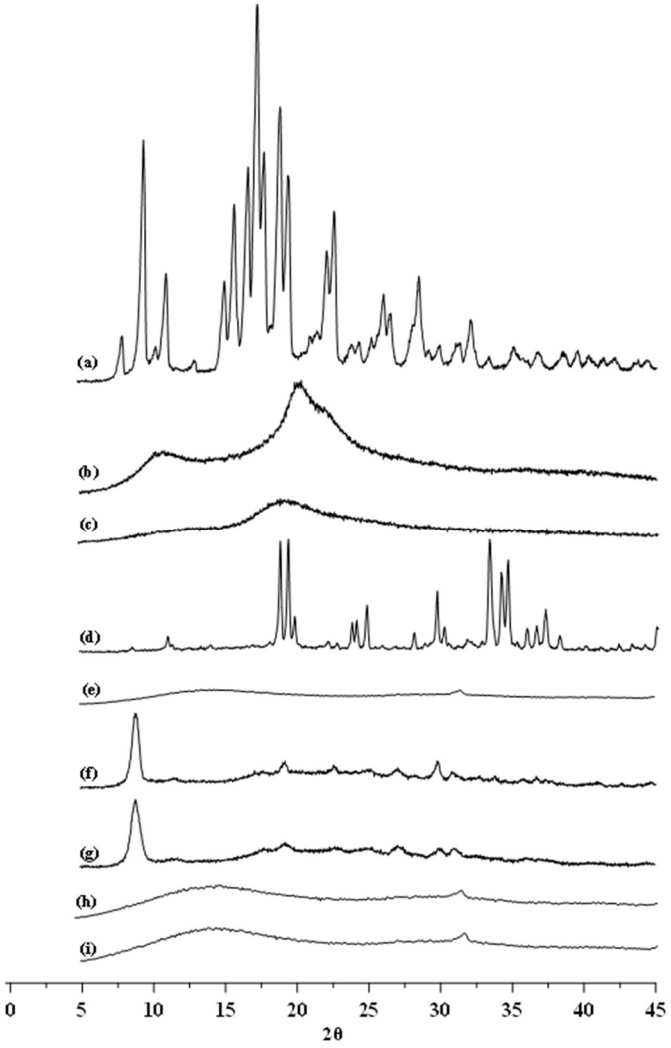

In vitro SIM release studies

The *in vitro* release of SIM from the enteric spray-dried microparticles was investigated in gradually pH-changing media and the results are shown in the Figure 9. As it can be observed, SIM exhibited a pH-dependent release profile. In the first hour, in the pH 1.2 hydrochloric acid solution, which would correspond to the time for gastric emptying, the SIM release from the SPD_{CD65} was 11.84, 9.21, and 9.03 % (Fig. 9a) and from the $SPD_{TPP/CD45}$ the release was 12.16, 10.09, and 8.82 % (Fig. 9b) for the microparticles prepared with chitosan nanoparticles to Eudragit® S100 ratios of 1:4, 1:6, and 1:8, respectively. The release of SIM did not occur in the subsequent 3 h in pH 4.5 phosphate buffer solution, indicating that this first fraction released corresponded to the fraction of the drug adsorbed at the surface of the spray-dried microparticles. When the medium was changed to buffer phosphate pH 7.2, which corresponds to the pH of the ileocecal region of the GIT, the remaining drug was released at a controlled rate from the microparticles. After 12 hours, the percent of SIM release from the SPD_{CD65} was 98.89, 99.17, and 99.69 % and from the $SPD_{TPP/CD45}$ was 98.35, 97.19, and 99.32 %, for the formulations prepared with chitosan nanoparticles to Eudragit® S100 ratios of 1:4, 1:6, and 1:8, respectively. Thus, these *in vitro* drug release results revealed that SIM was retained in the particles under acidic conditions, but was released as the environment pH changed from acidic to physiological pH, evidencing the enteric release properties of the microparticles. Besides that, the microparticles exhibited a time-dependent release profile, since SIM release occured in a sustained way in pH 7.2 Therefore, if the polymer dissolution begin in the small intestine (pH > 7.0), the controlled release would ensure drug release preferably in the colon.

Figure 9. SIM release profiles obtained from (a) SDP_{CD65} and (b) $SDP_{TPP/CD45}$ prepared with chitosan nanoparticle to Eudragit® S100 ratios of (♦) 1:4; (■) 1:6; and (▲) 1:8.

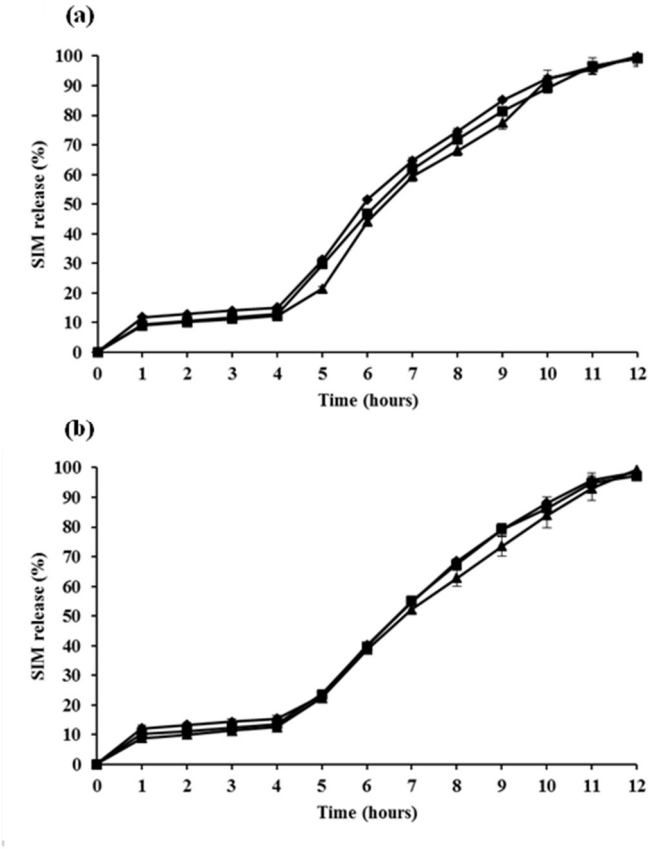

In order to verify if there were any statistical differences in the SIM release profiles regarding to the chitosan nanoparticles to Eudradit S100 ratio used in the formulations, the dissolution efficiency values (DE) were calculated for each dissolution media (Table 3). The analysis of the variance revealed that the DE in pH 7.2 phosphate

buffer was significantly different only when SDP_{CD65} was prepared with the higher amount of the enteric polymer (SDP_{CD65} 1:8), with a slower SIM release occurring in this case. Finally, the mean diameters of SPD_{CD65} measured after 5 hours of magnetic stirring in water adjusted to pH 7.2 were 592.17 nm, 584.23 nm, and 729.83 nm, with PDI values of 0.31, 0.37, and 0.34 for formulations prepared with nanoparticle/Eudragit® S100 ratios of 1:4, 1:6, and 1:8, respectively. For $SPD_{TPP/CD45}$ the sizes were 445.70 nm, 522.97 nm, and 814.47 nm, with PDI values of 0.45, 0.31, and 0.37 for the nanoparticle/Eudragit® S100 ratios of 1:4, 1:6, and 1:8, respectively. These results indicated that after this time the enteric polymer was quite dissolved, rendering a redispersible colloidal suspension.

Table 3. Dissolution efficiency (DE) obtained from SIM release from SDP_{CD65} and $SDP_{TPP/CD45}$.

Formulation	DE (%)[1] (Mean ± SD, n = 6)		
	pH 1.2	pH 4.5	pH 7.2
SDP_{CD65} 1:4	5.9 ± 0.2^{a}	7.5 ± 0.2^{c}	61.5 ± 0.9^{f}
SDP_{CD65} 1:6	4.6 ± 0.1^{b}	6.3 ± 0.2^{d}	60.3 ± 1.0^{f}
SDP_{CD65} 1:8	4.5 ± 0.1^{b}	6.0 ± 0.2^{e}	58.4 ± 0.5^{g}
$SDP_{TPP/CD45}$ 1:4	6.1 ± 0.5^{a}	8.0 ± 0.7^{c}	55.2 ± 0.4^{e}
$SDP_{TPP/CD45}$ 1:6	5.0 ± 0.4^{b}	6.4 ± 0.3^{d}	56.1 ± 1.2^{e}
$SDP_{TPP/CD45}$ 1:8	4.4 ± 0.4^{b}	6.3 ± 0.3^{d}	54.3 ± 1.6^{e}

[1]Equal letters indicate no statistical significance between the values. SDP_{CD65}: F_{cal} pH 1.2 = 159.40; F_{cal} pH 4.5 = 99.07; F_{cal} pH 7.2 = 19.81; $F_{critical}$ = 3.68; $SDP_{TPP/CD45}$: F_{cal} pH 1.2 = 13.31; F_{cal} pH 4.5 = 18.56; F_{cal} pH 7.2 = 3.36; $F_{critical}$ = 3.68. Significance level of 5%.

CONCLUSIONS

In the present study, SIM-loaded SBE-β-CD/chitosan nanoparticles were effectively prepared with or without the addition of TPP. The high SIM loading obtained by the addition of increasing amounts of SBE-β-CD to the formulations was probably due to the presence of interactions between the drug and the cyclodextrin, even though the inclusion complex formation could not be proved. Further, a spray-dryed enteric microparticles entrapping chitosan nanoparticles were obtained by using the enteric polymer Eudragit® S100. The *in vitro* release studies indicated that the microparticles would release SIM after 4 h after reaching the intestinal fluid, therefore, preserving the formulation during the passage through the gastric and small intestine environment (pH 1.2 and 4.5, respectively). Besides this pH-dependent release behaviour, the formulated enteric microparticles achieved sustained drug release over a period of 8 h in phosphate buffer pH 7.2 medium. In this way, colonic diseases such as colorectal cancer could be treated locally, opening a new therapeutic strategy by combining a delayed release system such as the Eudragit® S100 microparticles with the bioadhesive properties of chitosan nanoparticles.

ACKNOWLEDGEMENTS

This research was supported by Coordination for the Improvement of Higher Education Personnel Superior (CAPES, Ministry of Education, Brazil), which granted a scholarship to one of the authors.

DECLARATION OF INTEREST

The authors report no conflicts of interest.

REFERENCES

1. Wong WWL, Dimitroulakos J, Minden MD, Penn LZ 2002. HMG-CoA reductase inhibitors and the malignant cell: The statin family of drugs as triggers of tumor-specific apoptosis. Leukemia 16:508 – 519.

2. Hindler K, Cleeland CS, Rivera E, Collard CD 2006. The role of statins in cancer therapy. Oncologist 11:306 – 315.

3. Cho SJ, Kim JS, Kim JM, Lee JY, Jung HC, Song IS 2008. Simvastatin induces apoptosis in human colon cancer cells and in tumor xenografts, and attenuantes colitis-associated colon cancer in mice. Int. J. Cancer 123:951 – 957.

4. Qi XF, Kim DH, Yoon YS, Kim SK, Cai DQ, Teng YC, Shim KY, Lee KJ 2010. Involvement of oxidative stress in simvastatin-induced apoptosis of murine CT26 colon carcinoma cells. Toxicol. Lett. 199:277 – 287.

5. Chang HL, Chen CY, Hsu YF, Kuo WS, Ou G, Chiu PT, Huang YH, Hsu MJ 2013. Simvastatin induced HCT166 colorectal cancer cell apoptosis through p38MAPK-p53-*survivin* signaling cascade. Biochim. Biophys. Acta 1830:4053 – 4064.

6. Chourasia MK, Jain SK 2003. Pharmaceutical approaches to colon targeted drug delivery systems. J. Pharm. Pharmaceut. Sci. 6(1):33 – 66.

7. Bayat A, Dorkoosh FA, Dehpour AR, Moezi L, Larijani B, Junginger HE, Rafiee-Tehrani M 2008. Nanoparticles of quaternized chitosan derivatives as a carrier for colon delivery of insulin: *Ex vivo* and *in vivo* studies. Int. J. Pharm. 356:259 – 266.

8. Ashgar LFA, Chandran S 2006. Multiparticulate formulation approach to colon specific drug delivery: Current perspectives. J. Pharm. Pharm. Sci. 9(3):327 – 338.

9. Singh, BN 2007. Modified-release solid formulations for colonic delivery. Recent Pat. Drug. Deliv. Formul. 1:53 – 63.

10. Philip AK, Philip B 2010. Colon targeted drug delivery systems: A review on primary and novel approaches, Oman Med. J., 25:70 – 78.

11. Prasanth VV, Jayaprakash R, Mathew ST 2012. Colonic specific drug delivery systems: A review on various pharmaceutical approaches. J. Appl. Pharm. Sci. 2(1):163 – 169.
12. Dash M, Chiellini F, Ottembrite, RM, Chiellini E 2011. Chitosan – A versatile semi-synthetic polymer in biomedical applications. Prog. Polym. Sci. 36:981 – 1014.
13. Agrawal P, Strijkers GJ, Nicolay K 2010. Chitosan-based systems for molecular imaging. Adv. Drug Delivery Rev. 62:42 – 58.
14. Park JH, Saravanakumar G, Kim K, Kwon, IC 2010. Targeted delivery of low molecular drugs using chitosan and its derivates. Adv Drug Delivery Rev 61:28 – 41.
15. Gulbake A, Jain SK. 2012. Chitosan: a potential polymer for colon-specific drug delivery system. Expert Opin. Drug Deliv. 9:713-729.
16. Hejazi R, Amiji, M 2003. Chitosan-based gastrointestinal delivery systems. J. Control. Release, 89:151 – 165.
17. Rinaudo, M 2006. Chitin and chitosan: properties and applications. Prog. Polym. Sci. 31:603 – 632.
18. Amidi M, Mastrobattista E, Jiskoot W, Hennink, WE 2010. Chitosan-based delivery systems for protein therapeutics and antigens. Adv. Drug Delivery Rev. 62:59 – 82.
19. Hammam JH 2010. Chitosan based polyelectrolyte complexes as potential carrier materials in drug delivery systems. Mar. Drugs 8:1305 – 1322.
20. Senyigit T, Sonvico F, Barbieri S, Ozer O, Santi P, Colombo P 2010. Lecithin/chitosan nanoparticles of clobetasol-17-propionate capable of accumulation in pig skin. J. Control. Rel. 142:368 – 373.
21. Tan Q, Weidong Liu W, Guo C, Zhai G 2011. Preparation and evaluation of quercetin-loaded lecithin-chitosan nanoparticles for topical delivery. Int. J. Nanomedicine 6:1621 – 1630.
22. Mahmoud AA, El-Feky GS, Kamel R, Awad GEA 2011. Chitosan/sulfobutylether-β-cyclodextrin nanoparticles as a

potential approach for ocular drug delivery. Int. J. Pharm. 413:229 – 236.
23. Wu J, Shen Q, Fang L 2012. Sulfobutylether-β-cyclodextrin/chitosan nanoparticles enhance the oral permeability and bioavailability of docetaxel. Drug Dev. Ind. Pharm. 39(7):1010 – 1019.
24. Fülöp Z, Saokham P, Loftsson T 2014. Sulfobutylether-β-cyclodextrin/chitosan nano- and microparticles and their physicochemical characteristics. Int. J. Pharm. 472:282 – 287.
25. Teijeiro-Osorio D, Remuñan-López C, Alonso MJ 2009. Chitosan/cyclodextrin nanoparticles can efficiently transfect the airway epithelium *in vitro*. Eur. J. Pharm. Biopharm. 71:257 – 263.
26. Jingou J, Shilei H, Weiqi L, Danjun W, Tengfei W, Yi X 2011. Preparation, characterization of hydrophilic and hydrophobic drug in combine loaded chitosan/cyclodextrin nanoparticles and in vitro release study. Colloids Surf. B Biointerfaces 83(1):103 – 107.
27. Trapani A, Lopedota A, Franco M, Cioffi N, Ieva E, Garcia-Fuentes M, Alonso MJ 2010. A comparative study of chitosan and chitosan/cyclodextrin nanoparticles as potential carriers for the oral delivery of small peptides. Eur. J. Pharm. Biopharm. 75(1):26 – 32.
28. Jain A, Jain S, Jain R, Kohli DV. 2015. Coated chitosan nanoparticles encapsulating caspase 3 activator for effective treatment of colorectal cancer. Drug Dev. Transl. Res. 5:596-610.
29. Tummala S, Kumar MNS, Prakash A. 2015. Formulation and characterization of 5-fluorouracil enteric coated nanoparticles for sustained and localized release in treating colorectal cancer. Saudi Pharm. J. 23:306-314.
30. Higuchi T, Connors, KA 1965. Phase-solubility techniques. Adv. Anal. Chem. Instrum. 4, 117–212.
31. Loftsson T, Hreinsdóttir D, Másson, M 2005. Evaluation of cyclodextrin solubilization of drugs. Int. J. Pharm. 302:18-28.

32. Fan W, Yan W, Xu Z, Ni H 2012. Formation mechanism of monodisperse, low molecular weight chitosan nanoparticles by ionic gelation technique. Colloids Surf. B 90:21 – 27.
33. Krauland AH, Alonso MJ 2007. Chitosan/cyclodextrin nanoparticles as macromolecular drug delivery system. Int. J. Pharm. 340:134 – 142.
34. ICH 2005. Harmonised tripartite guideline: validation of analytical procedures: text and methodology Q2 (R1).
35. European Pharmacopoeia 2008, 6th ed., Council of Europe: Strasbourg. p 266 – 274.
36. Jun SW, Kim MS, Kim JS, Park HJ, Lee S, Woo JS, Hwang SJ 2007. Preparation and characterization of simvastatin/hydroxypropyl-β-cyclodextrin inclusion complex using supercritical antisolvent (SAS) process. Eur. J. Pharm. Biopharm. 66:413 – 421.
37. Wen X, Liu Z, Zhu T 2005. Mass spectrometry and molecular modeling studies on the inclusion complexes between α, β-cyclodextrins and simvastatin. Chem. Phys. Lett. 405:114 – 117.
38. Süle A, Szente L, Csempesz, F 2009. Enhancement of drug solubility in supramolecular and coloidal systemsn J. Pharm. Sci. 98(2):484 – 494
39. Gan Q, Wang T, Cochrane C, McCarron P 2005. Modulation of surface charge, particle size and morphological properties of chitosan-TPP based nanoparticles intended for gene delivery. Colloids Surf. B 44:65 – 73.
40. Crcarevska MS, Dodov MG, Goracinova K 2008. Chitosan coated Ca-alginate microparticles loaded with budesonide for delivery to the inflamed colonic mucosa. Eur. Pharm. Biopham. 68:565 – 578.
41. Ambike AA, Mahadik KR, Paradkar A 2005. Spray-dried amorphous solid dispersions of simvastatin, a low T_g drug: *in vitro* and *in vivo* evaluations. Pharm. Res. 22:990 – 998.
42. Shantha SL, Harding DRK 2002. Synthesis and characterization of chemically modified chitosan microspheres. Carbohydr. Polym. 48:247 – 253.

43. Fukuda M, Miller DA 2008. Influence of sulfobutyl ether β-cyclodextrin (Captisol®) on the dissolution properties of a poorly soluble drug from extrudates prepared by hot-melt extrusion. Int. J. Pharm. 350:188 – 196.
44. Gierszewska-Druzynska M, Ostrowska-Czubenko JO 2010. The effect of ionic crosslinking on thermal properties of hydrogel chitosan membranes. PCACD 15:25 – 32.
45. Mehta KA, Kislalioglu MS, Phuapradit W, Malick AW, Shah NH 2001. Release performance of a poorly soluble drug from a novel, Eudragit®-based multi-unit erosion matrix. Int. J. Pharm. 213: 7 – 12.
46. Pinto LMA, Fraceto LF, Santana MHA, Pertinhez TA, Junior SO, Paula E 2005. Physico-chemical characterization of benzocaine-β-cyclodextrin inclusion complexes. J. Pharm. Biomed. Anal. 39:956 – 963.
47. Zingone G, Rubessa F 2005. Preformulation study of the inclusion complex warfarin-β-cyclodextrin. Int. J. Pharm. 291:3 – 10.
48. Sarmento B, Martins S, Ribeiro A, Veiga F, Neufeld R, Ferreira D 2006. Development and comparison of different nanoparticulate polyelectrolyte complexes as insulin carriers. Int. J. Pept. Res. Ther. 12:131 – 138.
49. Cannavà C, Crupi V, Guardo M, Majolino D, Stancanelli R, Tommasini S, Ventura CA, Venuti V 2013. Phase solubility and FTIR-ATR studies of idebenone/sulfobutyl ether β-cyclodextrin inclusion complex. J. Incl. Phenom. Macrocycl. Chem. 75:255 – 262.
50. Silverstein R, Webster FX, Kiemle D 2005. Spectrometric Identification of Organic Compounds, 7th ed., New York. p 71 – 109.
51. Cilurzo F, Minghetti P, Selmin F, Casiraghi A, Montanari L 2003. Polymethacrylate salts as new low-swellable mucoadhesive materials. J. Control. Rel. 88:43–53.
52. Aceves-Hernández JM, Hinojosa-Torres J, Nicolás-Vázquez I, Ruvalcaba RM, García RML 2011. Solubility of simvastatin: a theoretical and experimental study. J. Mol. Struct. 995:41 – 50.

DISCUSSÃO GERAL

As estatinas compõem uma classe de fármacos inibidores competitivos da HMG-CoA os quais previnem a conversão da HMG-CoA redutase em ácido mevalônico, uma etapa limitante na via da biossíntese de colesterol (STANCU & SIMA, 2001). Além do efeito redutor de colesterol, evidências sugerem que as estatinas possuem efeitos terapêuticos em uma variedade de doenças incluindo o câncer. A via da biossíntese do colesterol é também responsável pela síntese de diversas outras moléculas importantes dentre elas os isoprenóides geranilpirofosfato e farnesilpirofosfato. Estes derivados prenilados são responsáveis pela localização celular precisa e função adequada de diversas proteínas envolvidas em importantes vias de sinalização. Estas proteínas exercem efeitos em funções celulares essenciais incluindo proliferação celular, diferenciação e sobrevivência, bem como participam da regulação da morfologia e motilidade celular (BONETTI et al, 2003; CHAN et al., 2003; SLEIJFER et al., 2005). Sendo assim, a inibição seletiva da HMG-CoA pode ser uma nova estratégia para o tratamento do câncer.

Diante do exposto, o objetivo do trabalho foi desenvolver micropartículas gastroresistentes encapsulando nanopartículas de quitosana, visando a liberação local da sinvastatina na região colônica após administração oral para o tratamento do câncer colorretal. As nanopartículas foram preparadas pela técnica de interação iônica entre quitosana e tripolifosfato, na qual a formação das partículas ocorre espontaneamente através das interações eletrostáticas entre as cargas opostas destes polieletrólitos. Entretanto, as nanopartículas de quitosana e tripolifosfato não são apropriadas para a encapsulação de fármacos que possuem baixa solubilidade aquosa, como a sinvastatina. Desta maneira, a adição de taurocolato de sódio (STC) e de sulfobutiléter-β-ciclodextrina (SBE-β-CD) foram utilizadas como estratégias para aumentar a associação da sinvastatina nestes sistemas.

A adição do STC, um surfactante aniônico, nas CSNP teve como intuito aumentar a associação de sinvastatina às

nanopartículas e, pela presença de cargas negativas na sua estrutura, interagir eletrostaticamente com os grupamentos de carga positiva presentes na quitosana, auxiliando na formação das CSNP. Os valores de teor de sinvastatina foram afetados pela quantidade de STC adicionado às CSNP, variando de 83,6 à 225,14 μg/mL, sendo que a incorporação da sinvastatina aumentou com o aumento da concentração de STC. Além disso, a formulação que apresentou o maior teor de sinvastatina ($CSNP_{70}$; 70 mg de STC) foi capaz de aumentar a associação do fármaco em cerca de 3,3 vezes quando comparada às nanopartículas sem STC ($CSNP_0$; 66,9 μg/mL). Em estudo de citotoxicidade *in vitro*, a incubação da sinvastatina livre e das $CSNP_{70}$ em cultura de células de adenocarcinoma de cólon humano (HT-29) reduziu significativamente a viabilidade celular de maneira concentração e tempo dependente. As $CSNP_{70}$ contendo sinvastatina apresentaram melhores resultados em comparação à 5-fluoruracila (controle positivo) após 72 horas de incubação. Além disso, foi demonstrado que a sinvastatina livre e as $CSNP_{70}$ contendo sinvastatina foram capazes de induzir a morte celular por apoptose, inibir a migração celular e a capacidade das células HT-29 de formar colônias.

A segunda estratégia utilizada para aumentar o teor de sinvastatina nas CSNP foi a adição da SBE-β-CD, uma ciclodextrina aniônica capaz de formar complexos de inclusão com moléculas hidrofóbicas, aumentando a associação de fármacos com baixa solubilidade aquosa como a sinvastatina às nanopartículas. De igual maneira ao STC, as cargas negativas da SBE-β-CD são capazes de interagir eletrostaticamente com as cargas positivas da quitosana, formando nanopartículas. Neste estudo, além da adição de diferentes concentrações de SBE-β-CD nas nanopartículas de quitosana e tripolifosfato ($CSNP_{TPP/CD}$), uma segunda formulação foi desenvolvida apenas com quitosana e SBE-β-CD ($CSNP_{CD}$). As $CSNP_{CD}$ apresentaram teores entre 160,38 e 634,62 μg/mL, sendo que a incorporação da sinvastatina nas nanopartículas aumentou com o aumento da concentração de

SBE-β-CD adicionada. As $CSNP_{TPP/CD}$ apresentaram teores de sinvastatina variando de 239,49 à 476,15 µg/mL. A adição da SBE-β-CD às CSNP foi capaz de aumentar a associação da sinvastatina em até 13 vezes ($CSNP_{TPP/CD45}$; 476,15 µg/mL) em comparação ao teor obtido nas nanopartículas de quitosana e tripolifosfato (36,38 µg/mL). Comparando as duas estratégias testadas, a adição da SBE-β-CD às nanopartículas ($CSNP_{TPP/CD45}$) e a formulação de nanopartículas de quitosana e SBE-β-CD ($CSNP_{CD65}$) foram mais eficientes em aumentar a associação da sinvastatina. O teor de sinvastatina obtido nas $CSNP_{TPP/CD45}$ e $CSNP_{CD65}$ foi 2 e 3 vezes maior em relação ao teor de fármaco obtido nas $CSNP_{70}$, respectivamente. Esta maior associação de sinvastatina nas nanopartículas provavelmente ocorreu devido a interação entre o fármaco e a ciclodextrina. A eficiência de encapsulação da sinvastatina nas CSNP foi superior a 91 % para todas as formulações, demonstrando que a maior parte do fármaco encontra-se preferencialmente associado às nanopartículas.

Após o desenvolvimento das nanopartículas, a formulações que foram capazes de encapsular maiores quantidades de sinvastatina ($CSNP_{70}$, $CSNP_{TPP/CD45}$ e $CSNP_{CD65}$) foram encapsuladas em micropartículas de Eudragit® S100, um copolímero do ácido metacrílico e metilmetacrilado que possui um pH de dissolução acima de 7,0. Esta parte do trabalho teve como objetivo evitar a liberação da sinvastatina na porção superior do trato gastrointestinal e ao mesmo tempo assegurar sua liberação na região colônica. Além disso, diferentes proporções de nanopartículas/Eudragit® S100 (1:4, 1:6 e 1:8) foram testadas com o intuito de avaliar o efeito da concentração de Eudragit® S100 na liberação da sinvastatina. A microencapsulação das CSNP baseou-se no fato do Eudragit® S100 possuir grupamentos carregados negativamente em sua estrutura e, desta maneira, ser capaz de interagir com a superfície carregada positivamente das CSNP, por meio de interações eletrostáticas.

Os estudos de liberação *in vitro* da sinvastatina a partir das micropartículas foram realizados em condições de pH crescente utilizando meio ácido clorídrico pH 1,2, meio tampão fosfato pH 4,5 e meio tampão fosfato pH 7,2. Os resultados obtidos confirmaram a obtenção de micropartículas gastroresistentes, visto que apenas uma pequena quantidade de fármaco foi liberada em meio ácido para todas as formulações testadas. Ainda, foi observado que quanto maior a proporção de nanopartículas/Eudragit® S100 (1:8), menor quantidade de fármaco foi liberado em meio ácido. Por outro lado, em meio tampão fosfato pH 7,2 ocorreu uma liberação sustentada da sinvastatina ao longo de 8 horas, confirmando que estes sistemas são capazes de se dissolverem em meio colônico, permitindo a liberação do fármaco no local da ação. Em relação a eficiência de dissolução, foi observado um maior controle da liberação da sinvastatina com o aumento da proporção de nanopartículas/Eudragit® S100 para as micropartículas encapsulando $CSNP_{70}$ e $CSNP_{CD65}$. Para as micropartículas encapsulando $CSNP_{TPP/CD45}$ não houve diferença estatística na liberação do fármaco independente da proporção de nanopartículas/Eudragit® S100 testada. Desta maneita, os sistemas de liberação desenvolvidos podem ser promissores para a liberação colônica da sinvastatina para o tratamento do carcinoma colorretal, visto que esta estratégia inovadora permite que as propriedades dos sistemas de liberação retardada sejam combinadas com a liberação local e bioadesividade das nanopartículas de quitosana.

CONCLUSÕES

- A preparação de nanopartículas de quitosana/tripolifosfato/taurocolato de sódio, quitosana/tripolifosfato/sulfobutiléter-β-ciclodextrina e quitosana/sulfobutiléter-β-ciclodextrina contendo sinvastatina pela técnica de interação iônica mostrou ser viável e de simples execução.
- A metodologia de espectroscopia de absorção no ultravioleta para determinação do teor de sinvastatina nas nano- e micropartículas mostrou ser sensível, linear, precisa e exata.
- Maiores teores de sinvastatina nas nanopartículas de quitosana/tripolifosfato foram obtidas através da adição de taurocolato de sódio (83,6 a 225,1 µg/mL), provavelmente pela formação de uma estrutura mais hidrofóbica.
- Maiores teores de sinvastatina foram obtidos através da adição de sulfobutiléter-β-ciclodextrina nas nanopartículas de quitosana/tripolifosfato (36,2 a 476,1 µg/mL) e através do desenvolvimento de nanopartículas de quitosana/sulfobutiléter-β-ciclodextrina (160,3 a 634,6 µg/mL), provavelmente pela interação do fármaco com a ciclodextrina.
- Os diâmetros das nanopartículas de quitosana variaram dependendo da concentração de taurocolato de sódio (338,9 a 576,3 nm) ou de sulfobutiléter-β-ciclodextrina (319,6 a 549,5 nm) empregada. Os valores de potencial zeta evidenciaram carga positiva refletindo a presença dos grupamentos amino da quitosana na superfície das nanopartículas.
- Os valores de eficiência de encapsulação da sinvastatina nas nanopartículas de quitosana foram

acima de 91%, indicando que o fármaco se encontra preferencialmente associado às partículas.

- As nanopartículas foram incorporadas de maneira eficiente em micropartículas de Eudragit® S100. O processo de spray-drying proporcionou um alto rendimento com diâmetros de partículas variando de 3,1 a 6,3 µm, teor de sinvastatina de 0,91 a 1,52%, potencial zeta negativo evidenciando a característica aniônica do Eudragit® S100, morfologia esférica de superfície lisa com regiões colapsadas e baixo teor de umidade.
- Análises de DSC e FT-IR confirmaram as interações eletrostáticas entre os componentes das formulações e as propriedades do estado sólido das nano- e micropartículas foram evidenciadas por DRX.
- A liberação da sinvastatina a partir das micropartículas foi pH e tempo-dependente, pois a liberação do fármaco foi evitada em meio ácido, porém ocorreu de maneira sustentada ao longo de 8 horas em meio tampão fosfato pH 7,2.
- A taxa de liberação da sinvastatina em pH 7,2 foi dependente da concentração de Eudragit® S100 utilizada somente para as micropartículas encapsulando as nanopartículas de quitosana/tripolifosfato/taurocolato de sódio ($CSNP_{70}$) e quitosana/sulfobutiléter-β-ciclodextrina ($CSNP_{CD65}$).
- A sinvastatina livre e $CSNP_{70}$ contendo sinvastatina exibiram citotoxicidade, causaram morte celular programada (apoptose), inibiram a migração celular e reduziram a habilidade das células de adenocarcinoma humano (HT-29) de formar colônias.

REFERÊNCIAS BIBLIOGRÁFICAS

ACHARYA, S., SAHOO, S. K. PLGA nanoparticles containing various anticancer agents and tumor delivery by EPR effect. *Advanced Drug Delivery Reviews*, v.63, p.170 – 183, 2011.

ACQUAVELLA, N., QUIROGA, M. F., WITTIG, O., CARDIER, J. E. Effect of simvastatin on endothelial cell apoptosis mediated by Fas and TNF-α. *Cytokine*, v.49, p.45 – 50, 2010.

AGNIHOTRI, S. A., MALLIKARJUNA, N. N., AMINABHAVI, T. M. Recent advances on chitosan-based micro- and nanoparticles in drug delivery. *Journal of Controlled Release*, v.100, p.5 – 28, 2004.

AGRAWAL, P., STRIJKERS, G. J., NICOLAY, K. Chitosan-based systems for molecular imaging. *Advanced Drug Delivery Reviews*, v.62, p.42 – 58, 2010.

ALI, H., SHIRODE, A. B., SYLVESTER, P. W., NAZZAL, S. Preparation, characterization, and anticancer effects of simvastatin-tocotrienol lipid nanoparticles. *International Journal of Pharmaceutics*, v.389, p.223 – 231, 2010.

ALMEIDA, V. L., LEITÃO, A., REINA, L. C. B., MONTANARI, C. A., DONNICI, C. L. Câncer e agentes antineoplásicos ciclo-celular específicos e ciclo-celular não específicos que interagem com o DNA: uma introdução. *Química Nova*, v.28(1), p.118 – 129, 2005.

AMBIKE, A.A., MAHADIK, K.R., PARADKAR, A. Spray-Dried Amorphous Solid Dispersions of Simvastatin, a Low Tg Drug: *In Vitro* and *in Vivo* Evaluations. *Pharmaceutical Research*, v.22(6), p.990 – 998, 2005.

AMIDI, M., MASTROBATTISTA, E., JISKOOT, W., HENNINK, W. E. Chitosan-based delivery systems for

protein therapeutics and antigens. *Advanced Drug Delivery Reviews*, v.62, p.59 – 82, 2010.

ASHGAR, L. F. A., CHANDRAN, S. Multiparticulate formulation approach to colon specific drug delivery: Current perspectives. *Journal of Pharmacy and Pharmaceutical Sciences*, v.9(3), p.327 – 338, 2006.

BALAN, V., VERESTIUC, L. Strategies to improve chitosan hemocompatibility: A review. *European Polymer Journal*, v.53, p.171 – 188, 2014.

BARDOU, M., BARKUN, A., MARTEL, M. Effect of statin therapy on colorectal cancer. *Gut*, v.59, p.1572 – 1585, 2010.

BERNKOP-SCHNÜRCH, A., DÜNNHAUPT, S. Chitosan-based drug delivery systems. *European Journal of Pharmaceutics and Biopharmaceutics*, v.81, p.463 – 469, 2012.

BI, Y., CAO, X., LIU, M., MENG, X., ZHAI, H. A smart delivery system in response to time, pH and enzyme for colorectal cancer therapy and its targeted release performance *in vitro*. *Materials Letters*, v.137, p.354 – 357, 2014.

BRANNON-PEPPAS, L., BLANCHETTE, J. O. Nanoparticle and targeted systems for cancer therapy. *Advanced Drug Delivery Reviews*, v.56, p.1649 – 1659, 2004.
BRIGGER, I., DUBERNET, C., COUVREUR, P. Nanoparticles in cancer therapy and diagnosis. *Advanced Drug Delivery Reviews*, v.54, p.631 – 651, 2002.

BROWN, A. J. Cholesterol, statins and cancer. *Clinical and Experimental Pharmacology and Physiology*, v.34, p. 135 – 141, 2007.

BAYAT, A., DORKOOSH, F. A., DEHPOUR, A. R., MOEZI, L., LARIJANI, B., JUNGINGER, H. E., RAFIEE-TEHRANI, M. Nanoparticles of quaternized chitosan derivatives as a carrier for colon delivery of insulin: Ex vivo and in vivo studies. *International Journal of Pharmaceutics*, v.356, p.259 – 266, 2008.

CARDWELL C. R., HICKS, B. M., HUGHES, C., MURRAY, L.J. Statin Use After Colorectal Cancer Diagnosis and Survival: A Population-Based Cohort Study. Journal of Clinical Oncology, v.32, p.1 – 11, 2014.

CHANG, H. L., CHEN, C. Y., HSU, Y. F., KUO, W. S., OU, G., CHIU, P. T., HUANG, Y. H., HSU, M. J. Simvastatin induced HCT166 colorectal cancer cell apoptosis through p38MAPK-p53-*survivin* signaling cascade. *Biochimica et Biophysica Acta*, v.1830, p.4053 – 4064, 2013.

CHO, S. J., KIM, J. S., KIM, J. M., LEE, J. Y., JUNG, H. C., SONG, I. S. Simvastatin induces apoptosis in human colon cancer cells and in tumor xenografts, and attenuantes colitis-associated colon cancer in mice. *International Journal of Cancer*, v.123, p.951 – 957, 2008.

CHOURASIA, M. K., JAIN, S. K. Pharmaceutical approaches to colon targeted drug delivery systems. *Journal of Pharmacology and Pharmaceutical Sciences*, v.6(1), p.33 – 66, 2003.

COELHO, J. F., FERREIRA, P. C., ALVES, P., CORDEIRO, R., FONSECA, A. C., GÓIS, J. R., GIL, M. H. Drug delivery systems: Advanced technologies potentially applicable in personalized treatment. *EPMA Journal*, v.1, p.164 – 209, 2010.

CORCOS, L., JOSSIC-CORCOS, C. L. Statins: Perspectives in cancer therapeutics. *Digestive and Liver Disease*, v.45, p.795 – 802, 2013.

CROISIER, F., JÉRÔME, C. Chitosan-based biomaterials for tissue engineering. *European Polymer Journal*, v.49, p.780 – 792, 2013.

DANHIER, F., FERON, O., PRÉAT, V. To exploit the tumor microenviroment: Passive and active tumor targeting of nanocarriers for the anti-cancer drug delivery. *Journal of Controlled Release*, v.148, p.135 – 146, 2010.

DASH, M., CHIELLINI, F., OTTEMBRITE, R. M., CHIELLINI, E. Chitosan – A versatile semi-synthetic polymer in biomedical applications. *Progress in Polymer Science*, v.36, p.981 – 1014, 2011.

DONG, Y., NG, W. K., SHEN, S., KIM, S., TAN, R. B. H. Scalable ionic gelation synthesis of chitosan nanoparticles for drug delivery in static mixers. *Carbohydrate Polymers*, v.94, p.940 – 945, 2013.

EVONIK INDUSTRIES. Disponível em: <www.evonik.com.br>. Acesso em: 10 de setembro de 2014.

FÀBREGAS, A., MIÑARRO, M., GARCÍA-MONTOYA, E., LOZANO-PÉREZ, P., CARRILLO, C., SARRATE, R., SÁNCHEZ, N., TICÓ, J. R., SUÑÉ-NEGRE, J. M. Impact of physical parameters on particle size and reaction yield when using the ionic gelation method to obtain cationic polymeric chitosan-tripolyphosphate nanoparticles. *International Journal of Pharmaceutics*, v.446, p.199 – 204, 2013.

FANG, J., NAKAMURA, H., MAEDA, H. The EPR effect: Unique features of tumor blood vessels for drug delivery, factors involved, and limitations and augmentation of the effect. *Advanced Drug Delivery Reviews*, v.63, p.136 – 151, 2011.

FERRARI, P. C., SOUZA, F. M., GIORGETTI, L. OLIVEIRA, G. F., FERRAZ, H. G., CHAUD, M. V., EVANGELISTA, R. C. Development and *in vitro* evaluation of coated pellets containing chitosan to potential colonic drug delivery. *Carbohydrate Polymers*, v.91, p.244 – 252, 2013.

FREIRE, A. C., PODCZECK, F., SOUSA, J., VEIGA, F. Liberação específica de fármacos no cólon por via oral. II – Tipos de sistemas utilizados. *Revista Brasileira de Ciências Farmacêuticas*, v.42(3), p.337 – 355, 2006.

FRIEND, D. R. New oral delivery systems for treatment of inflammatory bowel disease. *Advanced Drug Delivery Reviews*, v.57, p.247 – 265, 2005.

GALOPAN, A., YU, W., SANDERS, B. G., KLINE, K. Simvastatin inhibition of mevalonate pathway induces apoptosis in human breast cancer cells via activation of JNK/CHOP/DR5 signaling pathway. *Cancer Letters*, v.329, p.9 – 16, 2013.

GAUTHAMAN, K., FONG, C. Y., BONGSO, A. Statins, stem cells, and cancer. *Journal of Cellular Biochemistry*, v.106, p.975 – 983, 2009.

GEORGE, M., ABRAHAM, T. E. Polyionic hydrocolloids for the intestinal delivery of protein drugs: Alginate and chitosan – a review. *Journal of Controlled Release*, v.114, p.1 – 14, 2006.

GILL, S., THOMAS, R. R., GOLDBERG, R. M. Review article: colorectal cancer chemotherapy. *Alimentary Pharmacology & Therapeutics*, v.18, p.683 – 692, 2003.

HAFNER, A., LOVRIC, J., VOINOVICH, D, FILIPOVIC-GRCIC, J. Melatonin-loaded lecithin/chitosan nanoparticles: Physicochemical characterization and permeability through Caco-2 cell monolayers. *International Journal of Pharmaceutics*, v.381, p.205 – 213, 2009.

HAMMAM, J. H. Chitosan based polyelectrolyte complexes as potential carrier materials in drug delivery systems. *Marine Drugs*, v.8, p.1305 – 1322, 2010.
HEJAZI, R., AMIJI, M. Chitosan-based gastrointestinal delivery systems. *Journal of Controlled Release*, v.89, p.151 – 165, 2003.

HINDLER, K., CLEELAND, C. S., RIVERA, E., COLLARD, C. D. The role of statins in cancer therapy. *The Oncologist*, v.11, p.306 – 315, 2006.

KASPER, D. L., BRAUNWALD, E., FAUCI, A. S., HAUSER, S. L., LONGO, D. L., JAMESON, J. L. Harrison´s Principles of Internal Medicine – Volume I, 16th edition, p.527 – 531. United States of America, 2006.

KUMARI, A., YADAV, S. K., YADAV, S. C. Biodegradable polymeric nanoparticles based drug delivery systems. *Colloids and Surfaces B: Biointerfaces*, v.75, p.1 – 18, 2010.

INCA – INSTITUTO NACIONAL DO CÂNCER JOSÉ ALENCAR GOMES DA SILVA. Disponível em: <www.inca.gov.br>. Acesso em: 15 janeiro de 2016.

JAIN, A., JAIN, S., GANESH, N., BARVE, J., BEG, A. M. Design and development of ligand-appended polysaccharidic nanoparticles for the delivery of oxaliplatin in colorectal cancer. *Nanomedicine*, v.6, 179 – 190, 2010.

JI, J., HAO, S., WU, D., HUANG, D., XU, Y. Preparation, characterization and *in vitro* release chitosan nanoparticles loaded with gentamicine and salicylic acid. *Carbohydrate Polymers*, v.85, p.803 – 808, 2011.

KAUFMANN, S. H., EARNSHAW, W. Induction of apoptosis by cancer chemoteraphy. *Experimental Cell Research*, v.256, p.42 – 49, 2000.

KRISHNAIAH, Y. S. R., KHAN, M. A. Strategies of targeting oral drug delivery systems to the colon and their potential use for the treatment of colorectal cancer. *Pharmaceutical Development and Technology*, v.17(5), p.521 – 540, 2012.

KUMAR, M. N. V. R., MUZZARELLI, R. A. A., MUZZARELLI, C., SASHIWA, H., DOMB, A. J. Chitosan chemistry and pharmaceutical perspectives. *Chemical Reviews*, v.104, p.6017 – 6084, 2004.

LESLIE, A., CAREY, F. A., PRATT, N. R., STEELE, R. J. C. The colorectal adenoma-carcinoma sequence. *British Journal of Surgery*, v.89, p.845 – 860, 2002.

LIU, Z., JIAO, Y., WANG, Y., ZHOU, C., ZHANG, Z. Polysaccharides-based nanoparticles as drug delivery systems. *Advanced Drug Delivery Reviews*, v.60, p.1650 – 1662, 2008.

MAHMOUD, A.A., EL-FEKY, G.S., KAMEL, R., AWAD, G.E.A.Chitosan/sulfobutylether-β-cyclodextrin nanoparticles as a potential approach for ocular drug delivery. *International Journal of Pharmaceutics*, v.413, p.229 – 236, 2011.

MEI, L., ZHANG, Z., ZHAO, L., HUANG, L., TANG, X. L., TANG, J., FENG, S. S. Pharmaceutical nanotechnology for oral delivery of anticancer drugs. *Advanced Drug Delivery Reviews*, v.65, p.880 – 890, 2013.

MISHRA, J., DRUMMOND, J., QUAZI, S. H., KARANKI, S. S., SHAW, J. J., CHEN, B., KUMAR, N. Prospective of colon cancer treatments and scope combinatorial approach to enhanced cancer cell apoptosis. *Clinical Reviews in Oncology/Hematology*, v.86, p.232 – 250, 2013.

MOHANRAJ, V. J., CHEN, Y. Nanoparticles – A Review. *Tropical Journal of Pharmaceutical Research*, v.5(1), p.561 – 573, 2006.

MORA-HUERTAS, C. E., FESSI, H., ELAISSARI, A. Polymer-based nanocapsules for drug delivery. *International Journal of Pharmaceutics*, v.385, p.113 – 142, 2010.

NAGPAL, K., SINGH, S. K., MISHRA, D. N. Chitosan nanoparticles: A promising system in novel drug delivery. *Chemical and Pharmaceutical Bulletin*, v.58(11), p.1423 – 1430, 2010.

OLIVERA, M. A., YOSHIDA, M. I., GOMES, E. C. L., MUSSEL, W. N., VIANNA-SOARES, C. D., PLANETTI, G. A. Análise térmica aplicada à caracterização da sinvastatina em formulações farmacêuticas. *Quimica Nova*, v.33(8), p.1653 – 1657, 2010.

PARK, J. H., SARAVANAKUMAR, G., KIM, K., KWON, I. C. Targeted delivery of low molecular drugs using chitosan and its derivates. *Advanced Drug Delivery Reviews*, v.61, p.28 – 41, 2010.

PHILIP, A. K., PHILIP, B. Colon targeted drug delivery systems: A review on primary and novel approaches. *Oman Medical Journal*, v.25, p.70 – 78, 2010.

PISANTI, S., PICARDI, P., CIAGLIA, E., D´ALESSANDRO, BIFULCO, M. Novel prospects of statins as therapeutic agents in cancer. *Pharmacological Research*, v.88, p.84 – 98, 2014.

PRASANTH, V. V., JAYAPRAKASH, R., MATHEW, S. T. Colonic specific drug delivery systems: A review on various pharmaceutical approaches. *Journal of Applied Pharmaceutical Science*, v.2(1), p.163 – 169, 2012.

QI, X. F., KIM, D. H., YOON, Y. S., KIM, S. K., CAI, D. Q., TENG, Y. C., SHIM, K. Y., LEE, K. J. Involvement of oxidative stress in simvastatin-induced apoptosis of murine CT26 colon carcinoma cells. *Toxicology Letters*, v.199, p.277 – 287, 2010.

RINAUDO, M. Chitin and chitosan: properties and applications. *Progress in Polymer Science*, v.31, p.603 – 632, 2006.

SCHAFFAZICK, R. S., GUTERRES, S. S., FREITAS, L. L., POHLMANN, A. R. Caracterização estabilidade físico-química de sistemas poliméricos nanoparticulados para administração de fármacos. *Química Nova*, v.26(5), p.726 – 737, 2003.

SINGH, B. N. Modified-release solid formulations for colonic delivery. *Recent Patents on Drug Delivery & Formulation*, v.1, p.53 – 63, 2007.

SINHA, V. R., SINGLA, A. K., WADHAWAN, S., KAUSHIK, R., KUMRIA, R., BANSAL, K., DHAWAN. Chitosan microspheres as a potential carrier for drugs. *International Journal of Pharmaceutics*, v.274, p.1 – 33, 2004.

SONVICO, F., CAGNANI, A., ROSSI, A., MOTTA, S, DI BARI, M. T., CAVATORTA, F., ALONSO, M. J., DERIU, A., COLOMBO, P. Formation of self-organized nanoparticles by lecithin/chitosan ionic interaction. *International Journal of Pharmaceutics*, v.324, p.67 – 73, 2006.

SOPPIMATH, K. S., AMINABHAVI, T. M., KULKARNI, A. R., RUDZINSKI, W. E. Biodegradable polymeric nanoparticles as drug delivery devices. *Journal of Controlled Release*, v.70, v.1 – 20, 2001.

TOZAKI, H., KOMOIKE, J., TADA, C., MARUYAMA, T., TERABE, A., SUZUKI, T., YAMAMOTO, A., MURANISHI, S. Chitosan capsules for colon-specific drug delivery: Improvement of Insulin Absorption from the Rat Colon. *Journal of Pharmaceutical Sciences*, v.86(9), p.1016 – 1021, 1997.

TIWARI, R., PATHAK, K. Nanostructured lipid carrier versus lipid nanoparticles of simvastatin: Comparative analysis of characteristics, pharmacokinetics and tissue uptake. *International Journal of Pharmaceutics*, v.415, p.232 – 243, 2011.

VAUTHIER, C., BOUCHEMAL, K. Methods for the preparation and manufacture of polymeric nanoparticles. *Pharmaceutical Research*, v.26(5), p.1025 – 1058, 2009.

WANG, C. Y., LIU P. Y., LIAO, J.K. Pleiotropic effects of statin therapy: molecular mechanisms and clinical results. *Trends in Molecular Medicine*, v.14, p.37 – 44, 2008

WANG, M., THANAU, M. Targeting nanoparticles to cancer. *Pharmacological Research*, v.62, p.90 – 99, 2010.

WONG, W. W. L., DIMITROULAKOS, J., MINDEN, M. D., PENN, L. Z. HMG-CoA reductase inhibitors and the malignant cell: The statin family of drugs as triggers of tumor-specific apoptosis. *Leukemia*, v.16, p. 508 – 519, 2002.

WU, J., SHEN, Q., FANG, L. Sulfobutylether-β-cyclodextrin/chitosan nanoparticles enhance the oral permeability and bioavailability of docetaxel. *Drug Development and Industrial Pharmacy,* v.39(7), p.1010 – 1019, 2012

YANG, L., CHU, J. S., FIX, J. A. Colon-specific drug delivery: New approaches and in vitro/in vivo evaluation. *International Journal of Pharmaceutics*, v.235, p.1 – 15, 2002.

YU, X., PAN, Y., MA, H., LI, W. Simvastatin inhibits proliferations and induces apoptosis in human lung cancer cells. *Oncology Research*, v.20(8), p.351 – 357, 2013.

ZHANG, H., ALSARRA, I. A., NEAU, S. H. An *in vitro* evaluation of a chitosan-containing multiparticulate system for macromolecule delivery to the colon. *International Journal of Pharmaceutics*, v.239, p.197 – 205, 2002.

ZHANG, H., NEAU, S. H. *In vitro* degradation of chitosan by bacterial enzymes from rat cecal and colonic contents. *Biomaterials*, v.23, p.2761 – 2766, 2002.